THE UNIVERSITY
of EDINBURGH

THE UNIVERSITY *of* EDINBURGH
School of Engineering

Sedimentation dynamics in Waste Stabilization Ponds and implications for helminth eggs removal

Fides John Izdori

Thesis submitted in fulfilment of
the requirements for the degree of
Doctor of Philosophy
to the
University of Edinburgh — 2019

Declaration

I declare that this thesis has been composed solely by myself and that it has not been submitted, either in whole or in part, in any previous application for a degree. Except where otherwise acknowledged, the work presented is entirely my own.

Fides Izdori

December 2019

Thou tellest my wanderings: put thou my tears into thy bottle: are they not in thy book? *(Psalms 56:8)*

Abstract

Helminthic infections pose significant worldwide public health challenges, and standard therapy includes mass drug administration (for de-worming) and three monthly vaccinations. However, research suggests that improved sanitation, especially efficient wastewater treatment, is a potential methodology for eradicating helminth infections. In low and middle income countries, waste stabilization ponds (WSP) are considered a cost-effective and highest ranked wastewater treatment system, capable of removing helminth eggs through sedimentation. However, eggs are still recovered in some ponds effluents, resulting into environmental contamination. Understanding sedimentation processes, and causative factors in WSP may improve system design for helminth eggs removal, hence reduce infections. Therefore, this research explores the sedimentation processes in the Buguruni WSP- Tanzania, concentrating in particle modifications inside the pond, settlement patterns at the bottom and properties of sedimented particles at different locations inside the pond. The methodology employed covered analysis for particle size distribution (PSD), wastewater helminth eggs composition, and 3D hydraulic and sedimentation modelling in Delft3D. Data shows that, incoming particles have unimodal distribution with sizes ranging from 1 to more than 1000 μm, with almost half-half composition by supra-colloid and settleable particles. Inside the pond, there are settling and non-settling PSDs, characterized by unimodal and bimodal distributions respectively. Sedimentation takes place along the hydrodynamic path-line, up to about 100 m from the inlet, where flocs are

deposited in order of decreasing size; a phenomenon known as hydraulic sorting. Wastewater flocs fall under two categories according to their densities; lighter particles that are majority with a mode around 1000.45 kgm^{-3} and denser particles with a mode around 1020 kgm^{-3} for Buguruni facultative pond. Analysis shows that, the individual densities of helminth eggs do not play any role in their sedimentation, the eggs sediments immediately, within few meters of the inlet if incorporated into denser flocs, otherwise when incorporated into the lighter flocs, they have high probability of being transported to the outlet. Modelling and analysis of wastewater samples showed that, helminth eggs are mostly deposited close to the inlet, although a few eggs were recovered close to the outlet. The presence of high densities of the algae *A. fusiformis* observed is linked to high volume of particles with sizes between 1 and 100 μm, as well as lighter flocs in the pond. These algae, although useful for biological treatment of wastewater, they result into formation of buoyant flocs, hence poor sedimentation. This implies that, there is only a possibility of optimizing one process in primary facultative ponds, either biological action or sedimentation. However, research has shown that a large percent of BOD is contained in the supra-colloids range, hence may be sedimented and later anaerobically digested in sludge. Therefore, a significant area can be saved by constructing a system that favours sedimentation, followed by a sludge digester. This research also showed that, wind and discharge from rainfall, play an important role in sludge accumulation patterns, and that the increased discharge from rainfall may be resulting into pond 'self cleaning'. Therefore, neglecting maintenance of the pond, as well as the sewer system has potential severe health and environmental effects, impacting communities downstream of the WSP. It's proposed that, maintenance of the pond and sewer system and addition of flocculants, especially locally available and natural may improve the sedimentation process and hence helminth egg removal in WSP, and therefore future research should focus on this.

Acknowledgements

Through the time of my studies I received a lot of help and support from various people, without which this work would not have been possible. My family and friends, although I can not mention all by names, were a great pillar of strength and motivation throughout my studies.

I would like to thank my supervisors, Paolo Perona and Andrea Semiao for all the work they put into achieving this degree. Their guidance, advise and criticism whenever needed are invaluable. I particularly would like to thank Paolo for having so much faith in me, and Andrea for always prompting me to think outside the box.

I would like to thank The Commonwealth Scholarship Commission in the United Kingdom (CSC) for funding this research through its PhD scholarships for low and middle-income countries.

I thank my friends and colleagues; Dr Valimba, Dr Geoffrey Banda, Dr Vera Mugittu, Aluna Chawala, Henry Mruma and Upendo Laizer for all their support and particularly Dr Geoffrey Banda for reading my work. Also, the invaluable field assistance of Paul Paskal Masapa, Ally Said Kibuga and technical assistance from Godas Mwakasege, the laboratory technician from the Chemical and Mining Engineering department at the University of Dar es Salaam are highly appreciated.

During my study I had to spend a lot of time away from my family. My greatest gratitude goes to my husband, Alex Massawe for taking good care of our four children Audrey, Bridgette, Cedric and Denzel. I also thank my husband and children for all the support and understanding while undertaking my studies. I am forever grateful to Janet and Rehema, and my sister Digna Isdory, and sister in-law Glory Massawe for doing their best to look after my children in my absence. They say it takes a village to raise a child; the role played by my extended family; my in-laws (Casmir and Marietha), my parents (John and Phillipina), uncle Ben and aunt Bea will always be a reminder of what a great family I have.

Contents

List of Tables

List of Figures

List of Acronyms and Abbreviations

BOD - Biological oxygen demand
CW - Constructed wetlands
STH - Soil transmitted helminth
WSP - Waste stabilization ponds
USEPA - U.S. Environmental Protection Agency
RTD - Residence time distribution
PSD - Particle size distribution
PDD - Particle distribution distribution
WHO - World health organisation
NTD - Neglected tropical diseases
SDG - Sustainable development goals

Chapter 1

Introduction

1.1 Health burden related to helminths found in water

Parasites in wastewater pose a public health challenge (Mara and Faechem, 1999; Lloyd and Frederick, 2000), because they cause diseases such as helminthiasis: a serious health condition affecting nearly a quarter of the world's population (Hotez *et al.*, 2008b). Soil transmitted helminth (STH), especially *ascaris, trichiura* and hookworm are a major health concern due to their high resistance to environmental conditions and low infectious dose (Mara, 2004; Amoah *et al.*, 2017; Brooker *et al.*, 2006). Helminths infections result in poor health and retarded growth for school children, epileptic seizures, maternal death and lower efficacy of tuberculosis (TB) vaccination, leading to placental transfer of TB by pregnant women (Mwanjali *et al.*, 2013; Hotez *et al.*, 2008b). In Sub-Saharan Africa only, it is estimated that STH infects about 89.9 million school age children (WHO, 2002; Brooker *et al.*, 2006), with Mara and Sleigh (2010) reporting highest intensity of *ascaris* infection (eggs/g faeces) in children between 5 and 14 years of age. The

main mode of transmission of these parasites are via their eggs found abundantly in wastewater in developing countries and food crops irrigated with contaminated water (Jimenez-Cisneros, 2007). There are several types of helminths, some of which their eggs are displayed in Figure 1.2, the most common species being *ascaris, trichiura* and *taenia* (Shuval *et al.*, 1986; Sengupta *et al.*, 2011; Verbyla *et al.*, 2016; Ben Ayed *et al.*, 2009; Konaté *et al.*, 2013; von Sperling *et al.*, 2003). Prevalence of the different species vary between regions (Moodley *et al.*, 2008) and is influenced by environmental factors, mainly temperature and humidity (Brooker *et al.*, 2007, 2006).

1.1.1 Helminths transmission

Helminths are a type of worm-like organisms living and feeding on other living organisms (hosts) usually human beings and animals (Hotez *et al.*, 2008b). They can be categorized into three groups; trematodes, cestodes and nematodes. Trematodes (flukes) normally have an intermediate snail host and they infect humans by penetration through the skin. Cestodes (tapeworms) example *taenia* are parasitic, living in the digestive tracks of vertebrates and can grow up to 20 m in length. Nematodes (roundworms) including *ascaris, hookworms* and *trichiura* also known as soil transmitted helminths (STH) as majority of them are found in the top 15 cm layer of soil. These invertebrates that are either round or flat in shape, vary in size from 1 millimetre to several meters length. Several types of helminths such as *ascaris, trichuris, hookworms, oesophagostomum, h-diminuta, h-nana, taenia, ancylostoma, fasciola, trichostongylus* are reported in literature (von Sperling *et al.*, 2003; Shuval *et al.*, 1986; Sengupta *et al.*, 2011; Verbyla *et al.*, 2016; Ben Ayed *et al.*, 2009; Konaté *et al.*, 2013). *Ascaris* is the most abundant specie in low and middle income countries, appearing in large numbers almost everywhere. Most of the helminthes species found in wastewater

in the form of eggs may infect humans via different routes as depicted in Figure 1.1(a). Infection may be direct through ingestion of the eggs, for example for *ascaris*, or the eggs may hatch into an infective filarian form and penetrate the skin such as in the case of hookworms. The eggs may infect human beings through ingestion of contaminated food (crops and meat) or exposure to polluted water and soil, faeces, wastewater and sludge (Jimenez-Cisneros, 2007). Raw vegetables, if not properly washed with clean and safe water may contain eggs of helminths. Risk factors include inadequate water treatment, use of contaminated water for drinking, cooking, irrigation and to wash food, undercooked food of animal origin, and walking barefoot. After entering the bloodstream, the eggs travel to the duodenum where they hatch into larvae then to the intestine where they turn into complete worms. Inside the human body, a female helminth can lay up to 27 million eggs, some of which are passed in excreta (Figure 1.1b), and the whole cycle repeats (Jimenez-Cisneros, 2007). For *ascaris*, fertile eggs are produced only when a person is infected by both male and female worms. Infection with only female worms produces unfertilized eggs which will not hatch into worms while infection with male worms alone will not result into any eggs. The eggs contained in sewage are transported via sewer networks to the treatment plant (Figure 1.1c) or remain on-site for non-sewered systems. If not properly contained and de-activated, the eggs may end up in the environment leading to new infections.

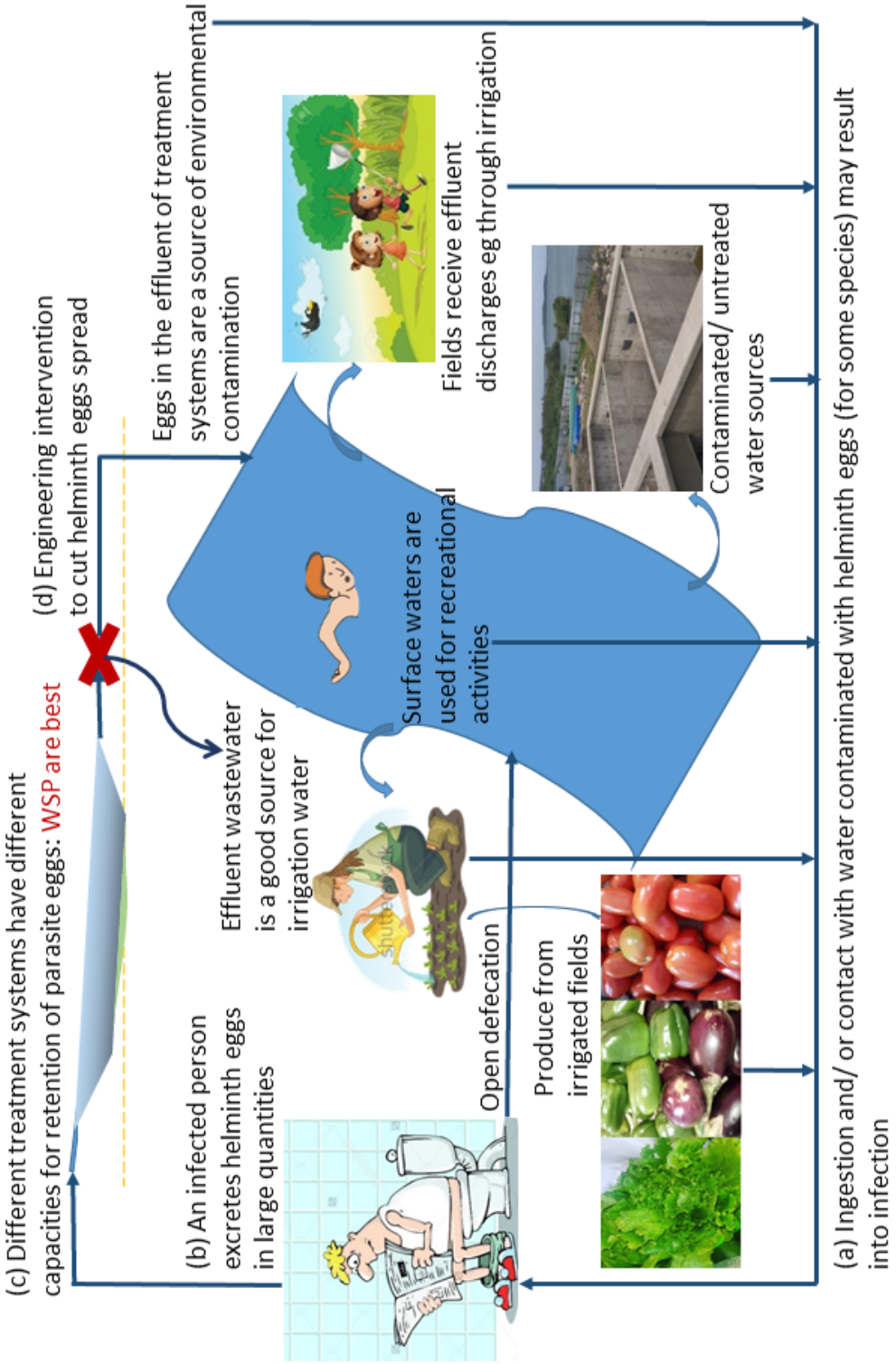

Figure 1.1: The interaction between helminth eggs, environment and humans.

1.1.2 Helminth eggs characteristics

Helminth eggs sizes range between 20 to 80 μm (examples in Figure 1.2), with specific gravity ranging between 1.056 to 1.3 (Jimenez-Cisneros, 2007; Sengupta *et al.*, 2011; Shuval *et al.*, 1986; David and Lindquist, 1982). Different egg types may have similar characteristics such as specific gravity and size (David and Lindquist, 1982). Although *taenia* and *physaloptera* are the smallest in terms of size, they are the heaviest (David and Lindquist, 1982). Most of the eggs are colored, except for *physaloptera* eggs which are colorless and therefore hard to identify (David and Lindquist, 1982). *Ascaris* eggs which vary in shapes tend to be spherical to oval, and are sticky. They are covered with layers which make them resistant to desiccation and therefore difficult to destroy. However, certain types of soil fungi and chemicals can penetrate and decompose ascaris eggs (Kunert, 1992; Keffala *et al.*, 2013) although in some instances the eggs shells were observed to remain intact (Kunert, 1992).

1.2 Helminths eggs removal from wastewater

Helminths infective agents are the eggs, because the worm cannot survive outside the host (Jimenez-Cisneros, 2007). Removal of the eggs (Figure 1.1d), and complete deactivation are among the best strategies for eliminating risk of developing these diseases (Jimenez-Cisneros, 2007). Although helminths are not microbes in nature, their eggs (ova) which are the infective agents are microscopic. The size of the helminth eggs falls within the range of suspended particles in wastewater hence they form a portion of suspended solids concentration, with high correlation established between helminths ova and suspended solids in wastewater (Jimenez-Cisneros, 2007; Chavez *et al.*, 2004; Shuval *et al.*, 1986). Therefore, methods used for removal of suspended solids such as sedimentation, filtration,

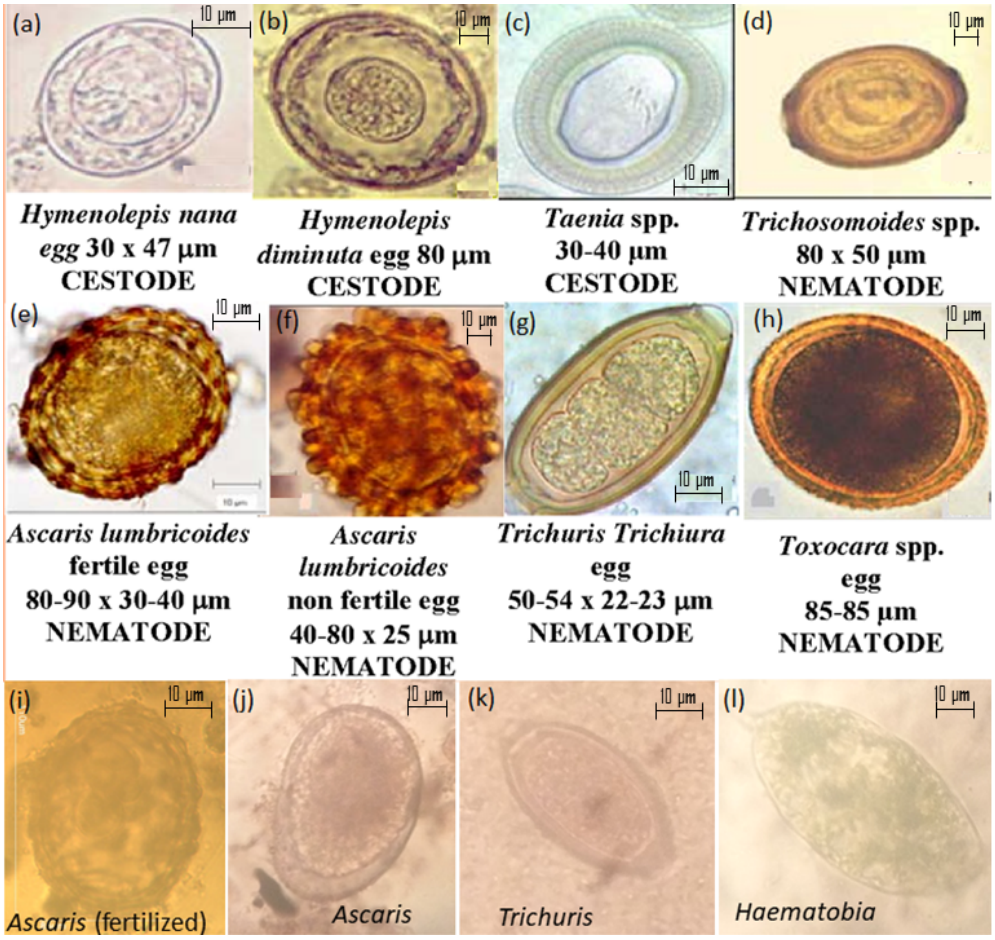

Figure 1.2: Helminth eggs observed in wastewater and sludge, extract from Jimenez-Cisneros (2007). The lower line (Plates i-l) are eggs recovered in our analysis.

adhesion and coagulation, are also employed in the removal of helminth eggs (Jimenez-Cisneros, 2007; Chavez *et al.*, 2004; Keraita *et al.*, 2008a; Stott *et al.*, 2003; Sengupta *et al.*, 2011). In waste stabilization ponds (WSP), the primary mode of helminths eggs' removal is the sedimentation process (Ayres *et al.*, 1991).

Different technologies for wastewater treatment including WSP, extended aeration, constructed wetlands, coagulation-flocculation, filters, Up-flow Anaerobic Sludge Blanket reactors and activated sludge systems have shown high removal efficiencies greater 97% (Keller, 2004; Tyagi *et al.*, 2008; Keraita *et al.*, 2008b; Jimenez-Cisneros, 2007; Stott *et al.*, 2003; Tyagi *et al.*, 2010; Keraita *et al.*, 2008a). In addition, reservoirs operated as batch systems with retention times of more than twenty days can remove HE (Jimenez-Cisneros, 2007). Simple dug-out ponds used for vegetable irrigation in Ghana were able to completely remove HE after three days by sedimentation (Keraita *et al.*, 2008a). Coagulation-flocculation is especially recommended when water is to be used for irrigation as it preserves nutrients while removing HE (Jimenez-Cisneros, 2007). Performance of constructed wetlands (CW) depend largely on bed length, with a bed length of 100 m providing complete HE removal (Reinoso *et al.*, 2008; Stott *et al.*, 2003).

1.2.1 Sedimentation in WSP

WSP are biological systems used widely for wastewater treatment due to their efficiency and relatively low operation and maintenance cost. A WSP system is normally made of three sets of ponds in series, each with a particular function and design. The first pond which is anaerobic ponds serves to reduce BOD through sedimentation of particulate matter in wastewater. Second pond which is known as facultative ponds is for reduction of BOD through the biological action of algae and the last pond which is maturation pond (also known as polishing ponds) is for removal of micro-organisms (bacteria etc) through natural die-off, predation

and UV light. For all of these pond types, it is recommended to have smaller ponds in parallel rather than having one very large pond as the flow conditions in a series of smaller ponds are more closer to a plug flow reactor (Mara, 2004). When an anaerobic pond precedes a facultative pond it is known as a secondary facultative pond, otherwise, if the first pond in the system is a facultative pond, then it is known as a primary facultative pond. Primary facultative ponds are very common, usually employed in the treatment of municipal wastewater when the incoming discharge is of medium strength. Systems with primary facultative ponds alone- excluding the other two pond units, are commonly used for treatment of municipal wastewater all over the world.

Although most of the waste stabilization is done by naturally occurring micro-organisms, sedimentation also plays a big role in reduction and removal of pollutants in all its units. Sedimentation is responsible for removal of about 60 % of BOD, inorganic pollutants and parasite eggs and cysts found in water. Also, sedimentation is the major removal mechanism for antibiotics as well as nutrients in primary ponds (Møller *et al.*, 2016; Mayo and Abbas, 2014). However, sedimentation is not designed in the traditional way (i.e by considering particle characteristics, normally the settling rate of the smallest particle expected to settle in the system) in these ponds despite common knowledge that the first pond is for sedimentation. Also, a large number of systems consist of primary facultative ponds within which the processes that normally take place in anaerobic and facultative ponds occur simultaneously. In this case sedimentation of helminth eggs is also expected to occur in the primary facultative pond. These ponds are shallower than anaerobic pond, and favour growth of algae which have a potential of forming buoyant flocs with wastewater particles, as well as introduces other particles in wastewater. Previous research has shown that, presence of other particles in water influences sedimentation of helminth eggs (Sengupta *et al.*, 2012a,b; Chavez *et al.*, 2004), although it is not clear through what mechanism.

Wastewater may be regarded as a biphasic medium containing pollutants (solids) as particles with sizes ranging between 0.001 and 1000 microns (Wu *et al.*, 2010; Azema *et al.*, 2002) and water. The reported values of specific gravity of wastewater particles have great variations, ranging between 1.2 and 1.3 for wastewater particles (Wu *et al.*, 2010; Levine *et al.*, 2017) and between 1.02 and 1.07 for activated sludge flocs (Sears *et al.*, 2006).

Due to general lack of sedimentation studies in wastewater treatment, most of studies reviewed here are for natural water bodies, water treatment sedimentation tanks and storm water detention ponds. Different particle sizes have different settling velocities and shear resistance, both of which affect their sedimentation (Ockenden, 1993; Lorang *et al.*, 2003) and resuspension (Lorang *et al.*, 2003). Particles have the ability to flocculate and form larger flocs under certain conditions, with subsequent higher settling velocities (Ockenden, 1993). Wastewater particle characteristics have impact on pollutants transport and removal (Semadeni-Davies, 2009), as different pollutants tend to be associated with particles of different sizes (Semadeni-Davies, 2009; Poister and DeGuelle, 2005; Levine *et al.*, 1991). Also, sewage with same suspended solids concentration but different particle size distribution have different removal efficiencies (Lawler *et al.*, 1980). Removal efficiency decreases with decrease in particle size as small particles are harder to settle and are therefore distributed throughout the supernatant (Al-Sammarraee *et al.*, 2009). Also, smaller particles tend to co-settle with large particle (Wu *et al.*, 2010; Azema *et al.*, 2002), as well as form flocs with bigger diameters (Semadeni-Davies, 2009; Azema *et al.*, 2002) resulting into particle size modification. Biological and physical processes such as turbulence may result into smaller particles that are harder to settle (Al-Sammarraee *et al.*, 2009; Levine *et al.*, 2017). Research show that, changing PSD can be used to optimize sediment ponds to have effective pond sizes (Semadeni-Davies, 2009; Wu *et al.*, 2010; Levine *et al.*, 1991), instead

of increasing HRT which may not result into any significant improvement (Wu *et al.*, 2010).

Flow patterns in ponds influence particle size distribution of the deposited materials (Krishnappan *et al.*, 1999; Dufresne *et al.*, 2010). Over long periods, this will result into particles of certain size to be highly concentrated in some areas of the pond and be scarce in others (Dominic and Aris, 2016).

In this research, hydraulic characteristic of the pond and particle size distribution are used to study the sedimentation process. Extensive research has been done on WSP but very few have actually looked on the sedimentation process inside WSP and how it affects the treatment process. It is anticipated that improving sedimentation in WSP maybe a way of reducing their land requirement, which is a major disadvantage of this system.

1.2.2 Efficiency of WSP in helminths eggs removal

WSP systems consisting of anaerobic, facultative and maturation ponds in series are generally able to remove HE by up to 100 % (Madera *et al.*, 2002; Stott *et al.*, 2003; Tyagi *et al.*, 2010, 2008). Also, WSP can successfully be used as secondary treatment to remove HE from other treatment systems such as Up-flow anaerobic sludge blanket (UASB) (von Sperling *et al.*, 2003; Tyagi *et al.*, 2010). If wastewater is to be used for irrigation, and if other interventions are used in combination with WSP, Mara and Sleigh (2010) demonstrated that only a 1 day HRT in anaerobic pond and 4 days HRT in facultative pond are enough to reduce HE concentration to desired concentrations in hyperendemic areas (areas with more than 100 eggs/L). Studies have shown that, anaerobic ponds removes HE by up to 95 % while facultative ponds remove by up to 99.9 % (Stott *et al.*,

2003). HE removal in tertiary maturation ponds is poor probably due to very low HE concentrations (Stott *et al.*, 2003).

Primary helminths' eggs removal in WSP is via sedimentation facilitated by the long HRT (Ayres *et al.*, 1991; Sengupta *et al.*, 2011; Stott *et al.*, 2003; von Sperling *et al.*, 2003), with a HRT of about 20 days providing complete removal (Ayres *et al.*, 1991; Shanthala *et al.*, 2007; Ayres *et al.*, 1992). Ayres *et al.* (1992) established a widely used mathematical model for prediction of nematode eggs removal from WSP (equation 1.1), with HRT as the main factor affecting removal efficiency (R). There were no significant difference in prediction equations for the different pond types so this equation was established for both (anaerobic, facultative and maturation ponds), and single ponds with 100 % removal efficiency were ignored (Ayres *et al.*, 1992). The equation is widely used for design and performance evaluation of WSP, giving results both in agreement (von Sperling *et al.*, 2003) and not in agreement (Verbyla *et al.*, 2013; von Sperling *et al.*, 2003; Verbyla *et al.*, 2016; Ben Ayed *et al.*, 2009; Reinoso *et al.*, 2008; Konaté *et al.*, 2013) with existing situations. The Ayres equation for removal efficiency (R) is given below:

$$R = 100[1–0.14e^{-0.38HRT}] \tag{1.1}$$

Where R is the removal efficiency of the system in percentage and HRT is the theoretical hydraulic retention time. However, other researches, such as Verbyla *et al.* (2013), have suggested using the actual HRT of the system, for example those obtained through tracer experiments due to possibility of hydraulic short-circuiting in the system.

However, studies show that HRT is not the only factor affecting sedimentation as given the same HRT, anaerobic, facultative and maturation ponds gave different removal efficiencies (Ayres *et al.*, 1991; Stott *et al.*, 2003) with best performance

given by facultative ponds and worst from maturation ponds (Stott *et al.*, 2003). Although Stott *et al.* (2003) speculated that fewer HE may be harder to remove, and that at lower concentrations other mechanisms, apart from sedimentation become more important, von Sperling *et al.* (2003) observed a 100 % removal from maturation demonstration scale ponds loaded with as low as 4 eggs/L. Also, given the same HRT, Shanthala *et al.* (2007) reported a better efficiency in batch system compared to continuous flow reactor, but Reinoso *et al.* (2008) sampled from a continuous fed system and obtained efficiency of more than 99.99 % HE removal. Perhaps this is a result of low discharge and long HRT (75.9 days) in the ponds sampled by Reinoso *et al.* (2008). Interestingly, despite the extremely long retention time of more than the recommended 20 days in facultative pond, Reinoso *et al.* (2008) noted only a 92.46 % reduction in HE concentration. This could still be a result of a continuous fed system, a more understanding on the effect of adding fresh eggs to removal of HE will be useful.

Hydraulic efficiency of WSP plays a major role in HE removal (Verbyla *et al.*, 2013). In developing countries where short circuiting and dead spaces in ponds are common, research on quantification of their impact on HE removal is needed. Changes in HRT of pond through short-circuiting, sludge accumulation and water turbulence may affect removal efficiency (Konaté *et al.*, 2013). Also, the implication of varying settling velocities, and fluctuating flow velocities brought about by turbulence events, to the pond retention time and hence HE removal is still missing. It is known that temperature, buoyant sludge particles and turbulence events may affect sedimentation process and could affect the removal efficiency (Mara, 2004; Sengupta *et al.*, 2011; Verbyla *et al.*, 2013), although von Sperling *et al.* (2003) sampled from ponds where temperature ranged between 18 °C to 29 °C and got results that were in agreement with the predictions from Ayres equation (equation 1.1).

The different egg types exhibit varying settling velocities between 0.22 to 1.53

m/h (Jimenez-Cisneros, 2007; Sengupta *et al.*, 2011; Ayres *et al.*, 1996; Shuval *et al.*, 1986; Ayres *et al.*, 1991), and these velocities influence their sedimentation (Konaté *et al.*, 2013; Sengupta *et al.*, 2011). The settling velocities are influenced by presence of wastewater particles (Sengupta *et al.*, 2011, 2012a). How the different egg types interact with particles of different nature, (i.e. organic and inorganic) and sizes is still not clear as both reduced and increased velocities have been observed (Sengupta *et al.*, 2011, 2012a). Chavez *et al.* (2004); Sengupta *et al.* (2012a) related HE removal to removal of fine particles. Also, the eggs do not possess any charge (they are neutral) which is important for flocculation, therefore the observed impact of coagulant addition (Chavez *et al.*, 2004; Sengupta *et al.*, 2012b) must be related to aggregation with other neutral particles.

1.2.3 Helminths Eggs in Sludge

In sludge, HE concentration follows the pattern of sludge accumulation, with higher sludge depth having more HE eggs (von Sperling *et al.*, 2003; Nelson *et al.*, 2004). The deposition patterns are not uniform and they vary from pond to pond, indicating that there are other external factors which are pond specific influencing their deposition. For example, Konaté *et al.* (2013) found most eggs in facultative pond were near the inlet and outlet while Nelson *et al.* (2004) found that eggs concentration decreased towards the outlet with very few eggs in the middle of a facultative pond. For aerobic ponds Nelson *et al.* (2004) found that eggs were deposited equally throughout the pond while Konaté *et al.* (2013) found maximum concentration near the centre. Also, Konaté *et al.* (2013) found eggs only at the middle of the maturation pond. Although the concentration of HE in sludge tend to decrease along the pond length (von Sperling *et al.*, 2003; Konaté *et al.*, 2013), there is no particular trend in the type of eggs (von Sperling *et al.*, 2003; Konaté *et al.*, 2013). The influence of time is not clear as the concentrations

of eggs have been observed to be both constant, increase and decrease with sludge age for different ponds (Nelson *et al.*, 2004).

1.2.4 Detection and enumeration of helminth eggs in water

Direct observation of helminth eggs from wastewater, sludge, soil and stool samples is hard due to their very low numbers. Therefore, methods used for their detection normally involve concentrating them through sedimentation and flotation of other materials. For sedimentation, a solution with a lower specific gravity than the eggs is used, and the sedimentation processes is speeded up by centrifugation. Lighter fatty and fecal materials are floated and extracted by ethyl acetate. Also, formalin may be used to fix the eggs, make them non-infectious as well as preserve their shapes.

Several methods for enumeration of HE eggs exist. As already stated, the key features of almost all of these methods are dissociation from organic matter, flotation, sedimentation, centrifugation (concentration), filtration and microscopic examination (Maya *et al.*, 2006; Ayres *et al.*, 1991; Moodley *et al.*, 2008). These methods perform differently interms of sensitivity, discrimination coefficients, precision, recovery effciency, and cost. Forexample, in comparison with Extrabes, modified Janeckso-Urbanyi and Leeds II method, Ayres *et al.* (1991) recommended the Bailenger method as the most appropriate for enumeration of both large and low numbers of HE in water, however, for low egg counts samples are increased to 10L. In another comparison that involved U.S.EPA, membrane-filter, Leeds I, and Faust methods to enumerate helminth eggs in both tap and wastewater in Mexico (Maya *et al.*, 2006), the U.S.EPA was selected as the best method. Furthermore, factors such as cost, availability and accessibility of chemicals, expertise

and equipments may result into modification of the standard methods to fit local conditions. The modified Bailenger method, outlined in Ayres *et al.* (1991) and summarized in Section 1.2.5, which requires 5L sample, was selected as the best method in terms of sensitivity, discrimination coefficients, precision, recovery efficiency, and cost.

1.2.5 The modified Bailenger and formol-ether concentration methods

Considering the availability of equipment and chemicals, as well the recovery efficiency discussed above, this research used the Bailenger and the formol-ether concentration methods to recover helminth eggs from wastewater samples. In the Bailenger method, a known volume of sample; 1L for raw wastewater and 10L for treated wastewater is used for analysis. Using an open-topped and straight-sided container, the sample is allowed to sediment for 1 to 2 hours, after which 90% of the supernatant is removed preferably by using a suction pump or siphon. The sediments are transferred into centrifuge tube(s), the container is rinsed with detergent solution and the rinsing is added into the centrifuge tube(s). The samples in the centrifuge tube(s) are then centrifuged at 1000 g for 15 minutes, after which the supernant is poured away, and if more than one centrifuge was used, the samples are combined into one centrifuge tube. The other centrifuge tubes are rinsed with detergent solution, the rinsing are added to the sample and centrifuged again at 1000 g for 15 minutes then the supernatant is poured out. The pellet at the bottom of the tube is then suspended in an equal volume of acetoacetic buffer, pH 4.5. Further two volumes of ethyl acetate or ether are added to the sample and the solution is mixed thoroughly in a vortex mixer, or shaken by hand. The sample is again centrifuged at 1000 g for 15 minutes whereby, it will now separate into three layers; non-fatty, heavier debris, including helminth

eggs, at the bottom layer, the clear buffer in the middle and the fatty and other light materials including fats at the top. The volume of the pellet at the bottom, which also contains helminth eggs is recorded before all the supernatant is poured out preferably in one smooth motion. Add five times the volume of Zinc Sulfate as that of the pellet, record the volume of the mixture (X ml), and then mix well, preferably using a vortex mixer, to produce a uniformly mixed mixture. An aliquot is quickly taken from the sample using a pasteur pipette and transferred to a McMaster slide where its left to stand on a flat surface for 5 minutes to allow the eggs to float to the surface before examination. The McMaster slide with the aliquot is then placed on the microscope stage and examined under 10× or 40× magnification. All the eggs seen within the grid in both chambers of the McMaster slide are counted. The number of eggs per liter is counted using equation 1.2.

$$N = \frac{AX}{PV} \tag{1.2}$$

Where N is the number of eggs per litre of sample, A is the number of eggs counted in the McMaster slide or the mean of counts from two or three slides, X is the volume of the final product (ml), P is the volume of the McMaster slide (0.3 ml for double chamber McMster slides) and V is the original sample volume (litres).

In the formol-ether method, similar procedures were followed for the first few steps until we had combined pellets of each wastewater sample in a single centrifuge tube. Then 10 mL of 10% formalin were added to the sediment, mixed well and left to stand for 5 minutes to effect fixation. About 1 to 2 mL of ethyl acetate were added and the mixture was shaken vigorously to homogenise it before centrifuging at 1500 rpm for 10 minutes. In thiscase, four layers resulted as follows; a top layer of ethyl acetate, plug of debris, layer of formalin and sediment at the bottom. The top three layers were poured out in one swift motion, leaving only the sediments

behind. The sediments were then mixed with the small amount of remaining fluid, one drop to a drop of saline and iodine were transferred on a glass slide, and covered with coverslip ready for microscopic examination for the presence of parasitic forms.

1.3 Statement of the problem

WSPs are generally regarded as the best low-technology and low-energy method for decreasing the helminthic load of contaminated water in low and middle income countries, through the sedimentation process. Despite the presence of a few basic models, very little is understood on the dynamics of the removal process inside the pond, since the ponds are normally designed as lumped systems, only considering the concentration of pollutants at the inlet and outlet. Moreover, there is usually little or no consideration of the sedimentation process in the design of WSP, but rather a provisional total retention time of 20 days in the system has been shown to achieve complete removal of helminth eggs. However, sedimentation in WSP is responsible for removal of a large number of pollutants such as BOD, nutrients, heavy metals and helminth eggs. It is therefore thought that improving the sedimentation process in WSP will result into better treatment efficiency, especially for helminth eggs, as well as reduce the required surface area for their construction, which is their main disadvantage. This research studies the sedimentation process in an operating primary facultative pond in Buguruni, Tanzania, to establish factors influencing the sedimentation process and hence sludge accumulation. Also, the influence of wastewater particles in the sedimentation of helminth eggs is explored to gain more understanding on helminth eggs removal in WSP and how to improve it.

1.4 Research Objectives

1.4.1 Main objective

The fundamental objective of this study is to explore the sedimentation process in waste stabilization ponds (WSP), so as to develop a deeper understanding of how it affects the sedimentation of helminths eggs, in order to improve and design procedures for their removal.

1.4.2 Specific objectives

(i) Characterize particle size of the incoming discharge and at different locations inside the pond;

(ii) Calibration of a sedimentation model to identify key factors in particle movement and settlement, and hence sludge accumulation patterns in the pond;

(iii) Development of mechanistic model for particles sedimentation in the pond and application to identification of areas with high probability of containing helminth eggs.

1.5 Research questions

These are related to key issues in sedimentation in WSP that would need better understanding.

(i) What are the physical characteristics of wastewater particles that are found in waste stabilization ponds?

(ii) Are there any spatial and/or temporal variations in these characteristics?

(iii) What fraction of particles falls within size class of helminth eggs?

(iv) What factors govern particles movement and deposition patterns?

(v) How do the ponds perform under varying influent discharge and concentration?

(vi) Is it possible to establish clear and distinct flow path-lines in the pond? What are their characteristic patterns?

(vii) Is there a contribution from environmental factors such as wind, rainfall run-off or any other site specific factors to flow path-lines and/ deposition patterns?

(viii) Can other particle characteristic data, such as particle size be used to back estimate particle densities which are onerous to obtain?

1.6 Study area

The study was conducted in Dar es Salaam city in Tanzania, which is the industrial, educational, and cultural centre of the nation, hosting about 8% of the nation's population. Dar es Salaam has an equatorial climate which is hot and humid, influenced by the North-East monsoon winds from October to March and the South-East monsoon winds from May to September. The area has two seasons with regard to precipitation, wet and dry. The wet season is further divided into three rainy sub-seasons, the Vuli (short) rains in late October-late December, Masika (Long) rains in mid-March to mid-May and an intermediate season in January-February receiving reduced rainfall amounts compared to Vuli and Masika seasons. The short rains season receives between 75 -100 mm of

rainfall per month which increases to 150-300 mm per month during the long rains. The average annual rainfall is about 1000 mm, with highest rainfall amounts occurring in April and December, but with very random rainy days. The remaining period which is from mid-May to October is normally dry. On the other

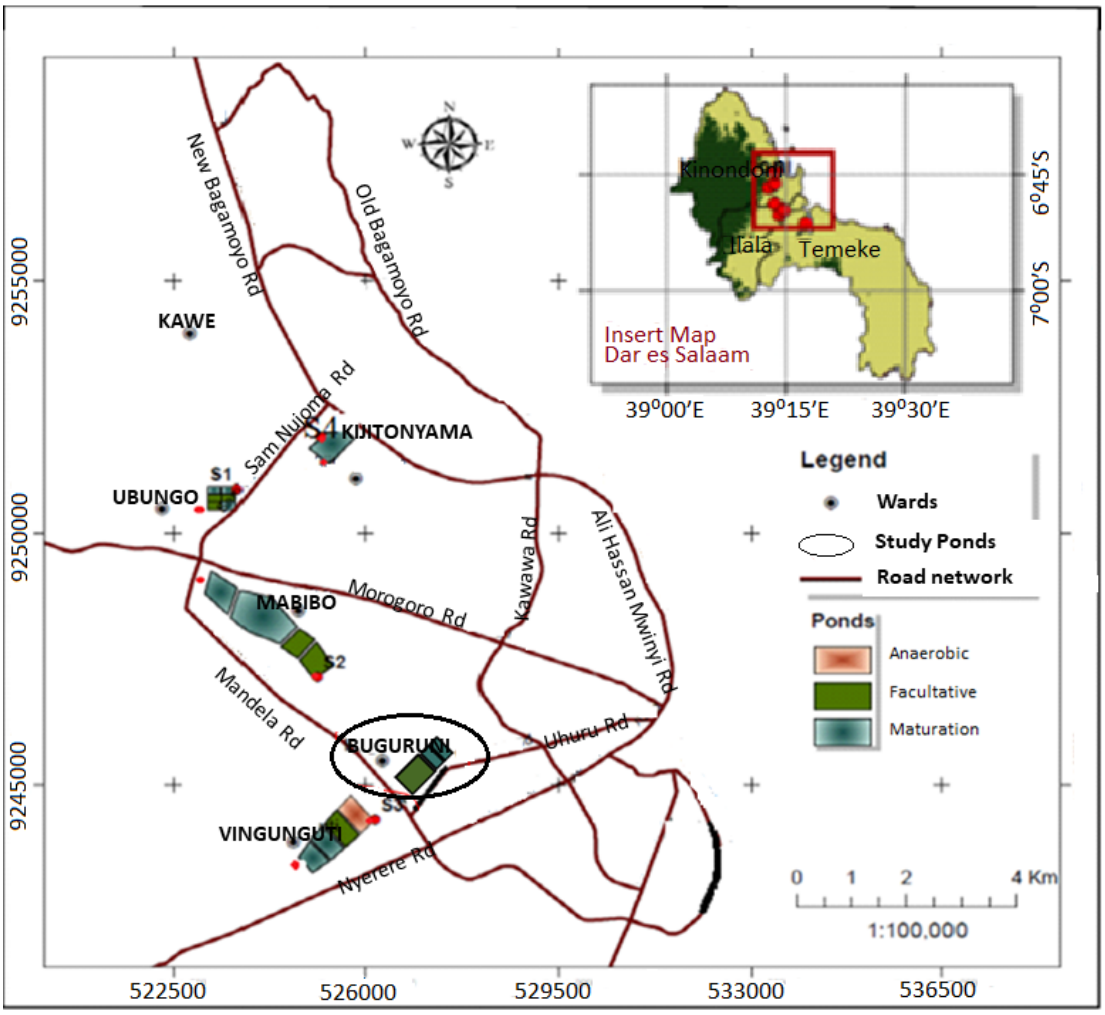

Figure 1.3: Location of the Buguruni WSP from the inset map of Dar es Salaam city (modified from Kihampa (2013))

hand, the study for the Tanzania coastal region that covered 30 years between 1977 and 2006, showed that the region has also two wind seasons according to the wind orientation Mahongo *et al.* (2012). The first season lasts from November through to March during which period wind blows mainly in the North-East

direction (45°), with average speed of 4.5 ms^{-1}. The second season is from April to October during which wind blows in the South-West direction (225°) in the morning and South-East direction (135°) in the afternoon, with an average speed of 2.5 ms^{-1}. Lowest winds are recorded in the afternoons of March to April, a period that coincides with high rainfalls (Ndetto and Matzarakis, 2013).

The annual average temperature is around 30 °C. Highest temperatures are recorded in January and February with an average maximum of 32.5 °C and average minimum of 24 °C. The lowest temperature are in July with an average maximum temperature of 29.5 °C and an average minimum of 19 °C. The diurnal change in temperature is around 9 °C.

The study pond system, Buguruni WSP (Figure 1.3, circled) is among the nine (9) waste stabilization pond systems servicing the city of Dar es Salaam, Tanzania. The pond system, consisting of one facultative pond and two maturation ponds, receives domestic waste water from the nearby areas of Buguruni and Tazara. The design discharge is 0.0077 m^3/s, but random measurement of discharge during the study period between December 2016 and December 2018 showed discharge ranging between 0.0044 m^3/s and 0.0085 m^3/s. The inlet is an open channel with a width of 60 cm fitted with a triangular V-notch weir with an angle of 90°, with a maximum capacity of 0.06 m^3/s, equivalent to a head of 30 cm which is the maximum height of the weir. About 5 random discharge measurements were done during the different data collection campaigns. The outlet is a 60 cm rectangular overflow weir.

The pond structure has a surface area of 1.62 ha and a depth of 1.2 m. The inlet side length is shorter (176 m) while the outlet length is longer (183 m). Wastewater flows by gravity from the inlet to the outlet. The pond is lined by concrete on the sides while the bottom consist of compacted clay, with a slope of 3 to 1.

1.7 Significance of the study

Tanzania is predicted to be among the water stressed countries by 2025 (DFID, 2008). Increased population and increased abstraction from the source which may soon become exhausted highlights the need for efficient use of the available water and conservation of water sources. In recent years, reuse of wastewater effluents especially for urban agriculture has gained popularity. However, wastewater contains pathogens, which includes helminth eggs in low and middle income countries, which cause helminthiasis, and therefore development of proper ways of managing and/or eliminating them is crucial. The research contributes to the available literature on helminths eggs removal and potential for reuse of wastewater for irrigation. The research is relevant to the community at large as it has a contribution to the efforts to improve sanitation through proper treatment of wastewater, and combat the spread of helminthiasis as well as enable re-use of wastewater in agriculture to generate income and reduce stress on fresh water sources. Research shows that, low levels of socio-economic life due to unemployment and low incomes are associated with poor housing and lack of access to adequate sanitary services and other social amenities, and prevalence of helminths infections. The problem is expected to worsen due to rapid urbanisation resulting from rural to urban migration. Also, in the Sustainable Development Goals (SDGs), ending the epidemics of neglected tropical diseases (NTDs), helminths being among them, by 2030 is among the recognized targets. The research is also in line with various programmes such as NTDCP (NTD Control Programme), for helminth elimination and control in Tanzania. Recognizing the severe health and economic impact of NTDs, the Government of Tanzania agreed to recognize NTDs in the new healthy policy and apportion a budget to combat them beginning in the 2019/2020 budget year (Makoye, 2018).

1.8 Contribution to Knowledge and Impact

The results of this research contribute towards efforts to improve public health as generated data on the parasitic species present, as well as provide indication of the incidence of infection in communities serviced by the Buguruni WSP in Dar es Salaam, Tanzania. The research is in line with the global target to eliminate morbidity due to soil-transmitted helminthiases (about 135,000 deaths/ year (WHO, 2002) by 2020. Although de-worming is the most used technique to reduce/ eliminate helminthic load, it is known and appreciated that it is only a short term solution and a long term solution may be obtained by treatment of excreta and wastewater (Mara and Pearson, 1999; Mara, 2004; WHO, 2002; Bethony *et al.*, 2006). The Neglected Tropical Diseases Support Center (NTD-ConnectOR) identifies the evaluation of the impact of WASH and Vector Control interventions as among the country operational research priorities for Tanzania. This research points out WSPs as concentration vessels for helminth eggs offering a cost-effective option for helminths control, and therefore should be included in the evaluation. Also, the increased demand for wastewater reuse and tighter effluent discharge limits call for design of better performing wastewater treatment systems. Thus, this research has contributed to understanding the sedimentation of helminth eggs inside the pond and factors affecting their settling. This information can be utilized to design the ponds to meet the required effluent characteristic for reuse. For scientists, this study advanced the knowledge of helminth eggs sedimentation, particularly the effect of the presence of other particles.

1.9 Thesis layout

This thesis is organised as follows;

Chapter 1: Introduction (Literature review, study area, problem identification, and research questions). This chapter introduces sedimentation process in WSP and is role in pollutants removal. Focus is then shifted to helminth eggs, their transmission and infection routes. This chapter gives an overview of the objectives of this research. It gives a brief background of the problem, scientific basis of this research and the research questions being addressed.

Chapter 2: Investigating particle size dynamics in WSP. This chapter studies particle size distribution and related variability inside the pond. This data is very important and forms the basis of this study as particle characteristics will be used to possibly correlate and represent different pollutants present in wastewater.

Chapter 3: Pond hydraulics and hydraulic sorting in WSP. In this chapter, a 3D hydraulic model is set on Delft3D to derive the flow conditions inside the pond. To achieve the objectives of this research, flow velocity vectors, travel path lines and travel time data to the different nodes defined in data collection plan are required and will be obtained through the model developed here. This chapter utilizes data from chapters 2 and 3 to establish the relationship between particle size and hydraulic characteristics of the pond. Then, derived probability distribution approach is used to reconstruct density of particles at different locations in the pond.

Chapter 4: Model for estimation of particle densities. Since the process for determination of wastewater particle densities is onerous, there is a need to develop methods that can estimate the particle densities from other characteristics that are readily obtainable, for-example particle diameters. Therefore in this chapter a model for back estimation of particle densities is developed and used to identify locations in the pond whose sludge has high probability of containing helminth eggs.

Chapter 5: The role of environmental variables in waste stabilization ponds' morphodynamics. In this chapter, a sedimentation model is set-up in Delft3D software incorporating different environmental variables such as wind, increased discharge and suspended solids concentration which may occur during the rainy season. The model is calibrated by comparing the resulted sludge depth to sludge depth measured in the field.

Chapter 6: Mechanistic model for particle sedimentation: application to helminth eggs in wastewater ponds. In this chapter, a simple model that accounts for spatial stochasticity of the distribution and deposition of particles depending on the incoming PSD and flow conditions in the pond is developed. Areas where helminth eggs are deposited are obtained by comparing the size of helminth eggs to mean size of deposited particles at different locations. Data collection protocol for helminth eggs is also undertaken in these areas to confirm the presence of helminth eggs.

Chapter 7: Conclusion and outlook. This chapter sums up the research by looking at the research questions raised at the introduction and how they were addressed or answered. Also, avenues for future research along the same lines are presented.

Chapter 2

Investigating particle size dynamics in WSP

The material presented in this chapter appears in:
Izdori, F., Semiao, A.J.C., Perona, P. Empirical characterization of particle size distribution spatial dynamics for helminth eggs detection in waste stabilization ponds (WSP). *Water 2018*, 10(2), 138.

2.1 Introduction

Wastewater contains a mixture of particles with sizes ranging from 0.001 to more than 1000 microns. Among them are parasites and parasite eggs. Parasites in wastewater are a public health concern (Mara and Pearson, 1999; Lloyd and Frederick, 2000), since they cause diseases such as helminthiasis, a serious health condition affecting nearly a quarter of the world's population (Hotez *et al.*, 2008a). Helminthiasis caused by ascaris, trichiura, and taenia, for example, result in poor health and retarded growth in school children, epileptic seizures,

maternal death, and lower efficacy of tuberculosis (TB) vaccination, leading to the placental transfer of TB by pregnant women (Hotez *et al.*, 2008a; Mwanjali *et al.*, 2013). The major infection mechanisms of these parasites are via their eggs found abundantly in wastewater in developing countries and food crops irrigated with contaminated water (Jimenez-Cisneros, 2007). The development of efficient wastewater treatment systems that are able to remove these eggs completely is crucial to controlling their spread. Helminths eggs' sizes in wastewater range between 20 and 80μm, and their specific gravity ranges between 1.056 and 1.3 (Jimenez-Cisneros, 2007; David and Lindquist, 1982; Shuval *et al.*, 1986; Sengupta *et al.*, 2011). Complete removal of the eggs is by sedimentation in waste stabilization ponds (WSP) (Sengupta *et al.*, 2011; Ayres *et al.*, 1991; Stott *et al.*, 2003; von Sperling *et al.*, 2003) when a hydraulic retention time (HRT) of about 20 days has been achieved (Ayres *et al.*, 1991, 1992; Shanthala *et al.*, 2007). However, actual HRT in WSP is normally lower than the designed HRT, thereby compromising their performance (Alvarado *et al.*, 2012b; Verbyla *et al.*, 2016, 2013), including the removal of helminth eggs (Verbyla *et al.*, 2013). Moreover, WSP are not designed for sedimentation, despite the universal acceptance that this is the main mechanism for helminth eggs removal, as well as a large percent of other pollutants. Also, primary facultative ponds are designed to receive particle-free raw wastewater (suspended solids concentrations less than 300 mg/L); therefore, the processes that normally take place in anaerobic and facultative ponds occur simultaneously here. In this case sedimentation of helminth eggs is also expected to occur in the primary facultative pond. These ponds are shallower than anaerobic ponds and contain algae that introduce other particles into the wastewater. Furthermore, literature shows that particles in wastewater can interact with parasite eggs and cysts and affect their sedimentation (Sengupta *et al.*, 2011; Jimenez and Alma, 2002; Kihampa, 2013; Sengupta *et al.*, 2012a,b). How these other particles influence the settling characteristics of eggs is still not clear, as both reduced and increased settling velocities in wastewater have been

observed (Sengupta *et al.*, 2011, 2012a). As a consequence of the lack of design for sedimentation and a fundamental understanding of the interactions between particles and helminth eggs in WSP, helminth eggs have been found in WSP effluents, even for ones with a HRT higher than 20 days, causing contamination and disease outbreaks. Since sedimentation leads to the modification of particle size distribution (PSD), studies on how particles sizes vary inside the pond may be used to study the sedimentation process in the ponds. This study explores particle size variations inside a facultative pond of an operating WSP to study influence of the sedimentation process influences particle size. The Buguruni WSP receives a daily inflow of around 691 m^3. After treatment, the effluent is discharged into Msimbazi River, which is highly encroached with people building houses and gardening very close to it. The river water is used for irrigation of vegetables along its course, and therefore the removal of helminth eggs and cysts is important to prevent their spread.

2.2 Materials and methods

The study was conducted in Buguruni pond, Dar es Salaam, Tanzania. The pond receives domestic waste water from the nearby areas of Buguruni and Tazara. The treatment system consists of one facultative pond and two maturation ponds, and sedimentation of helminth eggs is expected to occur mainly in the facultative pond. Water samples were collected from the facultative pond for both dry and wet periods to check if there are any seasonal variations. Using a 6.2 L van Dorn water sampler, shown in Figure 2.1a, with marks on the attached rope to show different depths, water samples were collected at nodes (Figure 2.2, circled numbers) from top, at depths of about 25cm below water surface and near the pond bottom. The pond dimensions are roughly 183 x 90 m^2 and therefore the cell size was chosen such that it was sufficient to capture the spatial characteristic

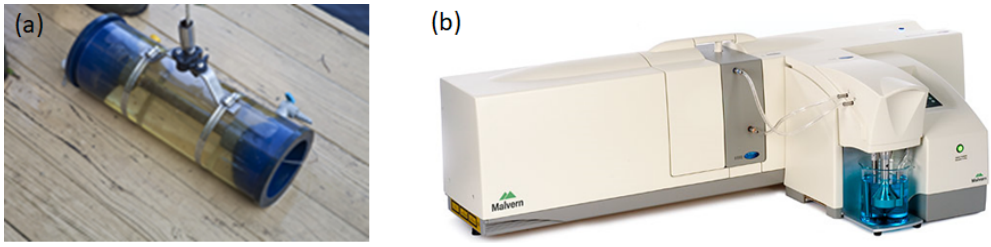

Figure 2.1: (a) The Van Dorn water sample used for sample collection at different depths in the pond and (b) Malvern Mastersizer 2000 particle size analyser.

without creating too many sampling points. A marked rope secured to the sides of the pond was used to mark the nodes, and navigation was done using a non-motorized boat. Immediately after collection, samples were taken to the Chemical and processing Engineering laboratory of the University of Dar es Salaam for particle size distribution analysis by the Malvern 2000 Mastersizer (Malvern Instruments, Malvern, UK), shown in Figure 2.1b. The Malvern Mastersizer 2000

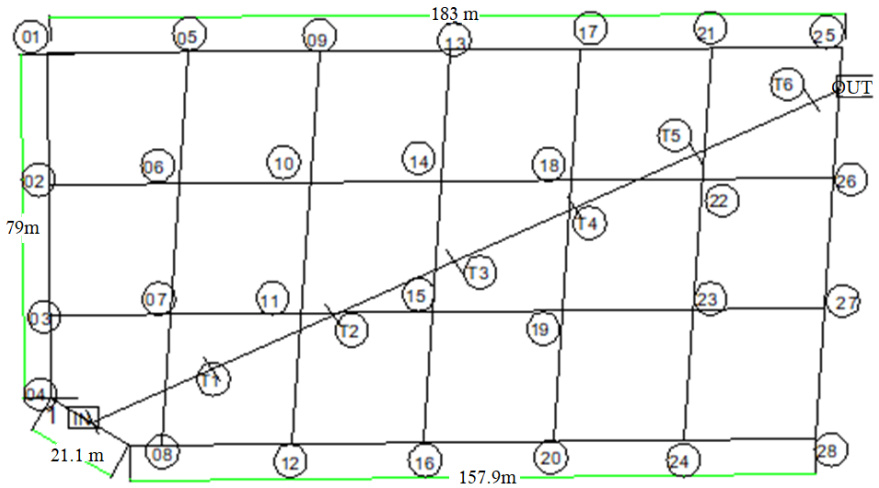

Figure 2.2: Sampling points for PSD analysis in the pond with node numbers given in circles.

predicts particle sizes based on how they scatter light as each size has its own unique scattering pattern. The Mastersizer captures the scattering pattern and then uses light scatter theories to calculate what particle size created them. There are two general light scatter theories; (i) the Fraunhofer and (ii) the Mie theories.

The Fraunhofer theory assumes scatter is produced by solid, opaque disc of known size, while the Mie theory assumes that the produced scatter is from spherical particles. The Fraunhofer has disadvantage that not many particles are disc shaped and opaque. The Mie theory, which is commonly used, requires that the user knows some particle characteristics such as refractive index and absorption. From the research by Sochan *et al.* (2014), the values of 1.0 and 1.52 for the absorption coefficient and refractive index, respectively, recommended for sewage and activated sludge suspensions were adopted. Both of the two light scatter theories are employed in particle size determination by the Malvern Mastersizer 2000 software.

2.3 Results and discussion

The study aimed at collecting data at the top and bottom of all the nodes (34 in total) shown in Figure 2.2, making a total of 68 samples. However, due to various technical and environmental factors, it was not possible to collect data in all the nodes during one sampling campaign. Firstly, it is important that wastewater samples are analysed for particle size distribution within few hours of sampling as particles tend to change their characteristics, there wasn't enough facilities to collect and analyse all 68 samples at once. Also, while the sun made it difficulty to continue collecting samples after 12 noon, during the rainy season the pond water was diluted, making it impossible to do analysis for some samples as the Malvern Mastersizer 2000 depends on light scattering and can only work when the sample has certain obscurity. Therefore, although several data sets were collected throughout the study period, this chapter utilizes only the data collected on the same day for both the dry and rainy season. Description of the PSD data inside the pond used in this chapter is given in Table 2.1. For the incoming wastewater,

data for all the samples collected is used to get the range of incoming particle sizes.

Table 2.1: Description of the data collected in different seasons, showing the number of data collected under different categories

	Dry		Wet	
	Top	Bottom	Top	Bottom
Data	18	13	21	26
Missing	16	21	13	8
Unimodal	2	5	1	15
Bimodal	16	8	20	11

2.3.1 Inflow volume fraction Particle Size Distribution

The PSD in terms of diameter of volume-equivalent spherical particles at the WSP inlet for both seasons is unimodal distribution skewed towards larger particle sizes (Figure 2.3a). The median (d_{50}) values range between 42.76 and 257.65 μm for all data. In some samples (15/12/2017 and 24/01/2018), the unimodal distribution has a kink-like shape on the side of particle size >100 μm, and the particle sizes end sharply before reaching the 1000 μm cut-off size of the Malvern mastersizer. Also, the modes of these two samples (15/12/2017 and 24/01/2018) are at a lower particle size compared to the others. Samples collected in different season did not show significant differences indicating no season PSD dependence.

The volume of particles corresponding to a prescribed size interval was obtained by calculating the area under the curve between the size intervals. Categorizing particles into their size fractions, i.e dissolved (<0.001 μm), colloidal (0.001-1 μm), supracolloidal (1-100 μm) and settleable (>100 μm) showed no significant variation for dry and wet weather (Figure 2.3b). Surprisingly, particles with

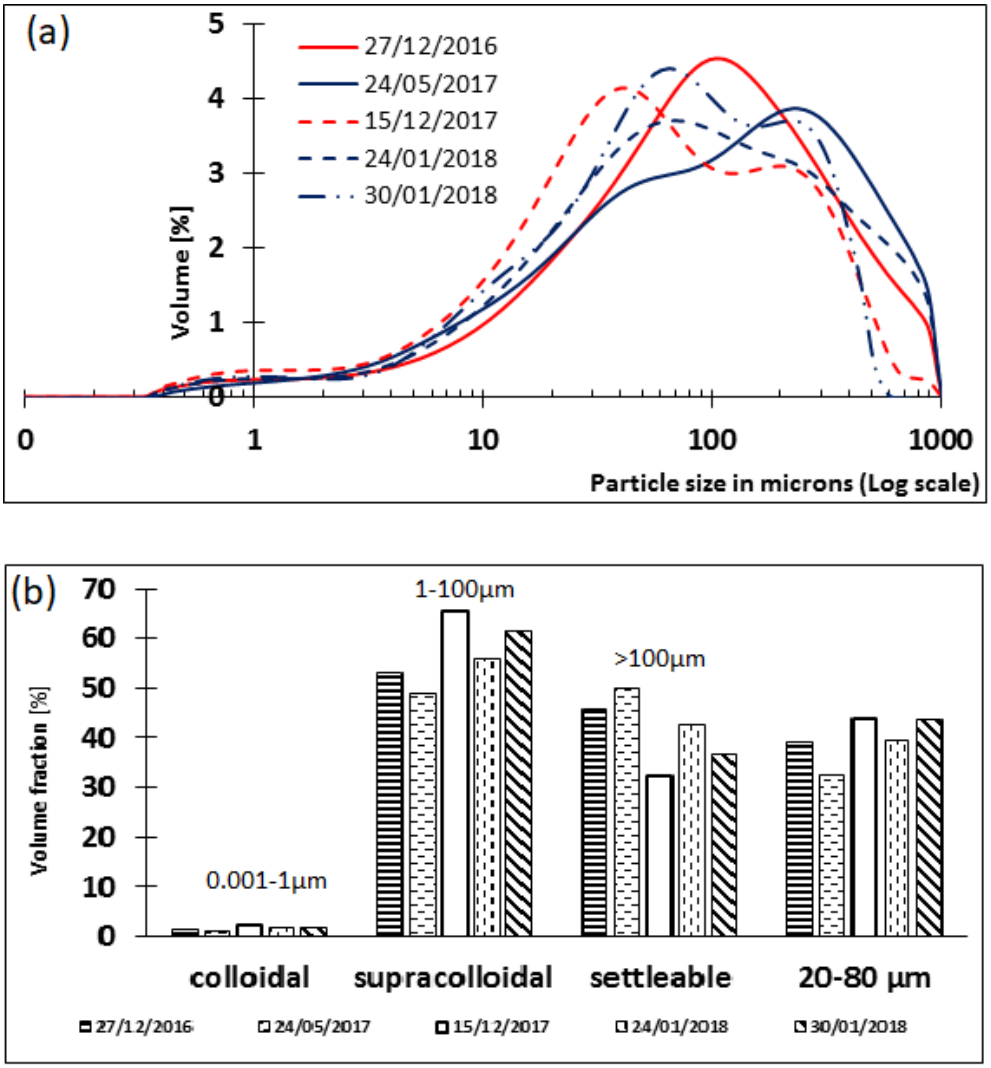

Figure 2.3: Incoming particle sizes at the inlet for different days (a) volume PSD (b) volume fractions of different size classes

sizes <1 μm (i.e. dissolved and colloidal) are very few (ranging between 1.12 and 2.18%), in contrast to existing literature where they contribute the largest percent of particles Levine *et al.* (1991). The values for supracolloidal fractions are between 48.9 and 65.4% and settleable between 32.4 and 49.9%. Therefore, wastewater flow into Buguruni WSP is composed largely of supracolloidal and settleable particles (possibly containing Helminth's eggs). This is in contrast with the reported fractions in literature whereby dissolved and colloidal particles form the largest fraction of particles in wastewater. It should be noted that the Malvern masterizer 2000 measure particles with size between 0.01 to 1000 μm, and therefore some of the colloid particles are outside this range. Inflow particles in the Buguruni ponds that fall within size class of helminth eggs (20-80 μm) range between 32.6 and 44% (Figure 2.3b). Therefore, efficient sedimentation of these particles will guarantee an efficient removal of helminth eggs.

2.3.2 In-pond seasonal PSD

Inside the pond, two types of PSD were identified for both dry and wet weather. The two distributions are a unimodal distribution(with one peak) and bimodal distribution (two peaks) (Figure 2.4). In dry weather, the bimodal distribution is found in almost all nodes at the top except at node 8 and 25 which are located close to the inlet and outlet respectively. This distribution is also found at the bottom of some nodes, from the inlet to around half pond length (nodes 9 and 12). Dry weather bimodal distributions have modes concentrated around similar sizes with the first peaks around 10 μm and the second peaks around 67 μm (Figure 2.4a). The bimodal distributions are characterized by more supracolloidal particles than settleable particles. On the other hand, the dry weather unimodal distribution is found in bottom samples collected from the nodes close to the inlet up to about half the pond length (nodes 12 and 13). The distributions at different

nodes (Figure 2.4b) are right skewed and are richer in settleable particles than supra-colloidal. The distributions have modes at different diameters and long tails towards the smaller particle sizes (less than 10 μm). This distribution is also found in nodes 8 and 25 at the top.

The similar modes on both top and bottom during the dry weather could represent well mixed conditions inside the pond. The shift towards coarser particle sizes in wet weather could be a result of change in inflow PSD due to defect pipes, as well as possible erosion of deposited materials due to increased flow caused by broken sewage system. In wet weather, the bimodal distribution is again found throughout the top, with the exception of node 8. This distribution is also found at the bottom of the pond but in wet weather the demarcation is not so clear as in dry weather. The wet weather modes shift to the right, with peaks around 15 microns and 100 μm (Figure 2.4a), and the separation of the two peaks is not as clear as it is for dry weather. Unimodal distribution during wet season is found only at nodes 8 at the top. At the bottom, although the demarcation is not clear, it can be seen that the bimodal distribution is around the inlet and then along the inlet- outlet path. The exception is at node 28 which is at the other side of the inlet. The long tails towards the smaller particle sizes (less than 10 μm) that were present during the dry weather disappear during wet weather (Figure 2.4 b).

2.3.3 The constituents of PSDs

The percentage of colloids in all samples range between 0 to 1.2%, supra-colloids 12.66 to 80.61% and settleables 14.22 to 87.34% as summarized in the tables below. Again the colloids form the smallest portion of the particle sizes. The dry weather unimodal distributions have more supra-colloidal particles at the top than bottom while for wet weather more supra-colloidal particles are at the bottom than the top. It should however be noted that the unimodal distribution appears

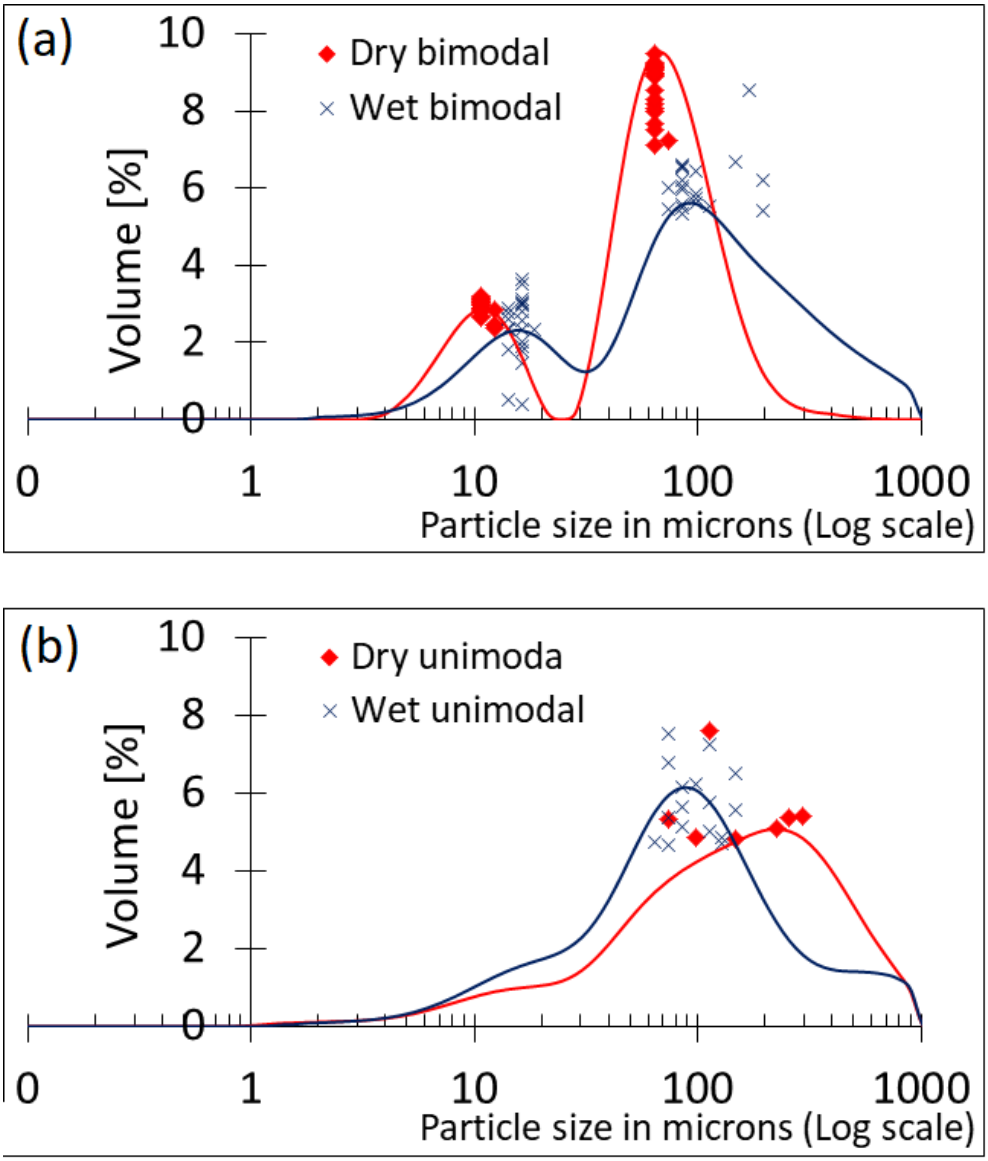

Figure 2.4: Variations in modes of (a) bimodal (b) unimodal distributions inside the pond

.

in only two nodes at the top (nodes 8 and 25) during the dry weather and only one node (node 8) during the wet weather. Settleable particles form the largest percent of particles at the bottom for both the dry and wet weather unimodal distribution. Overall, the unimodal distribution has slightly more settleable particles than supra-colloids in dry weather and more supra-colloids than settleable particles in wet weather.

Table 2.2: Percentage constituent of PSD for different seasons for the unimodal distributions

Fraction	Dry top	Dry bottom	Wet top	Wet bottom
Colloids	0.00 - 0.64	0.00 - 0.12	0.20	0.00 - 38.00
Supra-colloids	36.02 - 56.78	28.70 - 46.44	57.2	41.96 - 78.39
Settleables	42.58 - 63.97	53.43 - 71.30	42.61	21.23 - 58.04

The dry weather bimodal distribution has more supra-colloid particles at the

Table 2.3: Percentage constituent of PSD for different seasons for the bimodal distributions

Fraction	Dry top	Dry bottom	Wet top	Wet bottom
Colloids	0.00- 1.20	0.22 - 1.74	0.00 - 2.08	0.00 - 1.92
Supra-colloids	72.67 - 84.52	57.05 - 80.61	37.14 - 69.92	12.66 - 83.21
Settleables	14.22 - 26.44	17.65 - 42.63	29.30 - 62.85	16.19 - 87.34

top while the wet weather bimodal distribution has more supra-colloid particles at the bottom. The settleable particles are more at the bottom for both seasons. Overall, the bimodal distribution has more supra-colloids than settleable particles in dry weather. In wet weather the top has more supra-colloids than settleables while the bottom has more settleable particles than supra-colloids. The variations of the different constituents along the pond length is shown in Figure 2.5. The percentage of supra-colloidal particles do not have any significant variation along

the pond for the bimodal distributions at the top. For the dry weather, the percentages are similar in all the nodes while for the wet weather, node 7, 18, 22 and 23 have less supra-colloids compared to settleables. The bottom bimodal distributions also do not have any trend along the pond, but the supra-colloid particles continue to be more than settleables except at nodes 23 and 26 in the wet weather. On the other hand, the bottom unimodal distributions for the dry weather have more settleable particles with no particular trend along the pond length. The wet season bottom unimodal distribution has no trend along the pond as well, but has more supra-colloids than settleable particles except for nodes 9, 21, 22 and T6.

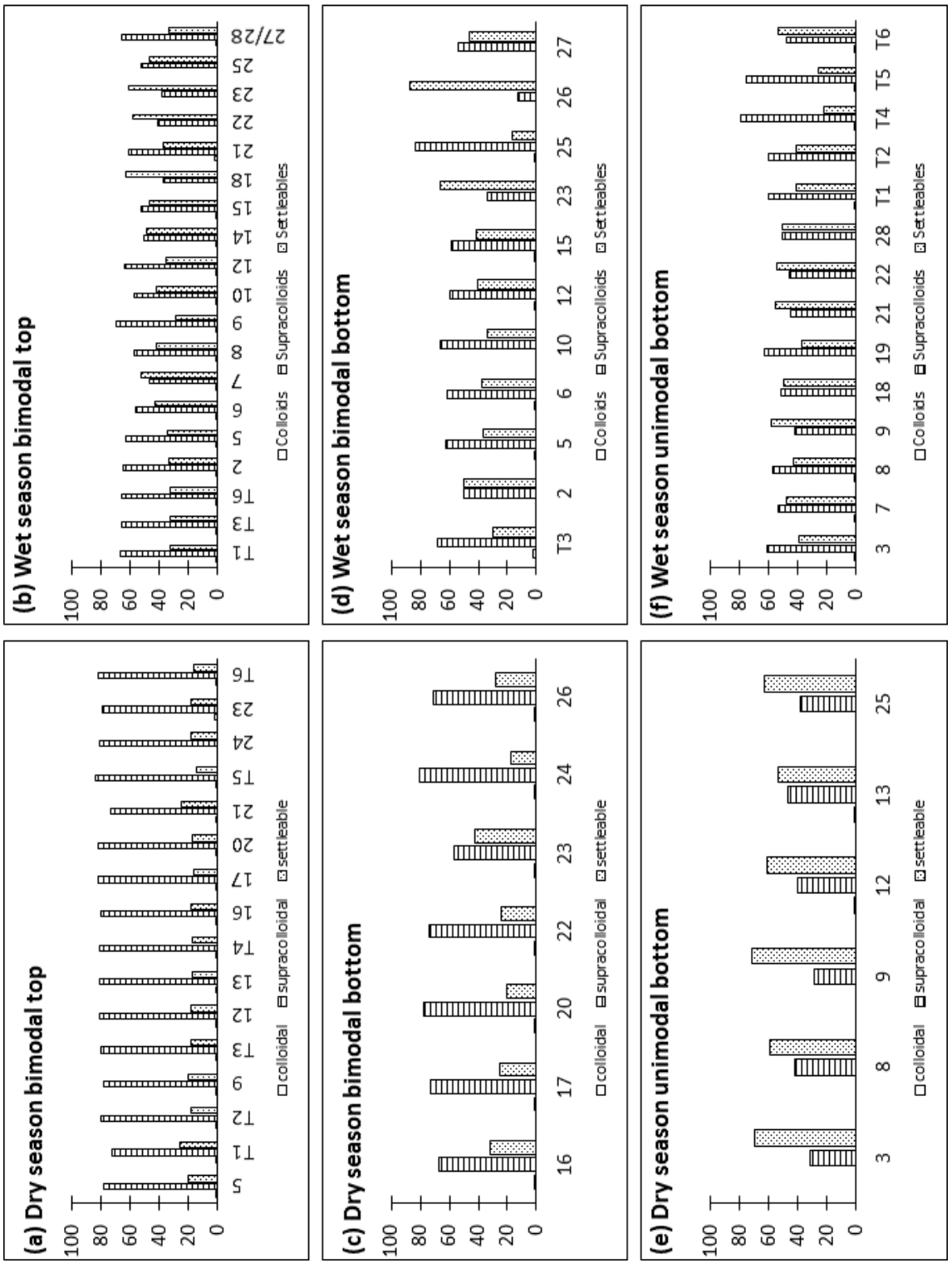

Figure 2.5: Composition of PSD in percentage volume at different locations inside the pond

From the description in sections 2.4 and 2.5 above, the unimodal distribution appears mostly at samples collected at the bottom while bimodal dominates samples collected at the top. Also, the unimodal distribution is richer in settleable particles while the bimodal distribution is richer in supra-colloids. Therefore, it may be concluded that the unimodal distribution represents the settling particles while the bimodal distribution represent non-settling particles.

2.3.4 Mapping of possible sedimentation areas

This was done through comparison of top and bottom PSD to reveal areas in the pond where sedimentation is taking place as well as those where resuspension of settled particles occurs. Firstly, areas with similar unimodal PSD at the top and bottom (Figure 2.6c), representing settling particles were identified as resuspension areas. As pointed before, these are locations with turbulence originating from change in cross section area and convective acceleration of the flow at the outlet and hence resulting re-suspension of settled particles. These were found in two nodes (8 and 25) during the dry weather, but in wet weather it was only at node 8 as the data for node 25 was too diluted for analysis. Node 8 is located close to the inlet while node 25 is close to the outlet of the WSP. Typically, these are areas with vorticity created by change in cross sectional area and therefore settled particles maybe re-suspended and a unimodal distribution is obtained. Secondly, areas with unimodal distribution at the bottom and bimodal distribution at the top (Figure 2.6a) were identified as areas where sedimentation is taking place. For dry weather, these are areas from around the inlet up to about half the pond length (nodes 12 and 13). In wet weather, there is not a clear demarcation but most of the nodes sampled (12 out of 18) fell under this category. Lastly, areas with similar bimodal distributions at the top and bottom (Figure 2.6b) were categorized as areas where there is no sedimentation. For dry

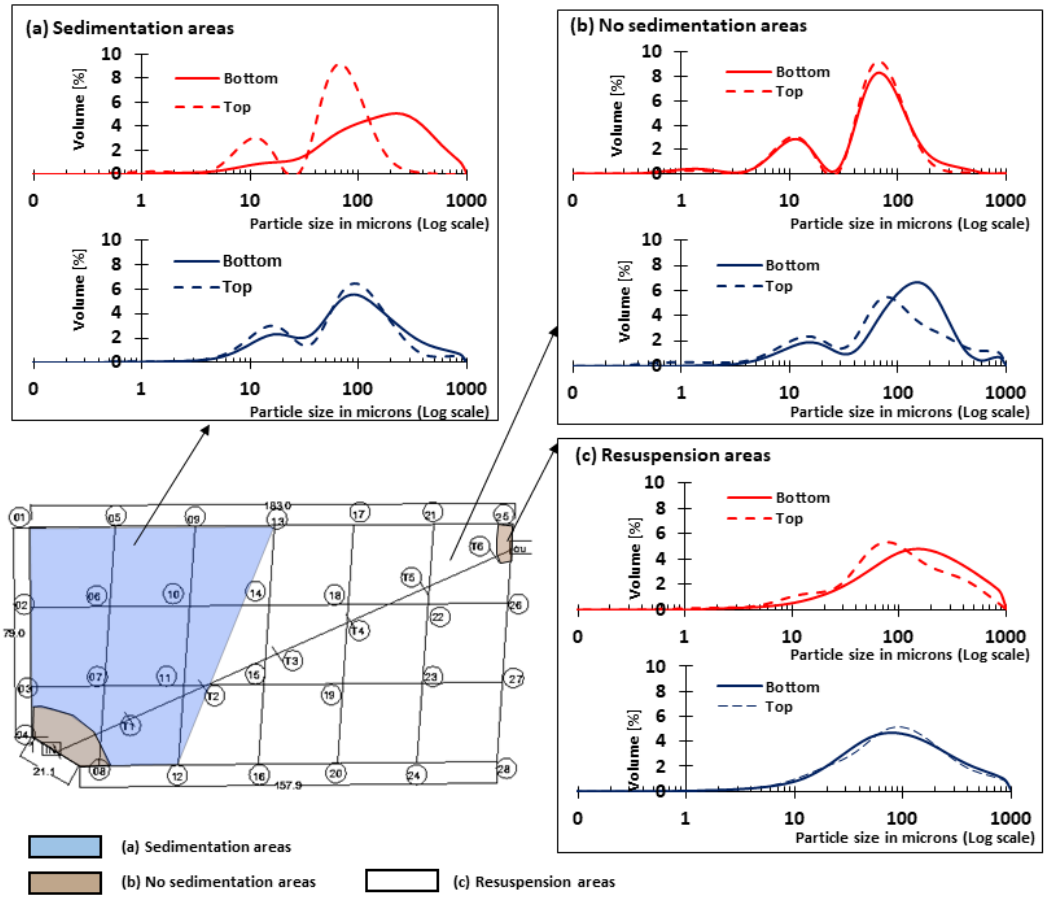

Figure 2.6: Comparison of PSD at the top and bottom of the pond for dry weather (red color) and wet weather (blue color). Node numbers are as shown in Figure 2.2.

weather these represented the remaining nodes from mid-point up to the outlet while for the wet weather the demarcation was not so clear. The similarity of PSD at the top and bottom indicates that a mixing process is taking place along the vertical direction.

There is a popular foot-path running on one side of the pond throughout the pond length (Figure 2.7c). This foot-path results into a lot of sand and other debris materials to be thrown and deposited inside the pond on that side (Figure 2.7a). Also, during wet weather, there is a potential of run-off coming into the pond through this path as it is badly worn in some areas such as the corner photographed in Figure 2.7a. Therefore this area has secondary sedimentation resulting from materials that are not related to incoming wastewater and are therefore discarded. Therefore, areas where sedimentation is taking place remain to be concentrated around the inlet as plotted in Figure 2.7d, and confirmed in the picture taken at the study area (Figure 2.7b).

2.3.5 Particles with sizes within the range for helminth eggs

Among the objectives of this research was to study the sedimentation of particles with size between 20 and 80 μm, which is the size range for helminth eggs as they have the highest chance of containing helminth eggs (Chavez *et al.*, 2004), which are detrimental to human health. Results show that these particles appear throughout the pond both at top and bottom, with an increased volume compared to that of the incoming particles indicating that they may be a result of floc formation as well as sludge creep/ saltation processes (Figure 2.8a,b). The particles do not exhibit any particular trend at the different locations, but their volumes are consistently higher at the top especially during dry weather indicating that these could be light suspended particles that may be carried out of the system,

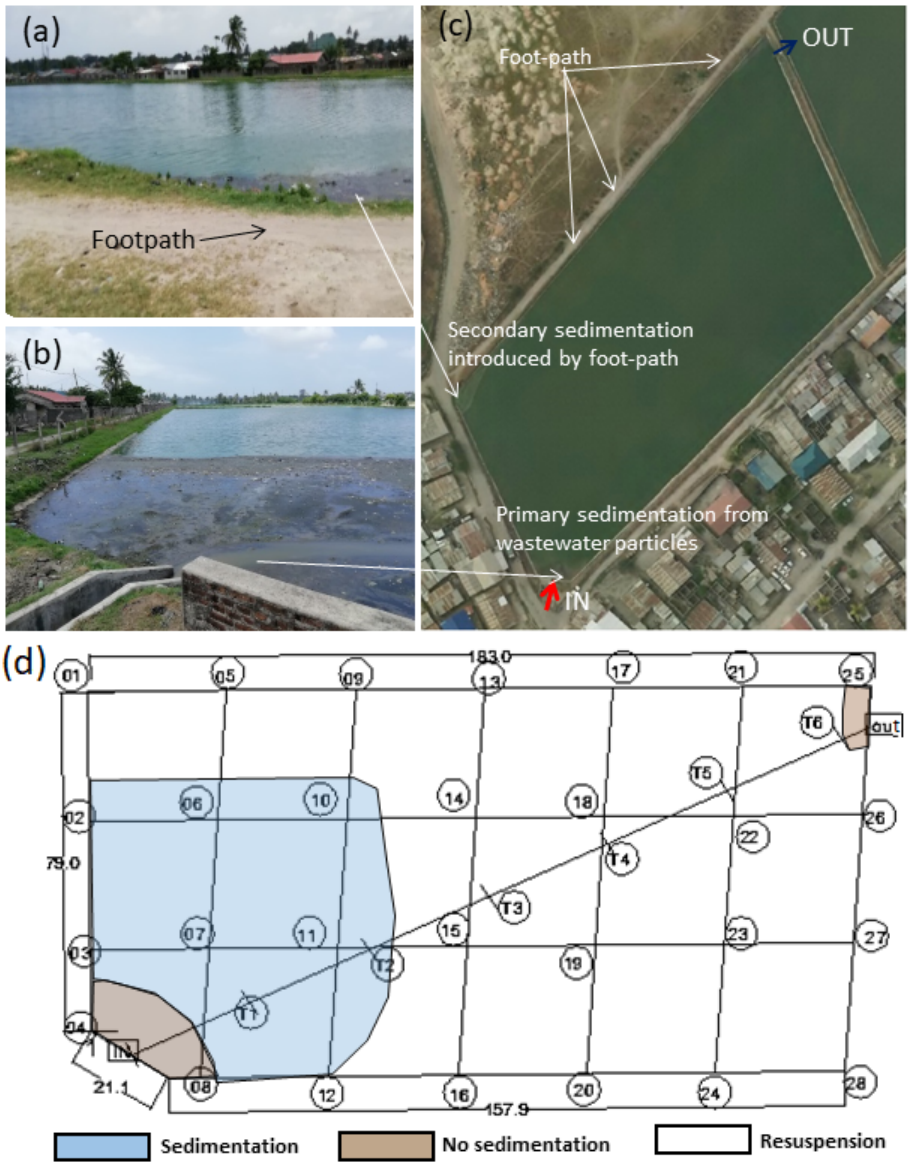

Figure 2.7: Photos of the different sedimentation zones in the pond. (a,c) is a popular footpath running parallel to the pond while (b) shows deposits at the inlet. Demarcation of areas of wastewater sludge deposits (d)

.

for instance during increased flow in rainy season. Their total volume fraction is slightly lower during the wet season perhaps due to shift of inflow particles towards the large particle sizes (>100 μm). Analysis for helminth eggs for water samples collected at the bottom was done using the formol-ether concentration method discussed in section 1.2.5, but very few eggs (only two eggs in 12 samples) were recovered. However, from the discussion above it can be seen that the persistence of helminth eggs in the environment due to discharge of polluted water is a result of the sedimentation dynamics in the pond. First, despite having higher settling rates which should enable them to settle immediately once they enter the pond, the eggs do not settle in isolation but rather form flocs with wastewater particles resulting into flocs with low settling rates. Secondly, the presence of creeping movement of settled sludge which is later re-suspended at the outlet is another potential cause of presence of helminth eggs in the discharge and hence contamination of the environment.

2.4 Conclusion

This chapter looked at how incoming wastewater particle sizes change inside a primary facultative pond of a WSP and is of key importance for all those water treatment plants where a primary sedimentation pond is missing. It was observed that particles coming into the pond are mainly supracolloids and settleables, although information about their densities was missing. Once inside the pond, the incoming PSD split into settling and non-settling PSDs, with an indication of particle breakage, as shown by the increased volume of smaller particles and hence appearance of a bimodal distribution. Sedimentation takes place mostly in the first half part of the pond, while the remaining part has suspended particles

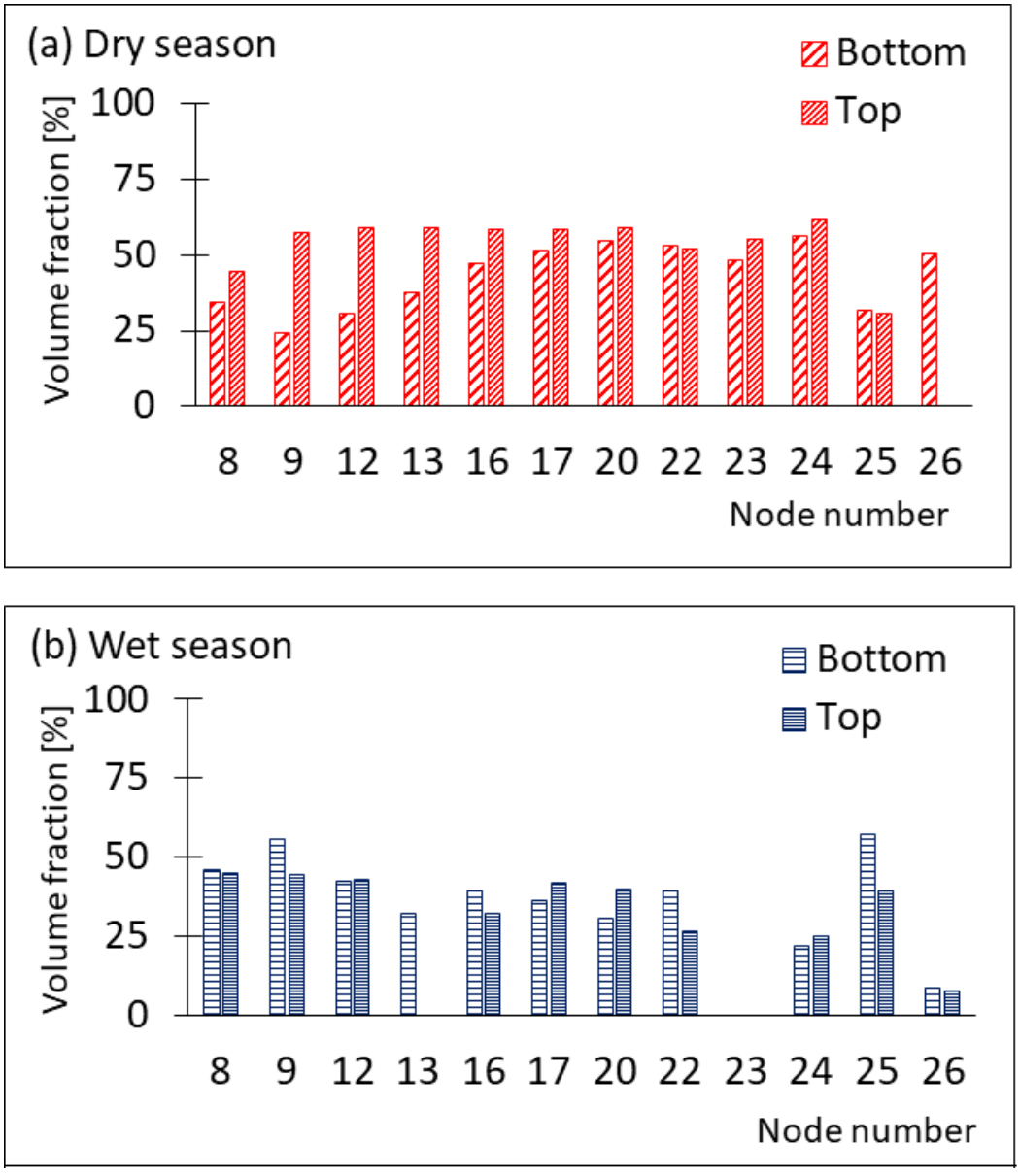

Figure 2.8: Variations of particles with size corresponding to helminth eggs (20-80 μm)

only. Particles with sizes between 20 and 80 μm (the size of helminth eggs) as well as settleable particles (>100 μm) are in abundance in suspension. Although these may not necessarily contain helminth eggs, they indicate a large potential for the eggs to remain in suspension and be carried out of the system. Further research on particle density variations inside the pond may enable tracing of the eggs based on their characteristics. However, measuring particle density is an extremely demanding effort. This asks for developing an inverse modelling technique for reconstructing the particle density distribution starting from the PSD difference at the top and the bottom and the travel times where sedimentation can occur. Travel times (which result in the HRT of the pond) are crucial to the operation of WSP (Alvarado *et al.*, 2012a; Verbyla *et al.*, 2016, 2013), and therefore the next task will be the development of a hydraulic model in Delft3D that is able to capture actual flow conditions in the Buguruni WSP. The PSD data presented here will be used, together with a hydrodynamic model developed in Delft3D, to derive the range of densities of wastewater particles at different nodes in the Buguruni WSP and hence trace where helminth eggs are most likely to be found.

Chapter 3

Pond hydraulics and hydraulic sorting in WSP

3.1 Introduction

Hydraulic conditions in the pond are important for removal of pollutants in WSP. These can be used to determine how long water is retained in the system (known as hydraulic retention time - HRT), degree of mixing as well as transport of pollutants to different parts of the pond and eventually the outlet. During the design process, flow conditions are important in determining the type of formulation to be used in determination of the rate constants for the biological reactions in the pond. The retention time is also linked to effluent quality of different pollutants, however, distinction should be made between the theoretical and actual HRT which is the actual time that water spends in a system. Actual HRT is a function of the distribution of flow velocities in the pond and may be affected by several factors including hydraulic short circuiting and dead-spaces

(zones). The occurrence and degree of these two phenomenon are fundamental in assessing the hydraulic performance of WSP.

Hydraulic conditions may be assessed by either plotting velocity vectors inside the pond or by the analysis of residence time distribution (RTD) curves from tracer experiments (Somes *et al.*, 1999). Traditionally, tracer experiments are used to derive RTD curves through the application of population balance models. The measurement of tracer concentration variations at the outlet with time can also be interpreted to establish mixing conditions in the pond (whether fully mixed or plug flow). However, tracer experiments especially in operating ponds are time consuming (recommended sampling period is 3-4 times the pond's HRT); and unreliable due to interference of other conditions such as wind and temperature stratification (systems not in steady state). On the other hand, application of hydraulic models are gaining popularity in assessing pond hydraulics. Hydraulic models have been shown to be capable of simulating hydraulic properties of a WSP very well (Pearson *et al.*, 2005; Vega *et al.*, 2003; Abbas *et al.*, 2006; Olukanni and Ducoste, 2011; Shilton, 2001; Sweeney *et al.*, 2005; Alvarado *et al.*, 2012a,b; Passos *et al.*, 2014b).

This section simulates the Buguruni primary facultative pond's hydraulic characteristics using the Delft3D software. Then the flow characteristics (velocities magnitude and direction) are extracted, from which other properties such as mixing conditions, presence of short-circuiting, dead spaces, flow path-lines and travel times are calculated. Due to the shallowness of the pond, it was thought that a 2D is sufficient to describe the pond hydraulics as well as tracing the settled particles trajectories down to the pond bed. However, a 3D model was also employed to explore the effect of wind on the flow characteristics as previous studies have shown that wind can be a dominant driving force of WSP hydraulics (Badrot-Nico *et al.*, 2009; Brissaud *et al.*, 2003; Gu and Stefan, 1995), introducing complex circulation patterns and differential movement of the top and bottom layers of the pond.

Badrot-Nico *et al.* (2009) observed stratification for low winds and complete mixing during high winds as well as wind-induced short-circuiting in an operational pond in France. Strong winds may result in re-suspension of settled sludge. Also, rainfall may result into altered inflow discharge characteristics especially when defective or poorly designed and maintained systems are involved.

It is known that hydrodynamics plays a very important role in sedimentation process and hence sludge accumulation patterns in the pond (Abis and Mara, 2005; Alvarado *et al.*, 2012a; Coggins *et al.*, 2017; Ouedraogo *et al.*, 2016; Murphy, 2012; Nelson *et al.*, 2004). The dependence of sludge accumulation patterns on hydraulic characteristics is common for sediment settling tanks (Camnasio *et al.*, 2013; Dufresne *et al.*, 2010; Kantoush *et al.*, 2008), and natural water bodies such as rivers, lakes and oceans (Onyango, 1992), and opens up a possibility of applying hydraulic sorting models to describe sludge characteristics in WSP. In hydraulic sorting models, particles are transported, deposited and entrained based on their sizes, shapes and densities (Onyango, 1992). These models are used widely to predict deposition of harmful/ toxic minerals; decide on disposal of dredged materials; and predict changes in the bed profiles of rivers, lakes and ocean (Onyango, 1992), which are also relevant to WSPs. However, the application of these models has so far been constrained to only coarse non-organic sediments as opposed to organic particles contributing a large percent of municipal wastewater. But, the particle composition of raw wastewater (mainly supracolloidal and settleables) and spatial variability in particles size distributions (PSD) observed in our previous study (Izdori *et al.*, 2018), as well as laminar flow conditions typical in WSP makes hydraulic sorting a possibility worth exploring.

Therefore, the influence of hydraulic characteristic of the pond on the sedimentation process was established by correlating bottom particle characteristics and flow parameters at different locations in the pond. It is thought that, the application of hydraulic sorting models to WSP maybe used to identify locations of

polluted sludge. Since the mean, median, and mode are different for the different PSDs, this section also explored which measure of central tendency can best be used to describe hydraulic characteristics of the sample.

3.2 Model set-up

Delft3D consists of different fundamental sub-modules for environmental hydraulic simulations: flow, water quality, wave generation and propagation, morphology and sediment transport (Deltares, 2016). This study utilized the hydrodynamic module. The Delft3D hydraulic model simulates velocity vectors of water in the pond in response to a variety of conditions and input parameters. The model domain was defined by grid and bathymetry shown in Figure 3.1(a, b), created using the pond dimensions and water levels. The magnitude and extent of velocity are solved on a square or rectangular grid covering the area of interest. The program offers pre-proccessing tools for creation of orthogonal grids (RGFGRID) and for preparation of grid data such as bathymetry (QUICKIN). The hydrodynamic model solves the Navier-Stokes equations for incompressible fluid, in ξ and η directions, given in equations 3.1 and 3.2 respectively, under shallow water and Boussinesq assumptions, integrated over the vertical to describe the velocity variations and other hydraulic parameters in two horizontal dimensions. The momentum equations are solved by implicit finite difference techniques.

$$\frac{\partial u}{\partial t}+\frac{u}{\sqrt{G_{\xi\xi}}}\frac{\partial u}{\partial \xi}+\frac{v}{\sqrt{G_{\eta\eta}}}\frac{\partial v}{\partial \eta}+\frac{\omega}{d+\zeta}\frac{\partial u}{\partial \sigma}-\frac{v^2}{\sqrt{G_{\xi\xi}}\sqrt{G_{\eta\eta}}}\frac{\partial \sqrt{G_{\eta\eta}}}{\partial \xi}+ \frac{uv}{\sqrt{G_{\xi\xi}}\sqrt{G_{\eta\eta}}}\frac{\partial \sqrt{G_{\xi\xi}}}{\partial \eta}-fv=-\frac{1}{\rho_0\sqrt{G_{\xi\xi}}}P_\xi+F_\xi+\frac{1}{(d+\zeta)^2}\frac{\partial}{\partial \sigma}(\nu_v\frac{\partial u}{\partial \sigma}) \quad (3.1)$$

$$\frac{\partial v}{\partial t} + \frac{u}{\sqrt{G_{\xi\xi}}}\frac{\partial v}{\partial \xi} + \frac{v}{\sqrt{G_{\eta\eta}}}\frac{\partial v}{\partial \eta} + \frac{\omega}{d+\zeta}\frac{\partial v}{\partial \sigma} + \frac{uv}{\sqrt{G_{\xi\xi}}\sqrt{G_{\eta\eta}}}\frac{\partial \sqrt{G_{\xi\xi}}}{\partial \eta}$$
$$- \frac{u^2}{\sqrt{G_{\xi\xi}}\sqrt{G_{\eta\eta}}}\frac{\partial \sqrt{G_{\eta\eta}}}{\partial \xi} + fu = -\frac{1}{\rho_0\sqrt{G_{\xi\xi}}}P_\eta + F_\eta + \frac{1}{(d+\zeta)^2}\frac{\partial}{\partial \sigma}(\nu_v\frac{\partial u}{\partial \sigma}) + M_\eta \tag{3.2}$$

Where u is the fluid velocity in the x- or ξ-direction, v is the fluid velocity in the y- or η-direction, ω is the fluid velocity in z-direction, $\sqrt{G_{\xi\xi}}$ and $\sqrt{G_{\eta\eta}}$ are coefficients used to transform curvilinear to rectangular coordinates, f is the Coriolis parameter (inertial frequency), d is the depth below some horizontal plane of reference (datum).

ξ and η are horizontal and curvilinear co-ordinates respectively

F_ξ and F_η are turbulent momentum flux in ξ and η directions.

P_ξ and P_η are gradient hydrostatic pressure in ξ and η directions.

M_ξ and M_η are source or sink of momentum in ξ and η directions.

The model simulates velocity vectors of water in the pond in response to a variety of conditions and input parameters. The magnitude and extent of velocity are solved on a square or rectangular grid covering the area of interest. The main inputs of the model are computational mesh, bathymetry, bed resistance, eddy viscosity, wind, water level and discharge boundary conditions. Delft3D consists of four fundamental sub-modules for environmental hydraulic simulations: hydrodynamics, water quality, sediment transport, ecological, particle tracking, morphodynamic and wave modules. This study utilized the hydrodynamic and particle tracking modules as outlined in the Delft3D user manual (Deltares, 2016).

The resulted velocity vectors are used to generate streamlines, (which are

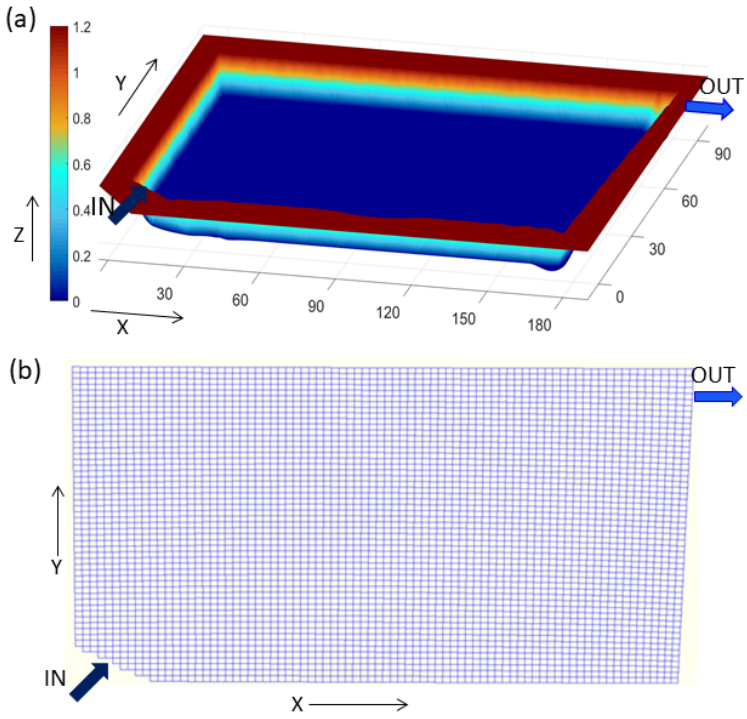

Figure 3.1: (a)Depth profile and (b) the mesh generated in Delft3D (figure not to scale), which are the main inputs into the hydraulic model.

assumed to be path-lines that particles follow), by the STREAMLINE function in MATLAB. The STREAMLINE function uses Forward Euler Prediction, which is a first order numerical procedure to solve ordinary differential equations, to predict the position of an object when the previous position is known. Results from the hydraulic model were also used in developing a hydraulic sorting model as outlined in Section 3.4.Other path-line characteristics are calculated as below; Path length L (m), a particle travels to a node (i) which is taken to be the same as L_t in equation (3.3), is calculated from the Cartesian coordinates X and Y as;

$$L = \sqrt{\sum_{1}^{n}(\Delta X_i^2 + \Delta Y_i^2)} \tag{3.3}$$

In doing this, equation (3.3) neglects the contribution of the vertical coordinate

ΔZ_i which is small compared to the horizontal coordinates. Average flow velocity (m/s), along a horizontal path-line to a node (i) is calculated from the velocity components along the Cartesian coordinates X and Y, which are u and v respectively, as;

$$V_m = \sqrt{\frac{\sum_1^n (u_i^2 + v_i^2)}{n}} \tag{3.4}$$

Time, T, taken by a particle to travel to a node (i) along the trajectory with a mean velocity V_m

$$T = \frac{L}{V_m} \tag{3.5}$$

The average particle size at a node (i) is read from Malvern Mastersizer 2000 results, where it has been estimated from the PSD data as:

$$D_m = \frac{\sum_1^n D_i^4 v_i}{\sum_1^n D_i^3 v_i} \tag{3.6}$$

Where D_m is the volume based mean particle diameter, D_i is the diameter of the ith particle and v_i its volume fraction.

Results from equations (3.3) to (3.6) represent node data. These are interpolated by the Krigging method in the SURFER9, a full-function 3D visualization, contouring and surface modelling package that runs under Microsoft Windows, to obtain spatial data covering the whole pond area.

3.3 Hydraulic characteristics of the pond

3.3.1 Spatial flow characteristics

Simulated flow velocity magnitudes and directions are represented in Figure (3.2). The hydraulic model is considered plausible since the computed average travel time to the outlet (28.8 days) is similar to the pond's theoretical retention time of 29.1 days obtained by dividing the pond volume with the design discharge. The average travel time to the outlet was obtained from Delft3D hydraulic model results by using equation (3.5) for each streamline, and then finding the average of all the travel times obtained. For the case without wind, velocity magnitudes are highest (in the order of $10^{-2}m/s$) in the proximity to both the inlet and outlet, most likely due to smaller cross-section areas of both the inlet and outlet (Figure 3.2a). Inside the pond, flow velocities are in the order of $10^{-4}m/s$ which is similar to what is reported in other researches (Shilton, 2001) and provides ideal conditions for sedimentation of wastewater particles. Inlet velocity is responsible for the flow and hence streamlines in shallow ponds due to the momentum derived from the inlet jet (Ouedraogo *et al.*, 2016; Camnasio *et al.*, 2013; Dufresne *et al.*, 2010; Kantoush *et al.*, 2008). The absence of recirculation could therefore mean that the inlet jet at Buguruni WSP is so small that its influence doesn't reach far into the pond, and that flow progresses steadily mainly due to difference in elevation between the inlet and outlet. Changing flow magnitude up to maximum capacity of the weir (the inlet channel is fixed with a V-notch weir) only increased the flow velocity magnitudes but the directions remained the same.

Introduction of the wind scenarios described in Section 1.6 in the simulation, resulted in modification of flow for the different wind scenarios as shown in Figures 3.2b-d. Wind blowing in the North-East direction is in the opposite direction as that of flow, that is it blows from the outlet edge towards the inlet edge, parallel

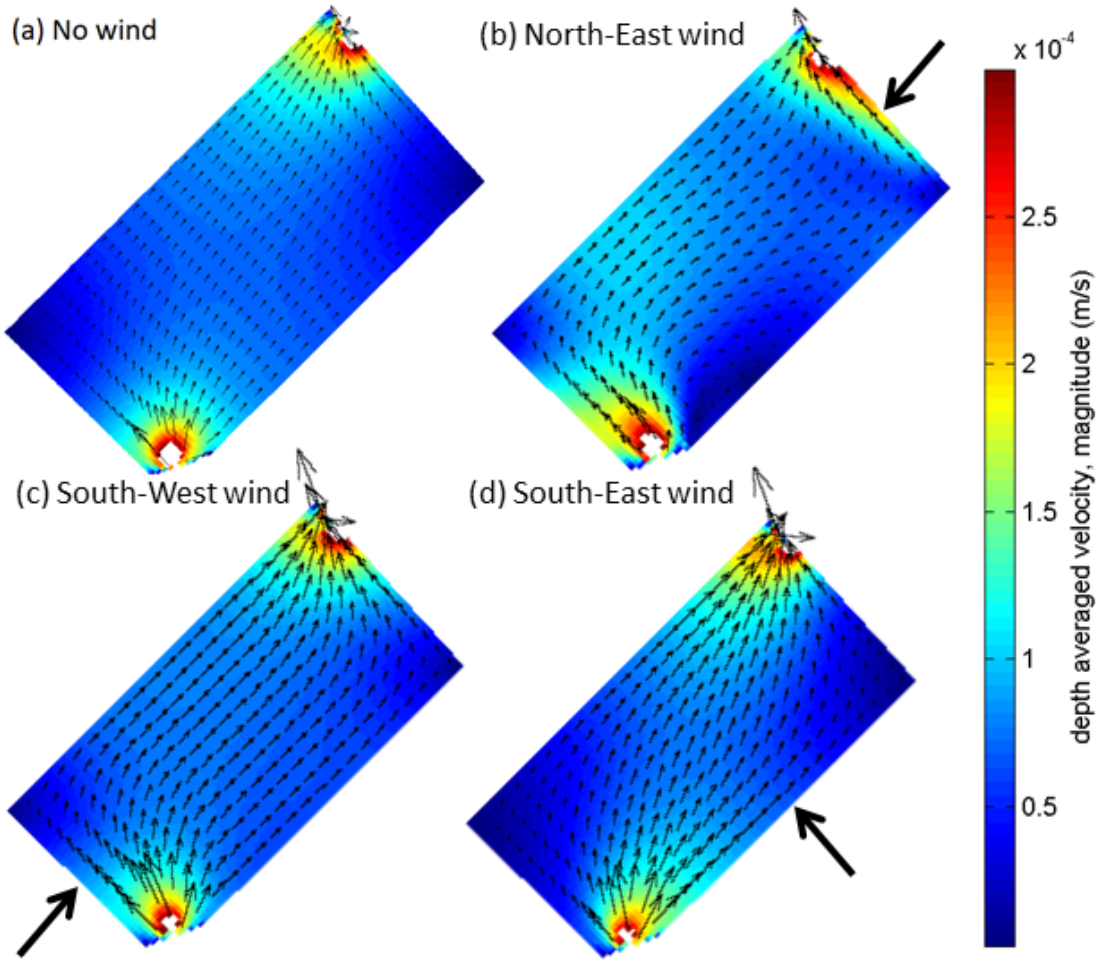

Figure 3.2: Flow magnitudes and vectors as simulated by a 3D-Delft3D for different wind scenarios

to the pond banks. The wind pushes the main flow path towards the outlet side (LHS) bank, resulting in higher flow velocities along this side (Figure 3.2b). The wind also introduces some flow re-circulation close to the inlet on the RHS bank. The South-West wind is in the opposite direction to the North-East wind and blows from the inlet edge towards the outlet edge, parallel to the banks. This wind pushes the main flow path towards the inlet side (RHS) bank, resulting into higher flow velocities on this side (Figure 3.2c). Lastly, the South-East wind blows from the outlet side (LHS) bank towards the inlet side (RHS) bank, parallel

to the pond edges. This wind seems to accentuate flow velocities along the main flow path-line i.e. inlet-outlet line (Figure 3.2d).

The North-East and South-West wind seem to decrease the areas with low flow velocities at the corners opposite to the inlet and the outlet. However, the North-East wind creates a low flow velocity area on the RHS bank close to the inlet. On the other hand, the South-East wind seem to increase the low flow areas on both the opposite corners to the inlet and the outlet.

3.3.2 Vertical flow profiles

In the vertical profile, different flow velocity patterns exist for different simulation conditions. In the absence of wind, the flow velocities show a vertical stratification down the pond depth, fluctuating around $7 \times 10^{-5} m/s$ with much higher values close to the inlet and the outlet (Figure 3.3a, c). The high flow velocities in these areas are the approach velocities as the cross section-area changes in the proximity of the inlet and the outlet respectively. Lowest flow velocities are observed in both LHS and RHS of the figure that represents the pond edges, whereby velocities are reduced as the flow comes into contact with the stationary sides of the pond. The velocity vectors are the same in all layers, pointing from the inlet to the outlet. Close to the inlet, vectors pointing downward are observed but they resolve to being horizontal in the middle of the pond (Figure 3.3a, b). A few meters close to the outlet there is again vertical velocity vectors, this time pointing upwards (Figure 3.3c).

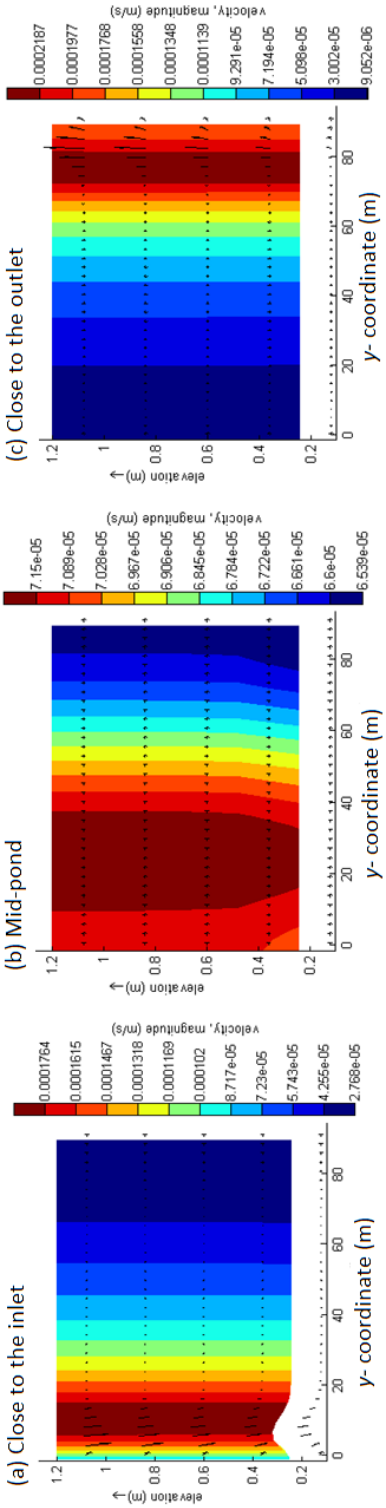

Figure 3.3: Flow velocity magnitudes down the pond depth in the absence of wind

.

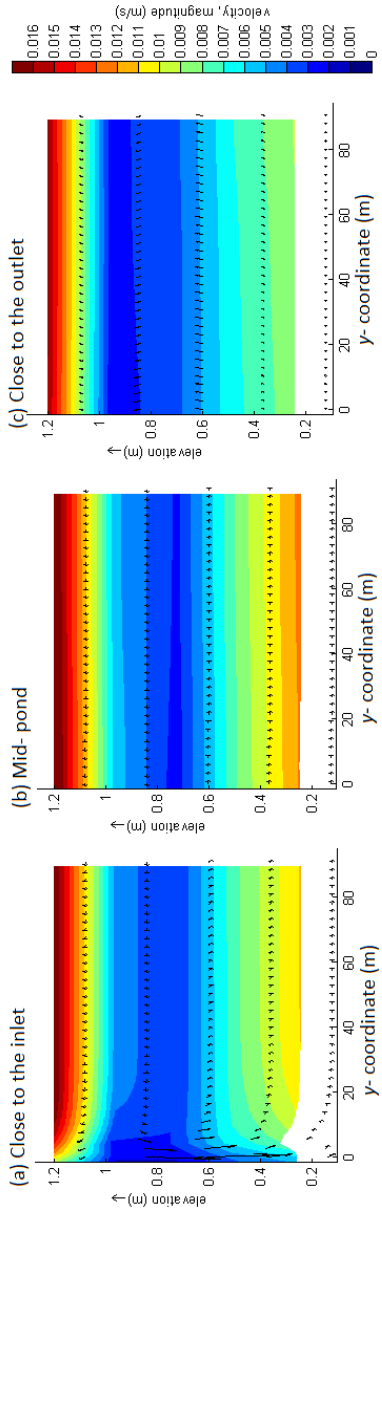

Figure 3.4: Flow velocity magnitudes down the pond depth for wind blow at North-East direction at the speed of 4.25 ms^{-1}

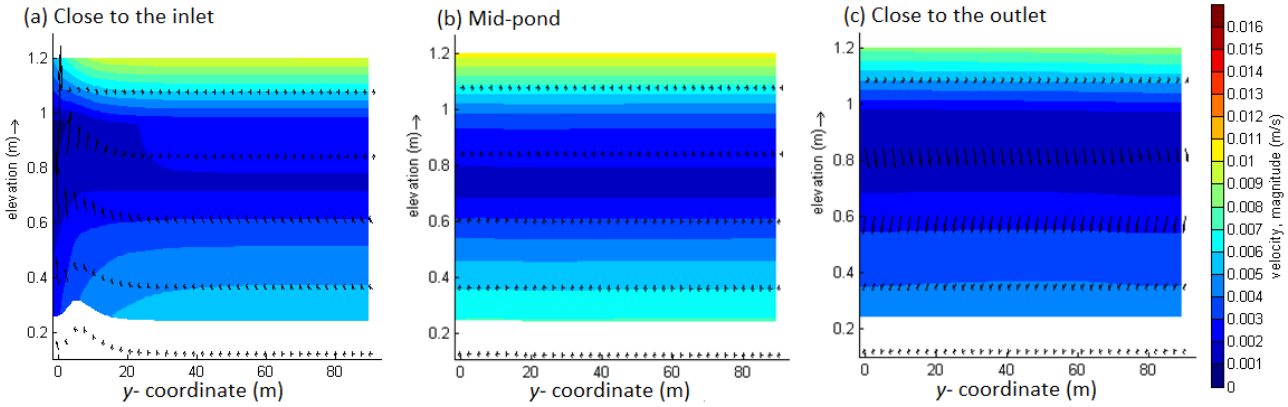

Figure 3.5: Flow velocity magnitudes down the pond depth for wind blow at South-West direction at the speed of 2.5 ms^{-1}

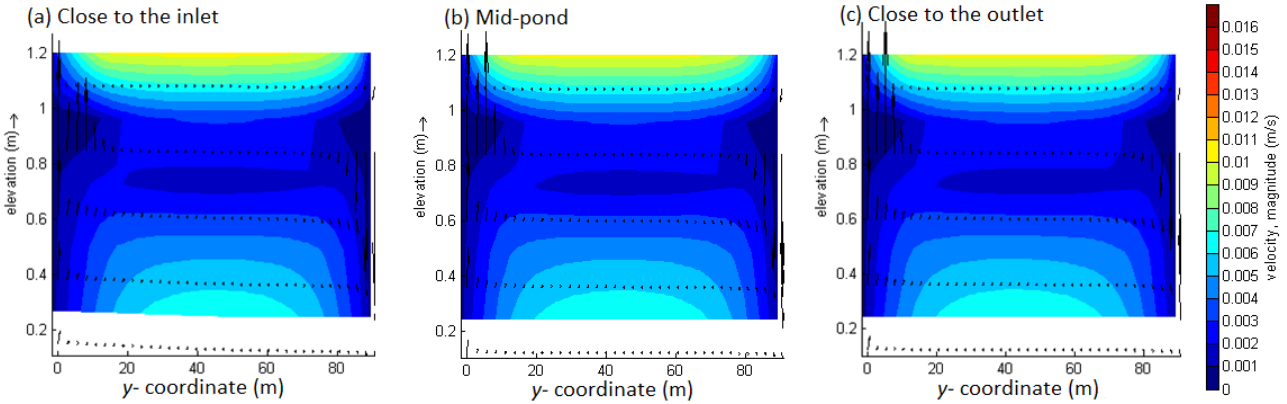

Figure 3.6: Flow velocity magnitudes down the pond depth for wind blow at South-East direction at the speed of 2.5 ms^{-1}

Profiles for scenarios with wind show a modification of the variations of flow velocity down the pond depth, this time causing horizontal stratification of flow velocities (Figures 3.4, 3.5 & 3.6). Highest velocities are observed at the top of the pond as expected, where the wind effect is maximum, reducing to a minimum at a depth of about 0.4 m from the top and then increasing again towards the bottom. Close to the inlet and outlet the velocity vectors are vertical, indicating vertical movement of flow around these areas (Figures 3.4, 3.5 & 3.6a, c). The flow velocity vectors even to horizontal in the middle of the pond indicating presence of only lateral flow (Figures 3.4, 3.5 & 3.6b). The North-East wind that blows in the period between November to April at an average speed of 4.25 ms^{-1} results in highest flow velocities magnitudes compared to all the other scenarios (up to 1.6 cms^{-1} and 1 cms^{-1} at the top and bottom respectively).

The vertical stratification and high flow velocities observed in simulations with wind are a potential source of short-circuiting, whereby wastewater spends less time in the pond than the design HRT. This may lead to transport to the outlet of lighter particles at the top, which in the absence of wind may have sufficient time to settle on their own or by forming flocs with other particles.

In the absence of wind, the pond has relatively similar low flow velocities except for areas close to the inlet and outlet only, that are a result of the incoming discharge. Imposing wind results into differential flow movement and higher flow velocities in all positions in the pond, dissolving the effect of the incoming discharge magnitude. In the differential flow movement caused by wind, the flow move in the wind direction for the top two layers (up to a depth of 0.4 m from the top) and in the opposite direction for the remaining bottom layers. However, depth averaged flow velocities for all wind scenarios are similar to the case without wind, both showing flow progressing from the inlet to the outlet (Figure 3.7).

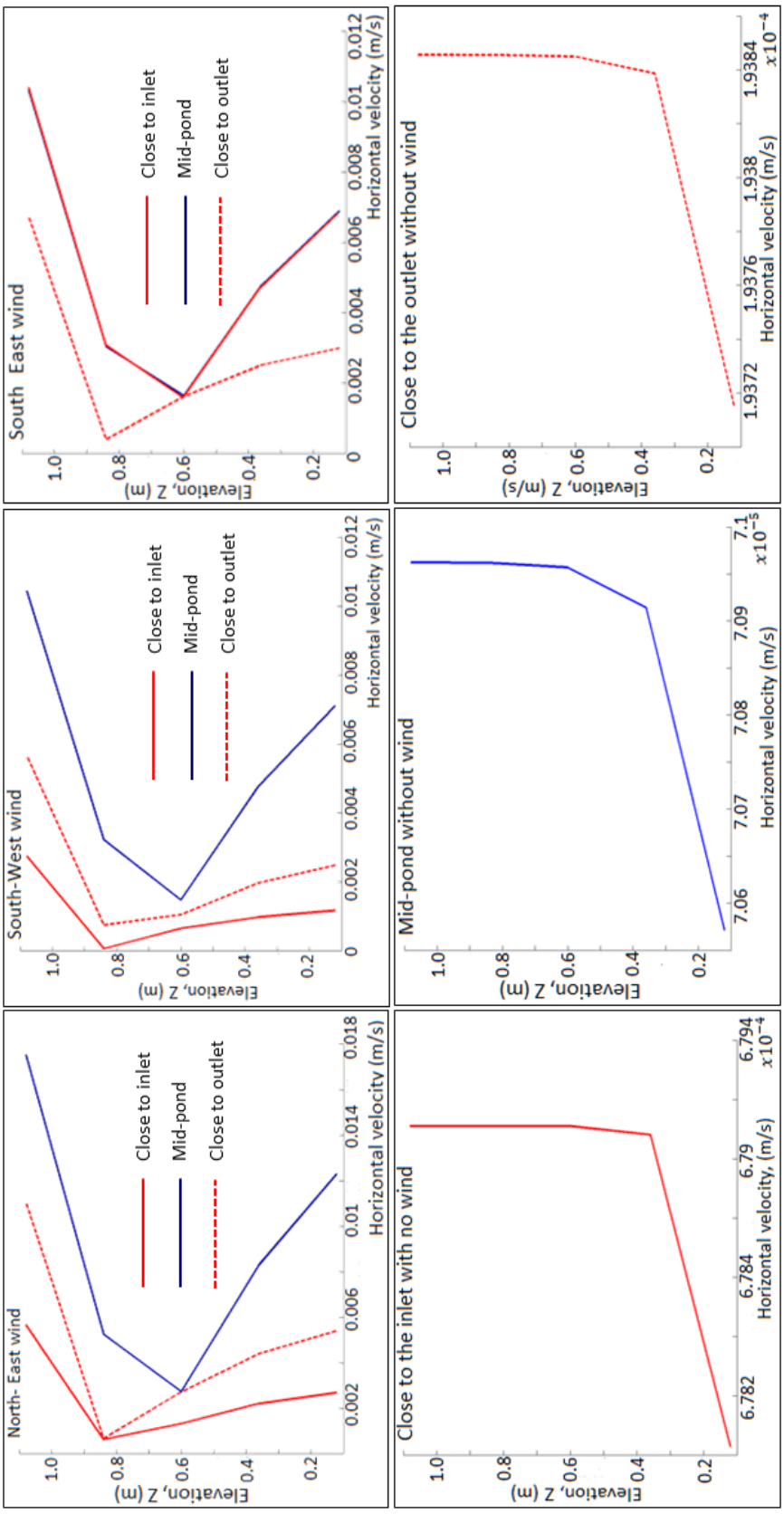

Figure 3.7: Average flow velocity magnitude variations down the pond depth for different wind scenarios

3.3.3 Particle path-lines and trajectories

Flow pathlines, representing the path travelled laterally by water particles to different locations in the pond and finally the outlet as constructed from the STREAMLINE function in MATLAB are shown in Figures 3.8. In all the scenarios (with and without wind), flow path-lines progress from the inlet to the outlet, with no recirculation as reported in other research (Ouedraogo *et al.*, 2016; Camnasio *et al.*, 2013; Dufresne *et al.*, 2010; Kantoush *et al.*, 2008). These flow-pathlines indicate plug flow conditions in the pond, which are ideal in the performance of WSP. This behaviour has also been reported by Shilton (2001) in a study of hydraulics of waste stabilization ponds. Areas on the corner opposite to the outlet exhibit very low flow velocities and streamlines do not pass through, indicating no movement of flow in this area. Areas with no flow are known as dead zones, and they result into significant reduction in the effective volume of the pond and the hydraulic retention time. Although the average retention time for the different scenarios show variations with the step-size, the shortest retention time was consistently found for the case when wind is blowing at the South-west direction with a speed of 2.5 ms^{-1} and the longest retention time occurred with a North-East wind with a speed of 4.25 ms^{-1} (Figures 3.8a-d). The South-west wind blows in the inlet-outlet direction hence enhancing fluid flow to the outlet while the North-East wind blows in the opposite direction to the inlet-outlet line, retarding fluid progress to the outlet and hence the resulted higher retention time. The case without wind yielded a retention time of 28.8 days which is close to the expected 29.1 days (Figure 3.8a).

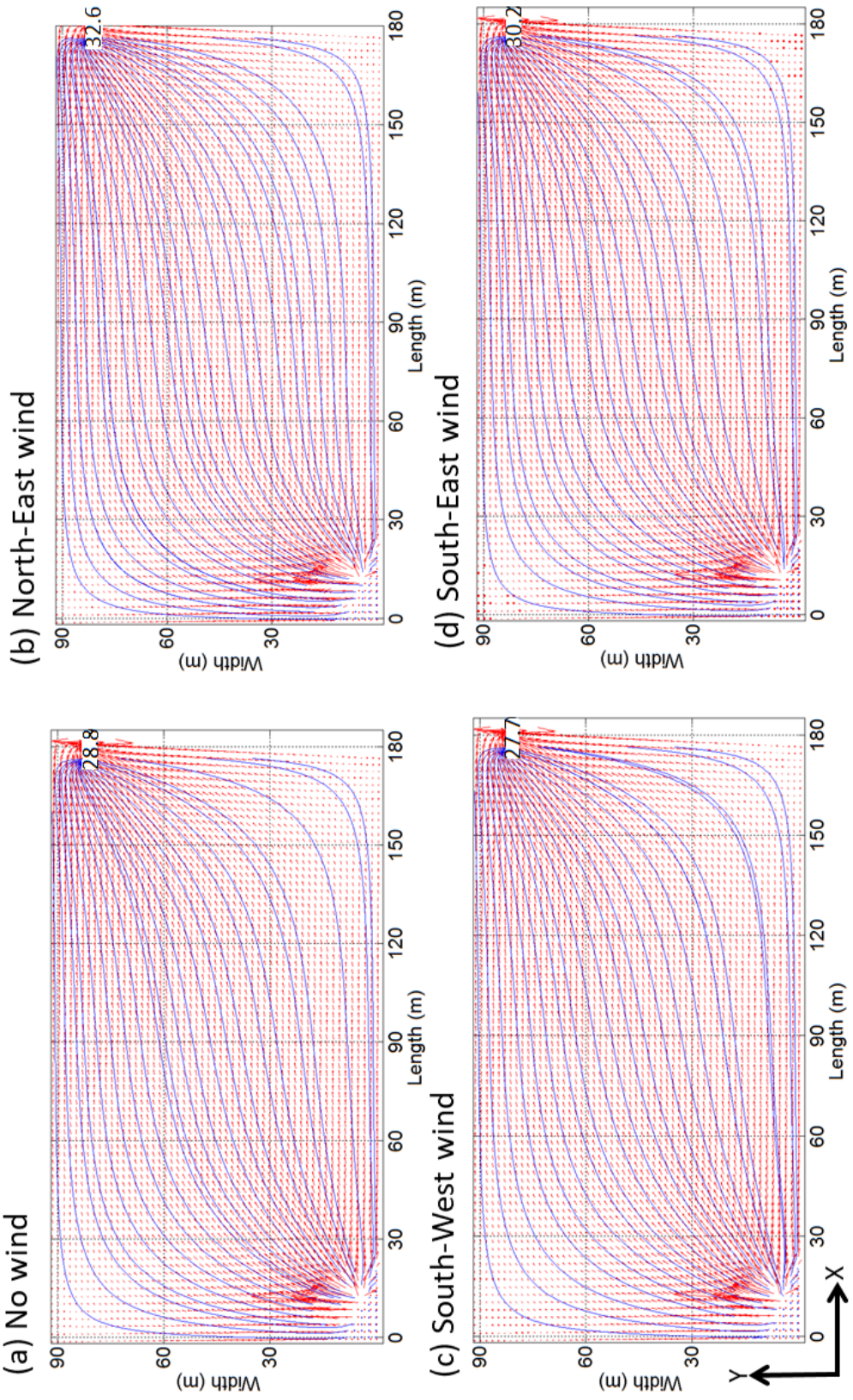

Figure 3.8: Flow path-lines to the outlet for different wind conditions

3.3.4 Travel path length and time

The path length to a node as well as the time taken for a particle to reach it were calculated using equations (3.3) and (3.5) and presented in Table 3.1 for both scenarios without and with wind. Without wind, travel path lengths range from 18 m (node 8 close to the inlet) to 221.2 m (node 25, close to the outlet). The average travel time followed the same trend with shortest travel time of 1.6 days for node 8 and longest travel time of 30.2 days for node T6. Since the depth averaged flow velocities for South-East and South-West winds are similar to that without wind, only parameters for the North-East wind were computed. The shortest travel length is that 12.8 m to node 7 and longest is 237.1 m to node 25. For travel time, the shortest is 0.9 day at node 8 and longest is 32.5 days to node T6.

The node data were then converted to spatial data in SURFER9 resulting into Figures (3.9 & 3.10). These show a steady progress of flow towards the outlet, forming quad-concentric lines of travel path length and time around the inlet. These are similar for both cases, but the shape is better defined for the case with wind. The parallel shape of travel path length and time curves imply laminar flow conditions in the pond, as well as minimal influence of wind on flow hydraulics. The theoretical HRT that represents the time that a particle spends in the pond, travelling from the inlet to the outlet, as calculated from the pond data (V/Q) is 29.1 days. Since our model estimates the travel time to the outlet of approximately 30 days for both cases with and without wind, it reasonably represents pond hydraulics Figure (3.10 a,b).

			Without wind		With NE wind	
Node	X	Y	Time [d]	Length [m]	Time [d]	Length [m]
8	30	0	1.6	18.0	0.89	21.5
3	0	30	2.3	23.4	2.4	15.2
7	30	30	2.7	31.6	1.6	12.8
T1	38	17	4.3	34.6	2.1	20
12	60	0	6.5	43.1	6.7	39.6
2	4	60	9.1	54.2	6.5	52.8
11	60	30	7.0	57.0	3.6	45
6	30	60	10.8	60.9	8.1	49.2
T2	66	29	6.9	61.9	8.4	54.9
16	90	0	12.2	70.3	11.9	70.8
15	90	30	13.0	77.3	11.1	77.8
10	60	60	13.0	82.6	9.6	67.6
T3	94	41	14.1	98.8	10.5	87.8
5	30	90	11.9	87.5	10.9	92.8
20	120	0	13.4	97.4	17.1	101.7
19	120	60	17.0	100.3	20.3	131.4
14	90	60	15.0	109.2	17.6	100.7
9	60	90	14.1	120.7	15.1	109.9
18	120	30	16.4	124.3	18.6	105.9
T4	122	57	17.9	124.8	22.3	120.7
24	150	0	20.3	126.5	23.4	132.9
23	150	30	22.5	128.4	26.8	134.9
13	90	90	12.7	145.6	18.7	153.3
22	150	60	27.6	154.1	26.5	144.3
T5	150	65	23.0	157.2	27.1	145.3
27	179	30	23.7	167.9	29.9	169.6
17	120	90	17.2	177.2	31.5	182.2
T6	177	78	30.2	182.3	32.5	179.8
26	181	30	31.2	189.1	27.9	183.9
21	150	90	20.5	210.9	27.1	204.3
25	183	0	25.4	221.2	29	237.1
	Maximum		**31.2**	**221.2**	**32.5**	**237.1**
	Minimum		**1.6**	**18.0**	**0.9**	**12.8**

Table 3.1: Hydraulic properties at different nodes for different wind scenarios

.

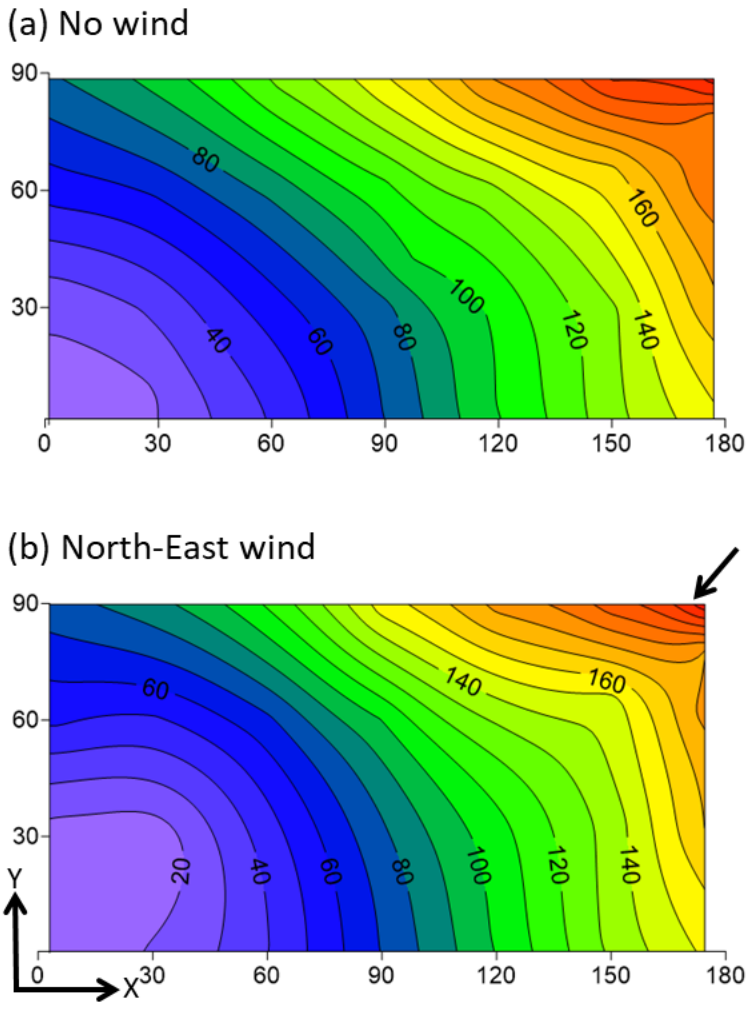

Figure 3.9: Travel path length [m] for different wind scenarios as indicated by the arrow

.

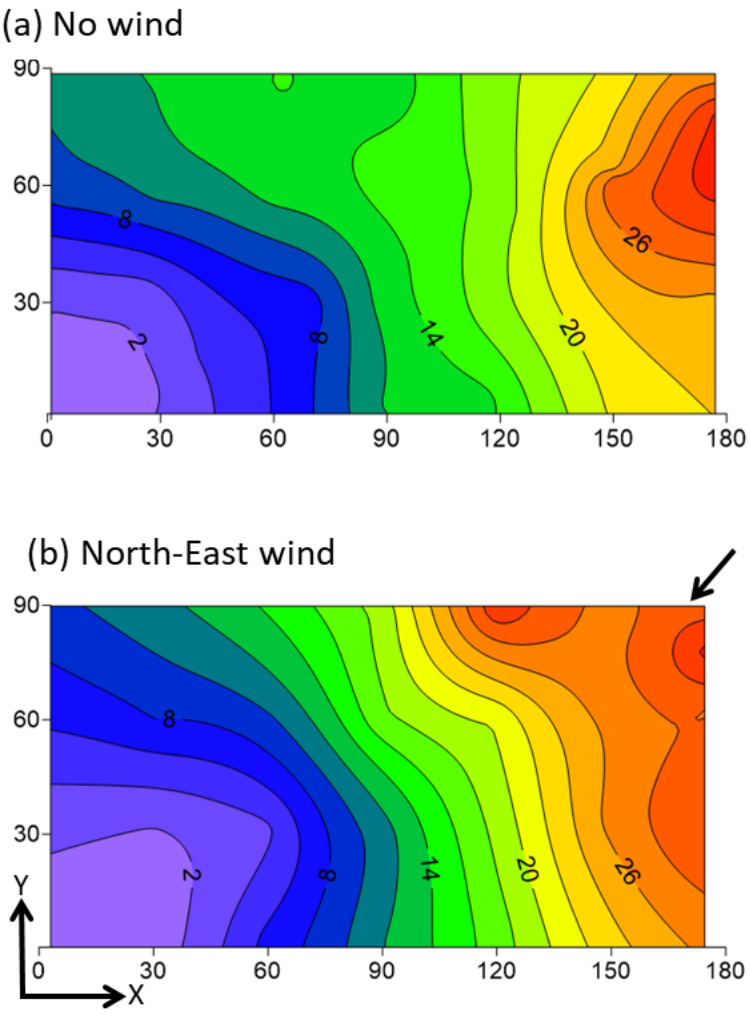

Figure 3.10: Travel time [days] for different wind scenarios as indicated by the arrow

.

3.4 Hydraulic sorting in the pond

3.4.1 Bottom particle size characteristics

Average particle sizes as calculated using data from Section 2.3.2 and using equation (3.6) ranged between 75.3 to 177μm. Higher average particle sizes were observed closer to the inlet but they progressively decrease along the travel path length to around mid-pond (Figure 3.11a). The decreasing average particle sizes are well defined in the areas with sedimentation identified in the previous chapter (area from the inlet enclosed by the dotted line in Figure 3.11(a). The lowest average particle size as can be deducted from this figure is 110μm. After mid-pond, the average particle sizes seem to decrease on the RHS edge while increase on the LHS edge. The larger particle size on the LHS edge could be a result of secondary deposition from the footpath running parallel to the pond as reported in Chapter 2. For areas closer to the outlet, the larger particle sizes are a result of re-suspension of the deposited materials occurring in this area.

The median particle sizes are lower than the average particle size in all sampled nodes (Figure 3.11b). Larger median sizes are observed close to the inlet and outlet consistent with the higher mean particle sizes. The sizes seem to decrease along the RHS edge while increase on the LHS edge, again similar behaviour as that of average particle size.

3.4.2 Relationship between deposited particle size and hydraulic characteristics

There exist a direct correlation between particle characteristics (represented by average particle size) and hydraulic characteristics as depicted in Figure 3.12.

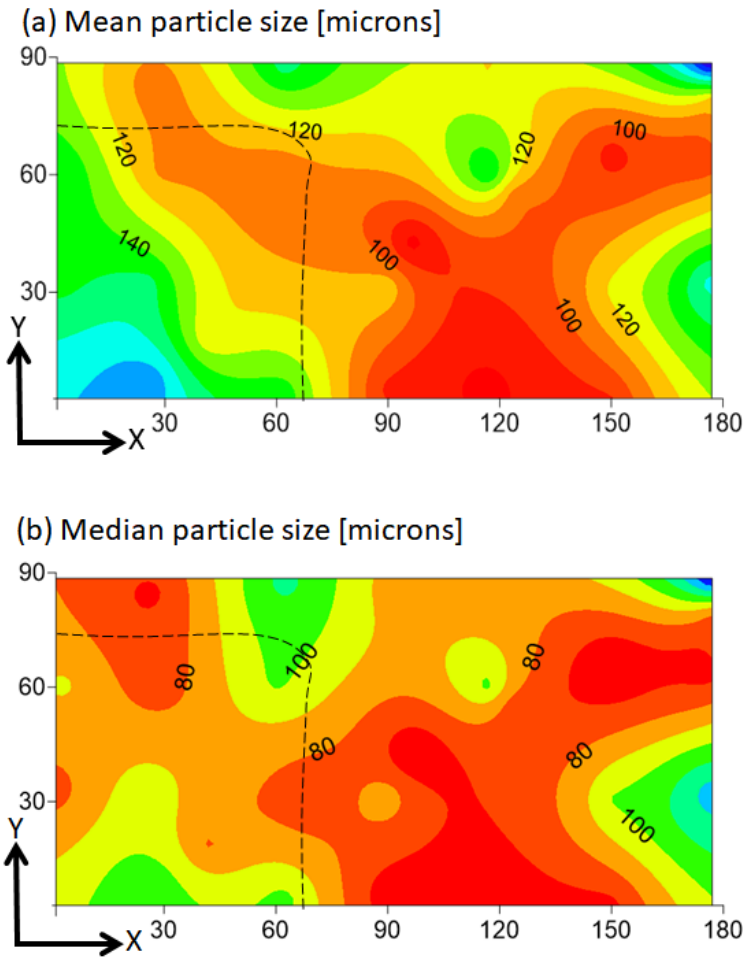

Figure 3.11: Particle size variations at the bottom of the pond. The dotted line marks the sedimentation areas as identified in the previous chapter

.

The correlation is strongest ($R^2 = 0.78$) for average particle size and path length, showing that, up to mid-pond, particles are deposited in order of their sizes, with larger particles deposited first closer to the inlet (Figure 3.12a). From mid-pond onwards toward the outlet, other processes probably diffusion dominates, and the average particle sizes are no longer decreasing along the travel path length. In fact, from mid-pond, the average particle sizes increase with the travel path length, which is in agreement with the Einstein's approximation equation for the diffusion of small spheres in fluid. Another strong correlation ($R^2 = 0.7$) exists for average particle size and travel time in days, showing that a sedimenting particle with average size of 100 μm may stay in suspension up to 16 days, while the larger particles are deposited earlier depending in order of their sizes.

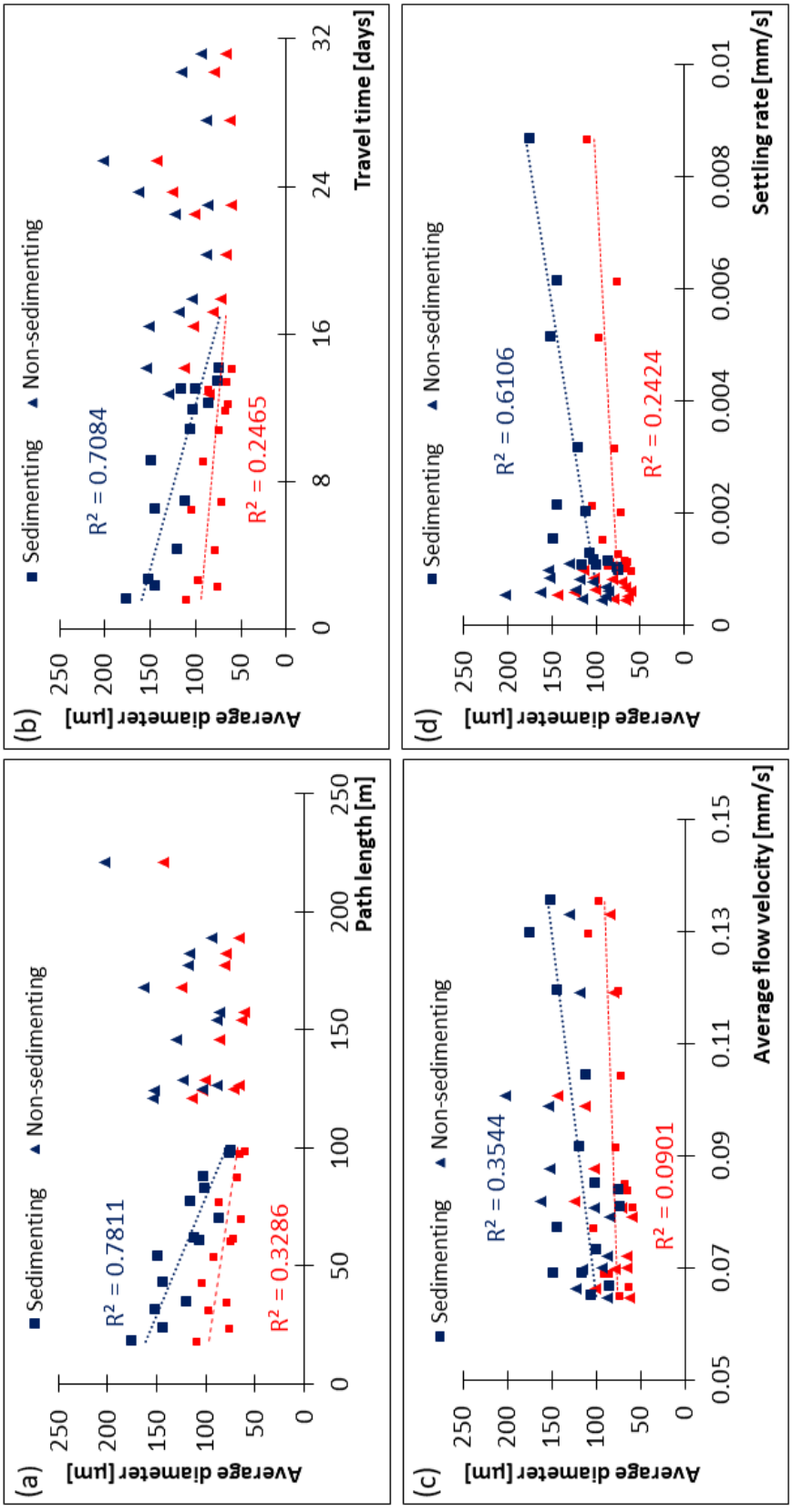

Figure 3.12: Correlation of particle characteristics and hydraulic parameters in the pond. Blue and red colors represent mean and median particle sizes respectively

Flow velocities do not seem to correlate with particle size (Figure 3.12c), and both sedimenting and non-sedimenting particles seem to exhibit similar flow velocities. Therefore the lateral progression/ advancement of particle is independent of their size which could account for the range of particle sizes (measured as PSD) at different location The above correlation analysis was repeated using median particle diameter. Similar trends were observed but at lower correlation coefficients and therefore it was considered better to use the average particle size as a representative size for particle size distribution.

3.4.3 Downstream fining

Particles were clustered in their respective size groups to study their variations with travel distance. Supracolloidal particles (1-100μm) were found in large percentages (52.5 to 94%) throughout the pond but their volume fraction is higher in areas without sedimentation (from mid-pond to the outlet) (Figure 3.13a &b). The areas with sedimentation have typically more settleable particles ($> 100\mu m$) ranging between 22.5 and 47.4%, and very little to none colloids. In areas with sedimentation, the volume of settleable particles decreased with increasing travel length as they settled out of the system, leaving behind smaller particles (Figure 3.13a). This phenomenon is known as downstream fining and is typical to areas with hydraulic sorting (Onyango, 1992).

3.5 Conclusion

This research modelled the hydraulic process in a primary facultative pond of a WSP, and linkage to the sedimentation process. It was observed that the pond has laminar flow with flow progressing from the inlet to the outlet, that persists

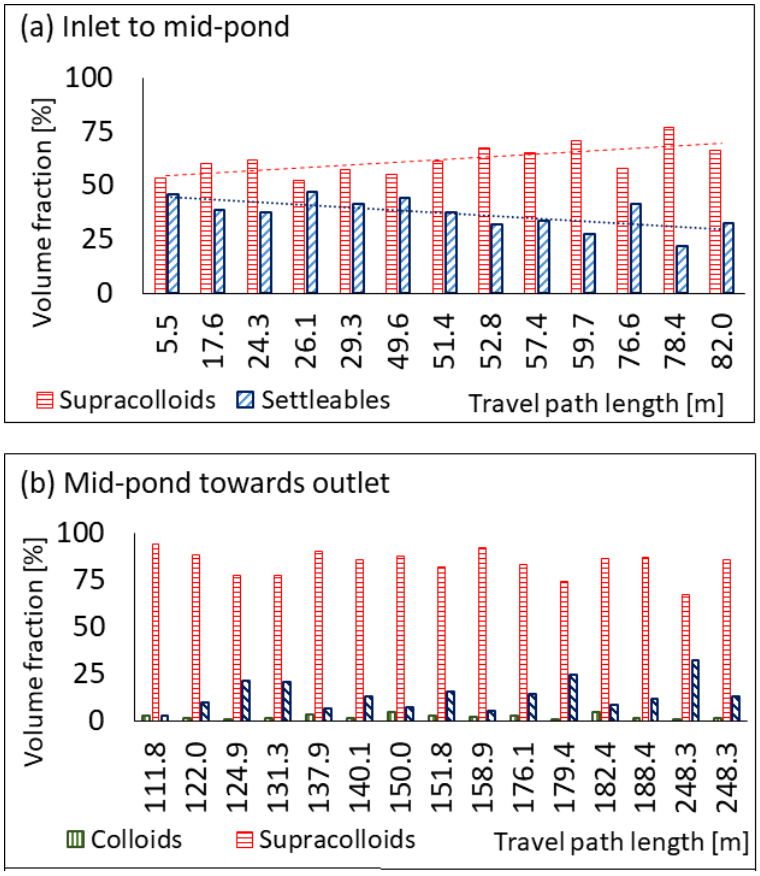

Figure 3.13: Variation in the volume fractions of different particles sizes (a) areas with sedimentation (b) areas without sedimentation

.

in the presence of wind. It should be noted that, systems designed for plug flow may actually exhibit mixed conditions if other parameters especially wind speed and direction are not taken into consideration. In contrast to other reported research, no any flow re-circulation (swirling) around the corners was observed for Buguruni WSP. Instead the corners opposite to the inlet and outlet have very low velocities and may be considered as dead spaces. The vertical flow vectors close to the inlet and the outlet explain the re-suspension of settled particles observed in the previous section. It was also observed that, hydraulic sorting occurs in the pond whereby particles are deposited in order of their sizes. This opens up the possibility of using hydraulic sorting model to locate different pollutants in sludge based on their hydraulic characteristics, i.e size and density.

Chapter 4

Model for estimation of particle density distributions (PDD)

4.1 Introduction

Physical characteristics of particles viz. size and density can be used to identify non-biodegradable pollutants such as helminth eggs in sludge. The presence of laminar conditions in the waste stabilization ponds facilitates the characterization of particles at different locations inside the pond. This is supported by the observed downstream decrease in mean particle size as well as percentage of larger particles as observed in Buguruni and outlined in Section 3.4. However, flocs have varying sizes and densities, complicating the application of this approach. Moreover, direct empirical measurements of waste water particle densities are very onerous to obtain. This chapter develops a model framework to estimate the spatial particle density distribution of wastewater particles (termed as PDD) using statistical approach and pond hydraulics simulated in Delft3D; and applies it to Buguruni WSP in Tanzania to locate helminth eggs in sludge. Since floc

density variations are complex, probabilistic approach is applied to account for the density of particles that sediment following hydraulic sorting only.

With the development of laser techniques for particle size analysis, particle sizes can be obtained fast and accurately through analysis of very small samples. The Stokes' equation which expresses the relationship between particle size and density difference, under the laminar flow conditions that normally exist in WSP enable estimation of particle densities. As particles in wastewater are incorporated in and settle out as flocs (Sengupta *et al.*, 2011), floc settling models are more suitable in estimation of densities of primary particles contained in a floc (Khelifa and Hill, 2006).

In this chapter, the distribution of the particle densities is re-constructed using an inverse method based on the derived distribution of marginal probabilities of diameters.

4.2 Model development

Buguruni WSP has a sewered system whereby, wastewater from washrooms and kitchens is collected and transported by pipes to the main sewer that carries it to the ponds. It is known that pollutants in wastewater are particles with sizes between 1 and 1000 μm, and about 50% are settleables (Izdori *et al.*, 2018). As the wastewater moves through the sewers, it is continuously mixed and therefore the pollutants are well mixed and randomly distributed. At the inlet, the pollutants (as particles) are discharged into the pond with the same advection velocity as that of the wastewater and settleables will immediately start descending to the bottom of the pond due to the gravitational acceleration.

When a particle is suspended in fluid, gravitational, advection, drag and diffusion

forces dictate its motion (Anderson, 1991; Haranas *et al.*, 2012). Gravitational force results from force of gravity, advection is caused by movement of the particle in the direction of fluid flow, drag is the resistance from fluid to particle movement, diffusion results from concentration and/or thermal gradients. Gravitational force (F_g) acts downwards and the rate of particle descent is influenced by the gravitational acceleration. This results into a more or less constant particle fall or terminal velocity (w_s) after a certain time interval. Advective force act in the direction of fluid flow, and is usually assumed that the particle advection velocity is the same as that of the fluid in which it is suspended. Diffusion is the movement of particles from area of high concentrations to those with low concentration, occurring with same magnitude in all direction for a well-mixed system. Considering the forces and assumptions above, the dotted line in Figure 6.1(a) shows the possible path that a particle may follow from the inlet towards the outlet, and gets deposited within the pond at a certain distance S from the inlet. The channel that encompasses the path traced by the particle is shown by the shaded area in Figure 6.1(a), assuming that only advection and settling dominates, and that there is minimal or no lateral movement of the particle. The particle path (i.e the shaded area) if cropped out and stretched will be the same as Figure 6.1(b).

Along the travel path, particles are deposited depending on certain characteristics. The observed spatial variations in the measured particle size distributions (PSDs) and average size (Izdori *et al.*, 2018) indicates the presence of hydraulic sorting as discussed in Chapter 3. The main factors for particle deposition in hydraulic sorting are the particle physical characteristics; that is shape, size and density (Onyango, 1992), hence minimum contribution from diffusion is expected. Ignoring the contribution from diffusion process, distribution of deposited particle sizes at a location S along the path-line can only be linked to changes in particle densities ρ_s, since constant density will result into single diameter in all sampling

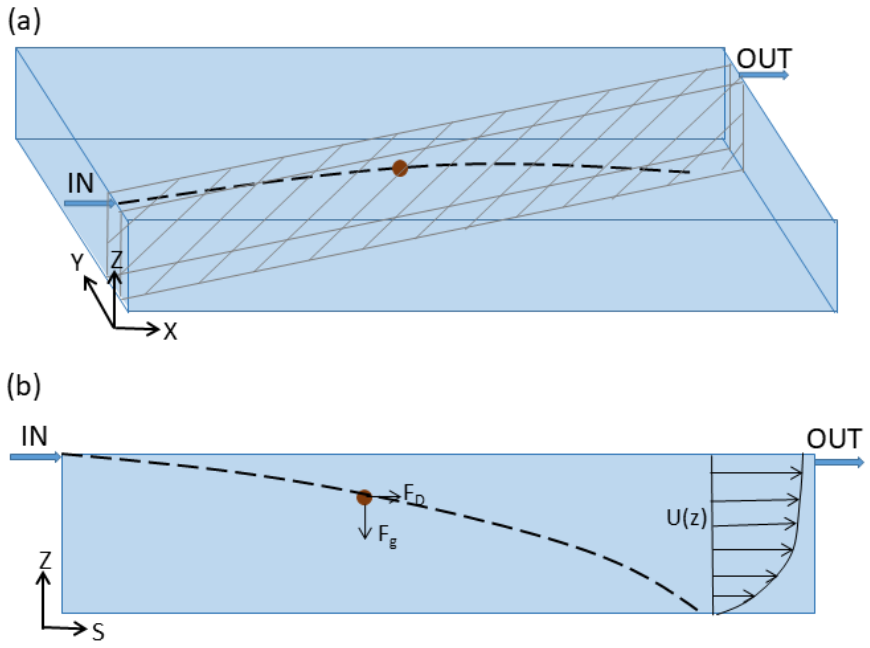

Figure 4.1: Model setup (a) Particle movement in 3D showed by the shaded area and (b) 1D representation of the path followed by the particle, shaded area in (a)

.

points and the PSD would be a peak around that diameter. The relationship is given by the deposition law predicting the distance, $L_{S(Z=h)}$ along the path-line where a particle of size D would travel within a water depth, h, after attaining the terminal velocity, w_s, and a laminar horizontal vertical velocity distribution profile, $U(Z)$, of the moving water (neglecting molecular diffusion hence assuming that particles progress by advection only). Doing some calculations in the idealized case of a straight 1D channel, such relationship is given by;

$$L_{S(Z=h)} = \frac{\rho g sin\alpha h^3}{3\mu w_s} \tag{4.1}$$

where g is gravitational acceleration, μ is the dynamic viscosity, ρ is the density of the water, and $sin\alpha$ is the slope of the equivalent straight channel responsible for the onset of the horizontal velocity. Considering the flow field, flow velocities

vary spatially hence we assign different equivalent slope angles to different nodes in the pond. w_s is the settling rate of wastewater particles as estimated from the Stokes law for a particle free falling in fluid given as;

$$w_s = \frac{g(\rho_s - \rho)d^2}{18\mu} \tag{4.2}$$

Where d is the particle size as measured using the Malvern Mastersizer 2000 and ρ_s is the density of the wastewater particles which is the unknown that we are looking to determine. However, wastewater particles are thought to exist as flocs, and therefore their settling rates may better be estimated using the modified Stokes equation for flocs as given in Khelifa and Hill (2006) as;

$$w_{s,m} = \frac{1}{18}\theta g \frac{(\rho_f - \rho)}{\mu} d_{50}^{(3-F)} \frac{D^{(F-1)}}{1 + 0.15Re^{0.687}}\phi \tag{4.3}$$

Where θ and ϕ represent the degree of sphericity and homogeinity of the flocs respectively, ρ_f is the density of flocs and D their sizes (diameters), Re is the flocs Reynold's number, d_{50} is the median particle diameter and F is the three-dimensional fractal dimension of flocs. If $Re << 1$, flocs are spherical $\theta = 1$ and nonporous (F = 3), and component particles are monosized $\phi = 1$, the equation simplifies to Stokes formula.

The settling time, τ_s, which is the time taken by particle to travel from the inlet at the top of the pond to deposition distance S at the bottom of the pond is obtained from the pond depth h and the modified average settling rate $w_{s,m}$ as;

$$\tau_s = \frac{h}{w_{s,m}} \tag{4.4}$$

Substituting the modified Stokes' equation (equation 4.3) into equation (4.1), we obtain

$$L_{S(Z=h)} = \frac{6\rho g sin\alpha h^3(1+0.15R_e^{0.687})}{\theta g(\rho_f - \rho)d_{50}^{3-F}D^{F-1}\phi} \tag{4.5}$$

Therefore, the relationship between diameter and density for particles/ flocs sedimenting at a distance $S(h)$ along a path-line is;

$$\rho_f = \rho\left(1 + \frac{6\rho g sin\alpha h^3(1+0.15R_e^{0.687})}{\theta g L_{S(h)}d_{50}^{3-F}D^{F-1}\phi}\right) \tag{4.6}$$

As the interest is to trace particles through their individual characteristics, it is useful to be able to establish characteristics of the individual (primary) particles making up the flocs. From Khelifa and Hill (2006), the effective density of flocs is related to the densities of primary particles making up the floc as:

$$\rho_f = \rho_s \frac{\sum_{i=1}^{k} d_i^3}{D^3} \tag{4.7}$$

where d_i and ρ_s represent the diameter and density of the primary particles making up the floc, respectively, while D and ρ_f are the floc diameter and density, respectively.

According to Khelifa and Hill (2006), equation (4.7) above can also be written as:

$$\rho_f - \rho = (\rho_s - \rho)(\frac{D}{d_{50}})^{F-3}\phi \tag{4.8}$$

where d_{50} is the median size of the component particles.

Equations (4.6) and (4.8) enable the establishment of the range of the densities of flocs and particles at different locations. The next task is to establish

the distribution of particle densities (PDD) at different locations. Let's name $p_x(D, \rho_s)$, the joint distribution of particle size and density at different locations in the pond. Then, the marginal distribution for diameters only for the deposited particles can be obtained from sampled data as;

$$p_S(D|\tau_s) = \int p_S(D, \rho_s) d\rho_s \tag{4.9}$$

or, analogously,

$$p_S(\rho_s|\tau_s) = \int p_S(D, \rho_s) dD \tag{4.10}$$

However, the joint distribution is unknown and cannot be measured. Therefore, a way is sough to reconstruct at least $p_S(D, \rho_s)$, which is the marginal density distribution of particles only.

Starting from sampled particle size distributions data, $p_S(D|\tau_s)$, at different distances S, whose hydrodynamic paths from the inlet is equal to L_S, the density distribution of particles (PDD) at different distances $p_S(\rho_s)$ can be established. Since the pond length L is larger than the water depth, d, then L_S at a node is the same for top and bottom.

As already stated, contribution from diffusion is assumed to be minimum and are therefore neglected for the time being. Therefore, there are no other sources of variability other than the particle density, and distribution of particle sizes at the measured point can only be explained by variability in their densities, ρ_s. Since we know the conditional distribution for particle sizes as measured at a given location, where particle deposit by following a path L_S in a time τ_S, then we can use the derived distribution approach in order to obtain the conditional distribution, $p_S(\rho_s|\tau_S)$ as per (Kottegoda *et al.*, 2008) as shown in equation 4.11 and elaborated in Figure 4.2. In this approach, the functional form relating

independent and dependent variables is assumed to be known with certainty. Therefore, it is possible to derive the PDF of the dependent variable from that of the independent variable.

$$p_S(\rho_s|\tau_S) = p_S(D(\rho_s))|\frac{dD}{d\rho_s}| \tag{4.11}$$

where $D(\rho_s)$ is obtained by inverting equation (4.6) and the term $|\frac{dD}{d\rho_s}|$ is the Jacobian of the transformation that renormalizes the distribution.

For the case of discrete distribution, then the derived distribution may be obtained straight forward as

$$p(\rho_s|\tau_S) = p(D|\tau_S) \tag{4.12}$$

This distribution $p(\rho_s|\tau_S)$, is thought to be conditional to the particular location at the bottom of the pond, calculated as $L_S = \bar{V} * \tau_S$ where $\bar{V}$ is the average flow velocity along the travel path-line and τ_S is the settling time as calculated from equation (4.4). Thus, different nodes in the pond that have the same travel path length L_S are expected to have the same distribution $p_x(\rho_s|\tau_S)$.

4.3 Results

4.3.1 Particles settling rates

The parameters of equation (4.1) are easily obtainable from pond parameters as well as the results of hydraulic modelling in the pond discussed in Chapter 3,

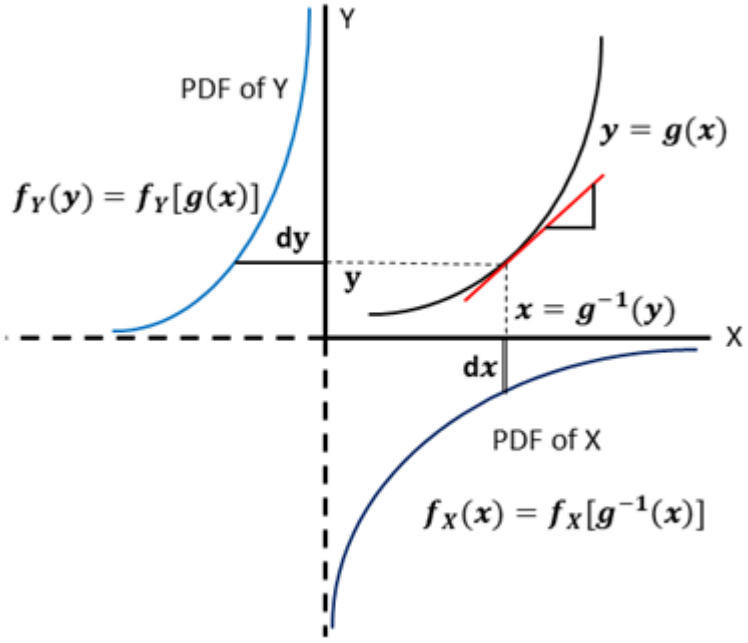

Figure 4.2: Derived distribution approach framework where dependent variable, $y = g(x)$ is a function of a single, continuous, and independent variable, $x = g^{-1}(x)$. $f_X(x)$ and $f_Y(y)$ are PDFs of x and y respectively (extract from Ramirez (2018)).

leaving the settling rate w_s as the only unkown. These parameters were used to estimate the range of settling rates in the pond, results of which are discussed here. Results show that, the settling rate is highest near the inlet and decreases towards the outlet (Figure 4.3). The highest settling rate for wastewater flocs in the primary facultative pond of Buguruni WSP is around 0.08 mm/s, observed in a narrow band at the inlet. From 0.08 mms^{-1}, the settling rate drops fast to 0.02 mms^{-1} about mid-pond and lower than 0.01 mms^{-1} onwards up to the outlet.

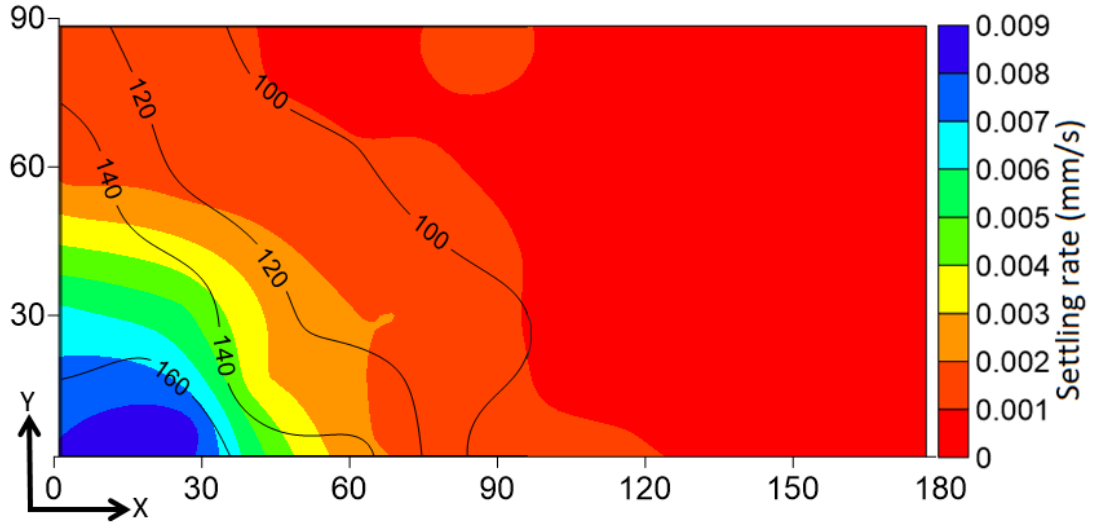

Figure 4.3: Spatial distribution of settling rates, w_s $[mms^{-1}]$ estimated from equation 4.1 and average particle sizes (represented by contour lines) from sampled data $[microns]$

Compared to settling rate of flocs reported in research, these appears to be very low (Figure 4.4, blue diamonds). This was thought to result from the low incoming discharge of 0.0077 m^3s^{-1} that results into low flow velocities in the pond hence low settling rates are permissible. A simulation with about 2.5X the normal discharge (0.02 m^3s^{-1}) was done in Delf3D. As expected, the resulted settling rate were higher, spreading over a wider range of densities than when the discharge was 0.0077 m^3s^{-1}. The estimated settling rates for nodes close to the inlet become similar to the reported settling rates of flocs in literature while those further from the inlet still have lower densities (Figure 4.4, red circles). Therefore, this shows

a potential of increasing discharge into the pond up to more than twice the design discharge without compromising the sedimentation process. It should however be noted that this will have a significant impact on the biological activities in the pond as the hydraulic retention time is also reduced (for the discharge of 0.02 m^3s^{-1}, the hydraulic retention time is reduced to 12 days).

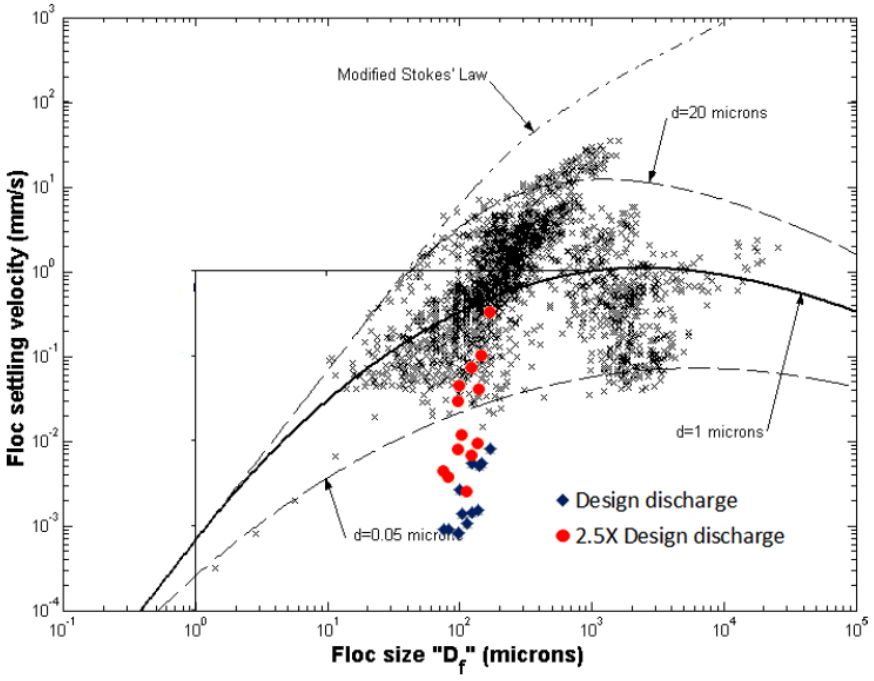

Figure 4.4: Comparison of estimated settling rates and other researches as extracted from Khelifa and Hill (2006)

4.3.2 Estimation of the fractal value, F

The fractal value of flocs is a number used to express the complexity of a floc's external shape, F can have any value between 0 and 3, with 0 representing totally fragmented particles while 3 is for primary particles. The fractal value can also give information on the mechanism of flocculation of particles (Logan and Wilkinson, 1990). From the information we have, the fractal value F can be

estimated by the expression proposed by (Johnson *et al.*, 1996) i.e. $F = n - 1$ where F is the fractal value and n the value of the power in the settling rate-particle diameter relationship.

Contour lines of average particle sizes at different locations in the pond where sedimentation is taking place were plotted using data from Chapter 2, and superimposed over the settling rate map (Figure 4.3). The trend is similar to that of settling rate, i.e. particle sizes decrease with increase in distance from the inlet, with 100 μm as the minimum average particle size for sedimentation. The settling rate shows a good power relationship with the average particle diameters, which is a property of fractal objects. Using log-log plot in Figures 4.5 and 4.6, the estimated fractal value of 2.6 suggests that flocs are formed through particle- cluster aggregation, whereby individual particles are incorporated into flocs resulting into higher fractal values ($2.5 < F < 3$), as opposed to cluster-cluster aggregation, which results into lower fractal dimensions ($1.6 < F < 2.2$, information extracted from Logan and Wilkinson (1990)). Determination of the fractal value for individual data collected at different dates resulted in values between 2.5 to 2.9 (Figure 4.6).

4.3.3 Floc densities

Equation (4.6) was used to estimate floc densities with the values of θ (representing floc sphericity) and ϕ (representing homogeneity of particles sizes) set to 0.3 and 0.8 respectively. The computed densities in the pond vary between 2019.2 and 1000 kgm^{-3} for flocs. Highest density values are found close to the inlet, decreasing inwards. At the nodes, floc densities decrease with increasing floc size possibly due to increase of porosity. Highest densities are observed for particles with a median class of 5 μm, dropping fast for the next median class of 15 μm after which the density values are slightly more than that of water that is 1000

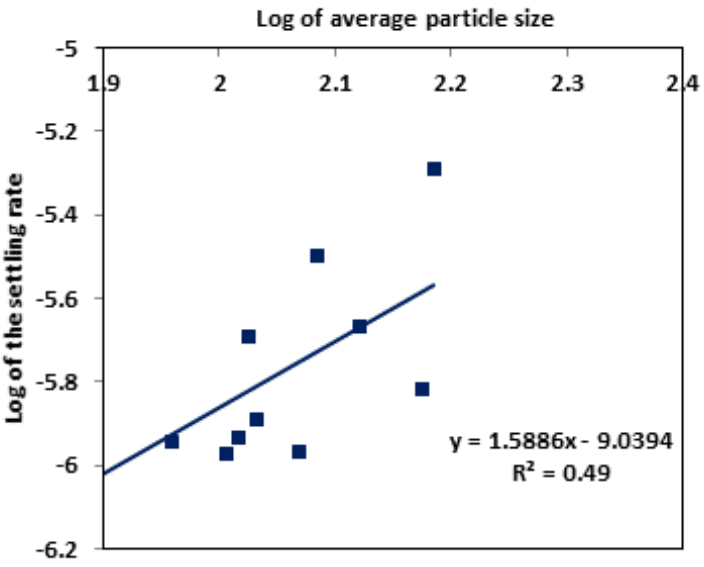

Figure 4.5: Estimation of the fractal value using the data represented in Figure 4.3.

kgm^{-3}. In most of the sampling locations (nodes), flocs as small as 60 μm already have densities close to that of water. This could be due to very low settling rates as shown in Figure 4.4, allowing even small particles to settle. Altering the values of θ and ϕ to represent spherical floc shapes and wide range of particle sizes respectively resulted into higher densities for only the smallest particle sizes, 30 μm and below, but the rest still had almost the same densities. Therefore the values of 0.3 and 0.9 for θ and ϕ respectively were adopted. This therefore implies that the flocs are of irregular shapes, and composed of particles with similar sizes. The pdf of densities shows almost constant probabilities for all the particle densities, with very mild peaks at around 1000 kgm^{-3}.

Comparison of our results and the measured as well as results from other models reported in Khelifa and Hill (2006) is shown in Figure 4.7. This publication was chosen as it combines measured data from 26 publications and five common models used in estimation of floc densities. The models, as referenced in Khelifa and Hill (2006) are Tambo and Watanabe (1979), Hawley (1982), McCave (1984), Kranenburg (1994) with d = 4 μm and Lau and Krishnappan (1997).

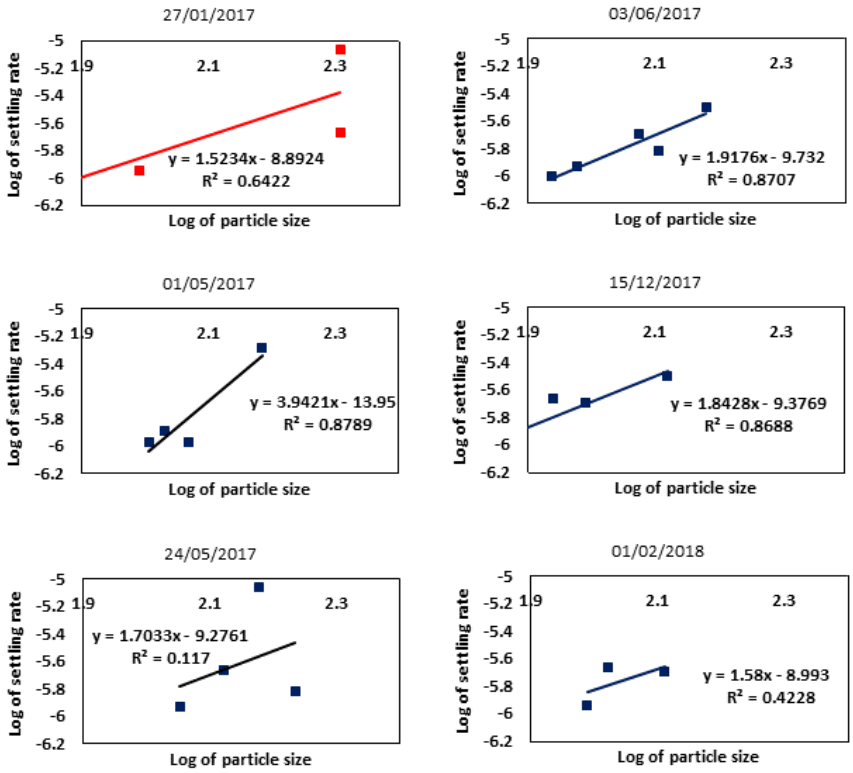

Figure 4.6: Relating average particle size and settling rate at nodes for data collected in different dates. The red color represent dry season while the blue color is rainy season.

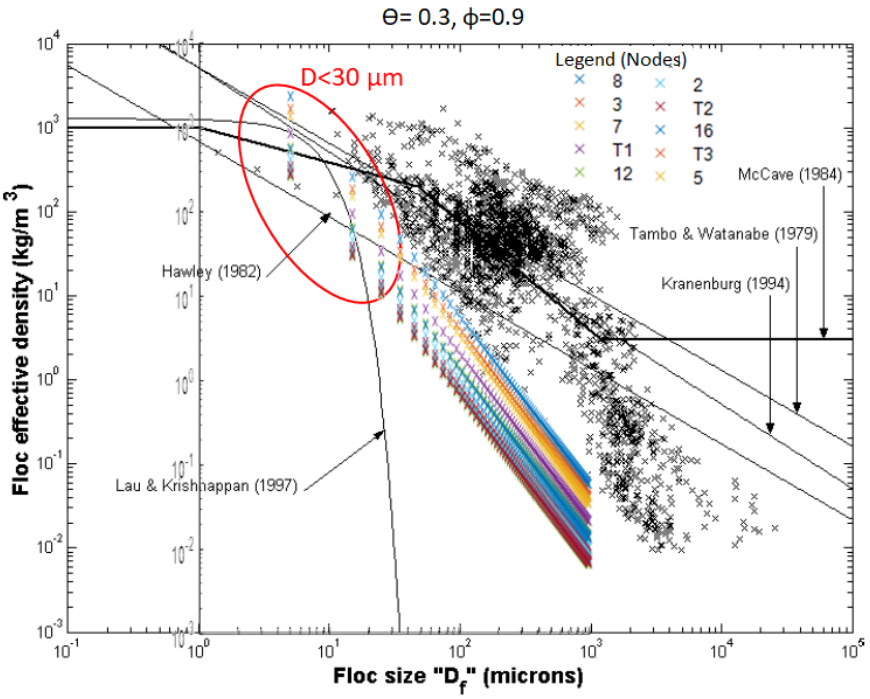

Figure 4.7: Comparison of our results and the measured (black cross-symbols) and modelled extracted from Khelifa and Hill (2006).

Since in reality density values are discrete, results from equation 4.12 were clustered into $1kgm^{-3}$ density intervals to form histograms with classes as shown in Figure 4.8. It is observed that most of particle densities fall in the range of 1000.45 to 1006.45 kgm^{-3}. The density value of 1000.45 kgm^{-3} which is almost the density of water seem to be common, with more than 50 % of particles having this density. The percentage of particles with densities between 1000.45 and 1006.45 kgm^{-3} varies from 64.1 at node 3 to 88.6 % at node 2. The percentage of particles in this density range seem to increase with travel path length towards the outlet (Figure 4.11, red coloured markers). These may represent the majority of wastewater flocs, that are found throughout the pond and settle gradually along their travel paths from the inlet to the outlet. The fact that the percentage of these particles increase with travel path length may imply that they form majority of particles in these areas. This is a result of heavy particles settling out of the system before first, leaving behind the lighter ones.

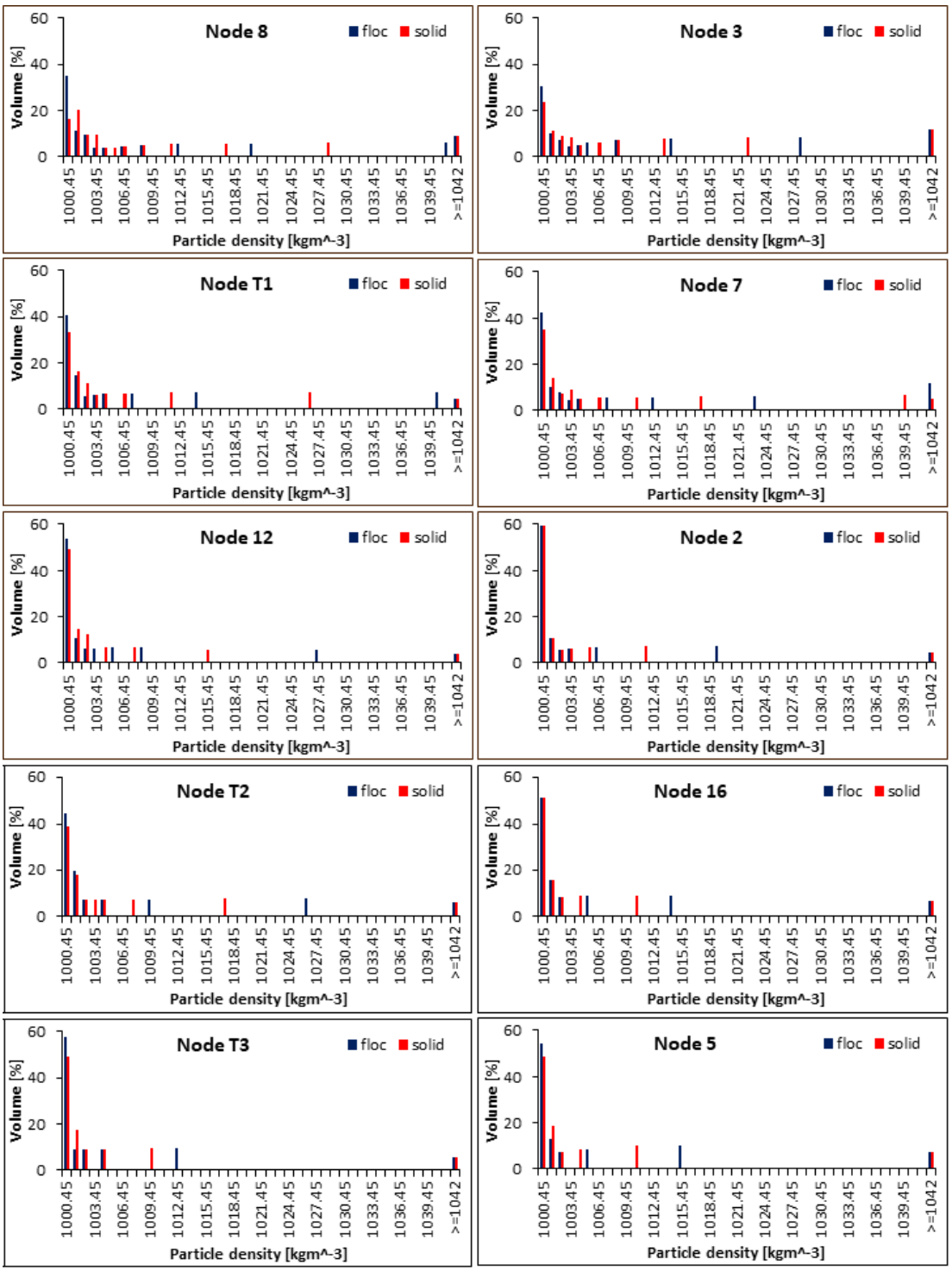

Figure 4.8: Histograms of densities at different locations in the pond.

The percentage of flocs with densities greater than 1010 kgm^{-3} from all nodes are combined in Figure 4.9. It can be seen that, a continuous range of densities exist between 1010 and 1030 kgm^{-3}, with a median density value of 1020 kgm^{-3}. The highest percent of these particles is 16.7% at node 3 and the lowest is 7.4% at node T1. The rest of density values up to 2019.2 kgm^{-3} are randomly scattered to different nodes. Estimation of the densities of primary particles making up the flocs using the model proposed by Khelifa and Hill (2006) revealed particle densities not very different from those of flocs (Figure 4.8, red histograms). The percent of particles with densities greater than 1010 kgm^{-3} varies from 13.9% at node T2 to 26.7% at node 3. The percentage of particles with this density range (greater than 1010 kgm^{-3}) seem to decrease along the travel path length, as shown in Figure 4.11, blue coloured markers. This means that, these are particles that get settled out of the system hence why they decrease.

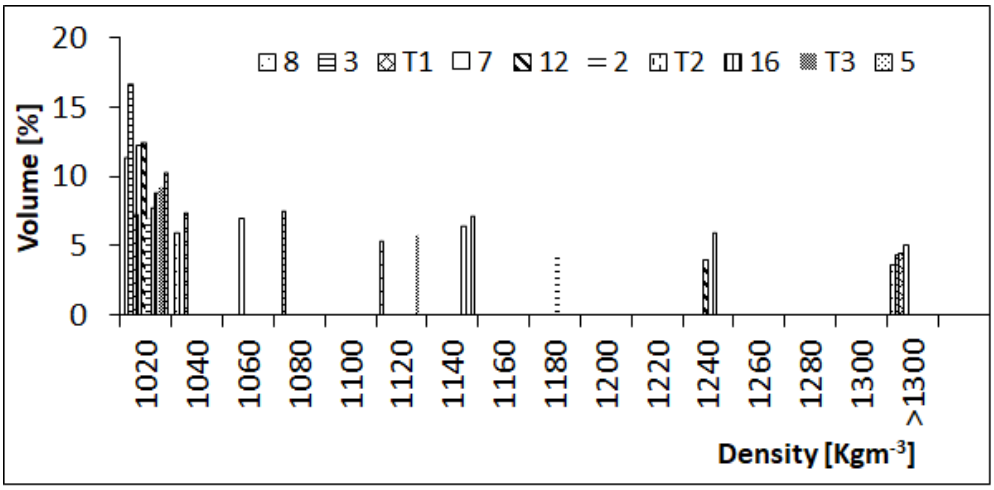

Figure 4.9: Percentage of particles with densities greater than 1010 kgm^{-3}. Numbers in the legend are for the different nodes.

All the samples of wastewater from top and bottom had a green color, indicating presence of micro-organisms presumably algae (Figure 4.10a). When observed under a microscope, a large number of zig-zag shapes were seen, which were identified as the filamentous cynobacteria *Arthrospira fusiformis* (Figure 4.10b). The

abundant presence of the cynobacteria *Arthrospira fusiformis* poses a possibility that these free floating micro-organisms are the major components of the lighter flocs. These micro-organisms have cell diameter ranging between 3–12μm, though occasionally it may reach up to 16 μm. The helix pitch of these cells typically ranges from 10–70 μm and its diameter from 20–100 μm.

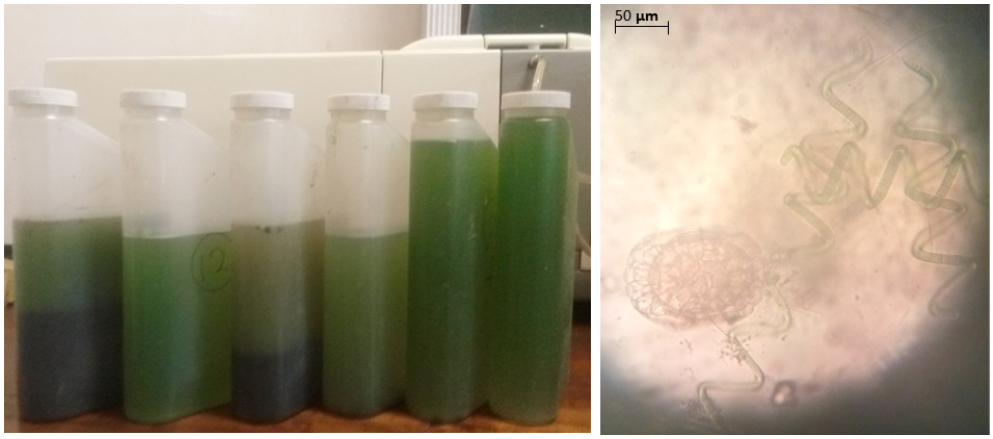

Figure 4.10: Photos showing presence of algae blooms in the pond. (a) 1L bottles containing samples collected in the pond (b) *Arthrospira fusiformis* (zig-zag shapes) as observed under the microscope.

Therefore, the densities of particles in Buguruni facultative pond may be categorized into two. The first group are the 'lighter' particles that are the majority, constituting up to 88.6 % of all particles in some nodes. These have densities between 1000.45 to 1006.45 kgm^{-3} and are believed to require flocculation for them to settle hence why their volume increases along the travel path length (Figure 4.11, red markers), as they get more time to form larger flocs with sufficient settling rate to sediment. The density of 1000.45 kgm^{-3} may be taken as a representative for this group as the highest volume of particles (more than 50 %) have this density. The second group are the 'denser' particles that do not require to form flocs as they already have sufficient settling rate to settle out of the system hence they settle immediately upon entering the pond and their volume decreases

along the travel path length (Figure 4.11, blue markers). This group seem to exhibit random density values at different nodes, with large gaps from one density value to the other. Also, it appears that there is no common density values for the different nodes. However, all the nodes appear to have density values between 1010 to 1030 kgm^{-3}. This form some kind of a continuous distribution between these two values with a median density at 1020 kgm^{-3}. The highest volume of particles at the different nodes have the density between these two values and therefore the density of 1020 kgm^{-3} may be used as a representative density for this group.

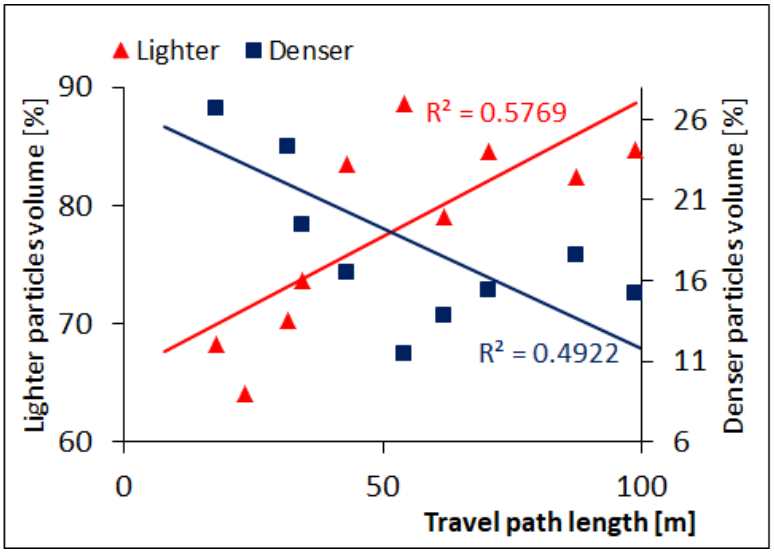

Figure 4.11: Variations particle volumes according to their density characterization along the travel path length.

4.3.4 Particles with densities similar to that of helminth eggs

Helminth eggs have densities between 1056 to 1300 kgm^{-3}. The percentage of particles falling under this category was calculated by summing up the probabilities of particles with densities above 1056 kgm^{-3} as there is a possibility

Node	Density	
	Particles [%]	Flocs [%]
8	9.2	9.2
3	12.1	12.1
T1	4.6	4.6
7	5.1	12.1
12	4.1	4.1
2	4.4	4.4
T2	6.0	6.0
16	6.5	6.5
T3	5.9	5.9
5	7.2	7.2

Table 4.1: Probability of finding flocs/ particles with the density similar to that of helminth eggs at different nodes.

of more than one egg to be contained in the floc hence producing much higher density values. Results show that, the volume of particles in this category ranges between 4.1 % at node 12 to 12.1 % at node 3 (Table 4.1). However, there is a possibility of helminth eggs to be contained in large flocs with lower densities than the range of 1056 to 1300 kgm^{-3}. This could explain the observed interaction of the different egg types with other particles, resulting in both reduced and increased settling velocities in wastewater as reported (Sengupta *et al.*, 2012a, 2011).

4.4 Conclusions

This chapter aimed at establishing the particle density variations inside Buguruni WSP. Results show that, particle densities fall in two categories; lighter particles with a representative density of 1000.45 kgm^{-3} and denser particles with a representative density of 1020 kgm^{-3}. The lighter particles are the majority

forming between 64.1 and 88.6 % of all particles in the nodes, and settle out by clustering to form larger flocs. They appear almost consistently in all nodes. The denser particles form about 13.9 % to 26.7 % of all particles in the nodes. These particles are believed to be capable of settling out of the system discretely, although may form flocs due to the flocculent nature of wastewater particles. Improving the estimation of settling rates and separating the floc sizes in the determination of the fractal value, F, could improve the model performance.

Chapter 5

Morphodynamics of waste stabilization ponds (WSP)

The material presented in this chapter appears in:
Izdori, F., Semiao, A.J.C., Perona, P. (2019). The role of environmental variables in waste stabilization ponds' morphodynamics. Frontiers in Environmental Science, 7, p159.

5.1 Introduction

Sludge accumulation patterns impact the pond hydraulics directly as a result of reduction in the effective pond volume and modified pond bottom surface (Murphy, 2012; Alvarado *et al.*, 2012a; Coggins *et al.*, 2017; Rodrigues *et al.*, 2015). Although some research suggests that sludge accumulations result into longer HRT (Alvarado *et al.*, 2012a) and do not cause any significant reduction in organic pollutants removal (Passos *et al.*, 2014a), nutrients removal especially nitrogen seem to be significantly affected by the presence of sludge (Passos *et al.*,

2014a). Also, helminth eggs content of sludge is associated with its distribution in the pond; that is, areas with higher sludge depth tend to contain more helminth eggs (von Sperling *et al.*, 2003; Nelson *et al.*, 2004). Therefore, the correct prediction of sludge accumulation patterns is important not only for the proper functioning of the pond, but also for identification of areas with sludge containing helminth eggs as well as a tool during design to select the best design option. Helminth eggs are resistant to inactivation and can survive for several years in the environment, hence proper handling of sludge in which they are present is important to prevent environmental contamination. Lack of information on sludge accumulation rates and distribution is a major factor for the poor management of sludge from WSP (Nelson *et al.*, 2004). It is thought that, correct prediction of areas with sludge containing helminth eggs can contribute to reduction of sludge treatment cost, as only the contaminated sludge will be treated through thermophilic sludge digestion at temperatures above 45°C that ensures their destruction.

Sedimentation and hence sludge accumulation patterns in WSP is complicated by the non-stationary nature of the inputs and environmental factors such as weather variables, that are mostly site specific. Sludge accumulation depends on hydraulic factors including pond geometry, inlet and outlet characteristics, mixing conditions, dead-zones, etc (Abis and Mara, 2005; Alvarado *et al.*, 2012a; Coggins *et al.*, 2017; Ouedraogo *et al.*, 2016; Murphy, 2012; Nelson *et al.*, 2004). Wind pattern and magnitude can be dominant driving forces of WSP hydraulics Badrot-Nico *et al.* (2009); Brissaud *et al.* (2003); Gu and Stefan (1995), therefore a strong influence of these variables in sludge accumulation is expected but there is no research exploring this. Ponds with single inlets as well as facultative ponds tend to have highest sludge deposits at the proximity of the inlet while those with multiple inlets and maturation ponds have uniformly distributed sludge patterns throughout their bottoms (Abis and Mara, 2005; Coggins *et al.*, 2017; Nelson

et al., 2004). Also in facultative ponds, sludge accumulation patterns follow flow velocity distribution, with higher flow velocities areas having higher sludge depths (Alvarado *et al.*, 2012a). Changes in sludge levels and patterns are also linked to environmental factors such as climate and secondary sources of particles including plants that shed seeds and leaves, and algal and bacteria populations in the pond (Papadopoulos *et al.*, 2003; Abis and Mara, 2005). Climatic and environmental factors are site specific and result into spatial differences in sludge accumulation rates and patterns between ponds.

The reviewed studies for sedimentation in shallow ponds involved experimental modelling in laboratory scale ponds, where the impact of environmental factors is minimal (Camnasio *et al.*, 2013; Dufresne *et al.*, 2010; Kantoush *et al.*, 2008). The numerical model studies such as that of (Alvarado *et al.*, 2012a; Coggins *et al.*, 2017; Ouedraogo *et al.*, 2016) looked at the impact of sludge accumulations in pond hydraulics, without accounting much for what influences the sludge accumulations. Therefore this study fills the gap between these two sets of studies by setting up a numerical sedimentation model that simulates the sludge accumulation patterns in the primary facultative pond of an operational Buguruni WSP in Tanzania. Also, the role of the different factors such as wind, influent discharge and suspended solids concentration is investigated.

5.2 Materials and Methods

The methodology for this research included on-site data collection and setting up of a sedimentation model in Delft3D. A very important step in sedimentation modelling is the setting up of a hydraulic model for the system. However, Delft3D has an option for including sedimentation as a process in the hydraulic model, an approach which was used in this research. The data sets needed to set-up and

calibrate the hydraulic and sedimentation model in Delft3D are described below. These are categorized into pond data (discharge, sludge levels, suspended solids concentration and pond geometry) and the hydrometry data that describes the climate of the area (if it is anticipated that there will be an influence on the pond hydraulics) and may include rainfall, wind and temperature.

5.2.1 Sludge and discharge data

The Buguruni WSP has a design discharge of 0.0077 m^3/s. The inlet channel is fitted with a V-notch weir for discharge measurement, with a maximum capacity of 0.06 m^3/s, equivalent to a head of 30 cm which is the maximum height of the weir. Random measurement of discharge during the study period between December 2016 and December 2018 showed discharge ranging between 0.0044 m^3/s and 0.0085 m^3/s. About 5 random discharge measurements were done during the different data collection campaigns. For sludge data, the 90 m $\times$ 183 m $\times$ 1.2 m WSP was gridded into 30 $\times$ 30 m cells and sludge level measurements were done twice (January 2017 and January 2018) at the nodes given in Figure 2.2, using the white towel method as described in (Mara, 2004). In the white towel method, a white towel (in this case a white muslin cloth) is wound on a long straight pole up to the height of the total pond depth. The pole is then dipped into the pond until it reaches the hard consolidated sludge and can no longer be pushed further. Upon pulling the pole out, sludge deposits will stick on the white cloth showing the end of deposited material. This was recorded as the sludge depth at that location. A clean muslin cloth was used for every node. Despite its simplicity, the white towel method will have a vertical error of about $\pm$ 5cm due to presence of slurry close to the pond bottom, capillarity and the towel absorption. The sludge depths were then processed in MATLAB to convert them into spatial data.

5.2.2 Hydro-meteorological data

The study aims at studying the impact of climatological parameters that may have effect on sludge accumulation. Increased discharge has virtually been observed during rainy season, most likely due to defective toilets and pipes allowing flow into the system. Discharge values ranging from the minimum observed discharge ($0.0044\ m^3s^{-1}$) up to about $0.02\ m^3s^{-1}$ were used to study the effect of discharge on pond hydraulics. Dar es Salaam has two wind seasons according to the wind orientation. The first season lasts from November through to March during which period wind blows mainly in the North-East direction (45°), with average value of $4.25\ ms^{-1}$. The second season is from April to October during which wind blows in the South-West direction (225°) in the morning and South-East direction (135°) in the afternoon, with an average speed of $2.5\ ms^{-1}$ (Mahongo, Francis, and Osima 2012). Hydraulic simulations for both of these three cases were run in Delft3D.

5.2.3 Hydro-morphodynamic model

The simulation was set up in the multi-dimensional Delft3D open source software supplied by Deltares; utilized the hydrodynamic and sediment transport sub-modules, detailed in Deltares (2016). In the sedimentation model, the mass balance (advection-diffusion) equation for sediment transport, equation 5.1, is solved using velocity and eddy diffusivities from the hydraulic model. The simulation was run for a period of 2 years at a 1 minute time-step to keep the Courant number less than the required minimum of $4\sqrt{2}$, with an initial water level of 1.2 m and suspended solids concentration of $0.35\ kgm^{-3}$. Discharge values ranging from the design discharge of $0.0077\ m^3s^{-1}$ (taken to represent the dry weather discharge in this study), up to the maximum of $0.02\ m^3s^{-1}$ and average

suspended solid concentrations ranging from the measured average value of 0.35 kgm^{-3} to a maximum of 5 kgm^{-3} were used in different combinations to represent the contribution of storm run-off inflow into the pond due to defective system.

$$\frac{\partial C}{\partial t} + \frac{U}{\sqrt{G_{\xi\xi}}}\frac{\partial C}{\partial \xi} = 0 \tag{5.1}$$

Where C is the concentration of sediments, U is the depth-averaged velocity in ξ-direction, $\sqrt{G_{\xi\xi}}$ is the coefficient used to transform curvilinear to rectangular coordinates.

For cohesive sediment fractions the fluxes between the water phase and the bed are calculated with the well-known Partheniades-Krone formulations outlined in equations 5.2, 5.3 and 5.4;

$$E^{(l)} = M^{(l)} S(\tau_{cw}, \tau^{(l)}_{cr,e}), \tag{5.2}$$

$$D^{(l)} = \omega^{(l)} c^{l}_{b} S(\tau_{cw}, \tau^{(l)}_{cr,d}), \tag{5.3}$$

$$c^{(l)}_{b} = c^{(l)}(z = \frac{\delta z_b}{2}, t), \tag{5.4}$$

Where; $E^{(l)}$ is the erosion flux $[kgm^2s^1]$, $D^{(l)}$ is the user-defined erosion parameter EROUNI $[kgm^2s^1]$ and $c^{(l)}_{b}$ is the erosion step function, 0 when maximum bed shear stress, τ_{cw} is greater than the user-defined critical erosion shear stress TCEUNI, $\tau_{cr,e}$ in $[N/m^2]$ and $\tau_{cr,d}$ is the user-defined critical deposition shear stress TCDUNI $[N/m^2]$.

5.3 Results and Discussion

5.3.1 Spatial-temporal sludge distribution

Measured sludge depth ranged from about 0.2 to 0.8 m in 2017 and 0.2 to 1.2 m in 2018. Measurements show that most sludge is deposited near the single inlet similar to observations from (Abis and Mara, 2005; Alvarado *et al.*, 2012a; Coggins *et al.*, 2017; Ouedraogo *et al.*, 2016; Murphy, 2012; Nelson *et al.*, 2004) (Figure 5.1). The sludge depth decreases gradually along the inlet- outlet path, from a maximum of 0.8 m (2017) and 1.2 m (2018) around the inlet to 0.3 m (2017) and 0.2 m (2018) at node T5 which is 150 m from the inlet. At node T6 which is almost at the outlet, the sludge depths seem to peak again in both years. In 2017, there are less deposits around the inlet but deposits extend more along the inlet-outlet path and along the inlet side bank. These extensions disappear in 2018 although their traces can be seen for example by the small island in the middle of Figure 5.1b. Profiles along the X-axis and Y-axis are presented in Figures 5.2 and 5.3 to get a detailed view on the sludge depth variations. For clarity, the longer edges will be referred to as banks and the shorter ones where the inlet and outlet are located will be referred to as inlet and outlet edges. The profiles are presented standing upstream of the inlet hence the inlet is on the right hand side (RHS) and the outlet on the left hand side (LHS).

The increase in sludge depth from 2017 to 2018 was obvious during data collection at the field as sludge deposits could be seen on the pond surface (see pictures on Figure 5.1c, d). The change in sludge depth as well as sludge distribution for the two periods is not uniform except at the inlet where there is consistent increase in sludge depth (Figure 5.1). The pond experienced serious sludge re-distribution in 2018, losing materials along both banks while gaining materials along the inlet edge.

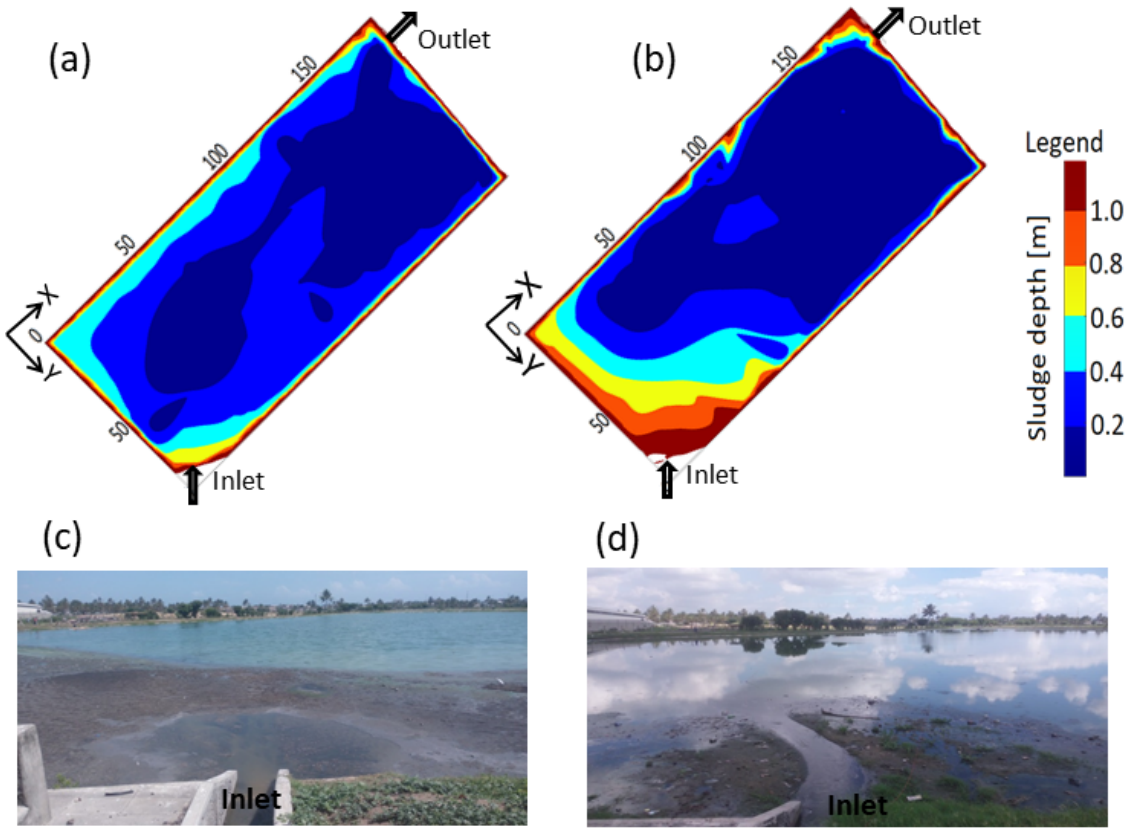

Figure 5.1: Measured sludge depth contours for (a) January 2017 (b) January 2018 and their corresponding pictures taken on-site for (c) January 2017 (d) January 2018. The outermost straight brown edges in the sludge contour pictures represent pond sides

The measured sludge profiles across the pond width show a mixture of both increased and reduced sludge depths for the period between January 2017 and January 2018 (Figure5.2). The inlet edge (X=0 m) has the highest increase in sludge depth extending the whole pond width while there is a decrease in depth throughout the outlet edge (Figure 5.2a and g respectively). For profiles inside the pond away from the X-axis boundary edges, there is an increase in sludge depth close to the inlet edge up to about 60 m from the inlet (X= 60 m, Figure 5.2c), after which a decrease in sludge depth across the whole pond width dominates

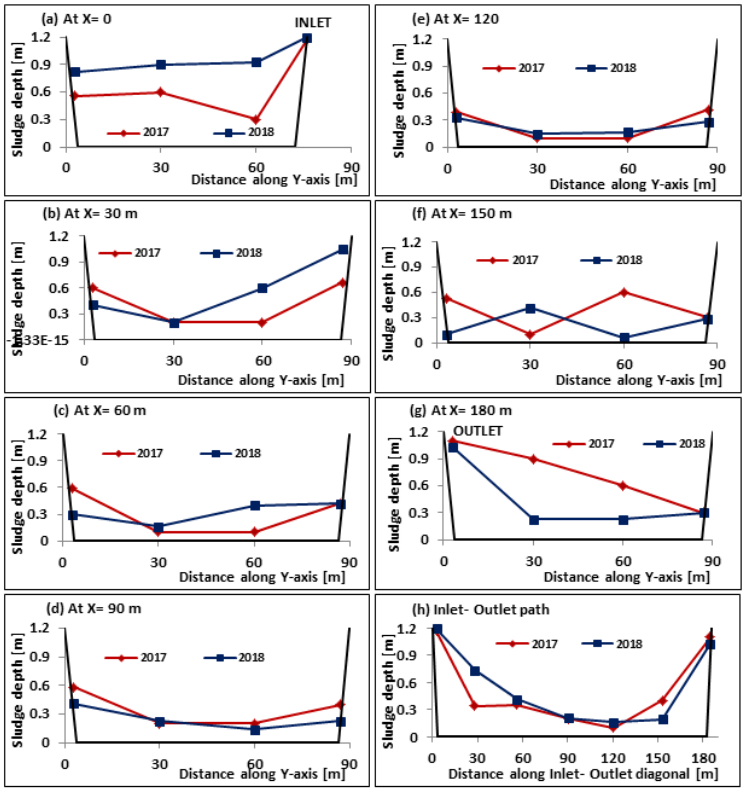

Figure 5.2: Sludge depth variations in sections across the pond width at 30 m intervals, standing upstream of the inlet making the inlet on the RHS (a-g), and along the inlet-outlet path (h)

up to the outlet edge. Sludge deposit around the inlet for systems with a single inlet is typical, multiple inlets give a distributed sludge deposition pattern.

The sludge profiles along the pond length generally show high sludge deposits around the inlet edge which decreases along the pond length and then picks up again around the outlet edge (Figure 5.3). The LHS bank (close to the outlet) had a decrease in sludge depth in 2018 (Figure 5.3a), except for areas close to the inlet where the sludge depth has increased. The rest of the profiles (Figure5.3 b - d) show sludge depth increase in 2018 in areas close to the inlet while decreasing towards the outlet, with the highest decrease observed at the outlet edge for the profile at Y= 30 m (Figure 5.3b). The general trend is sludge accumulates

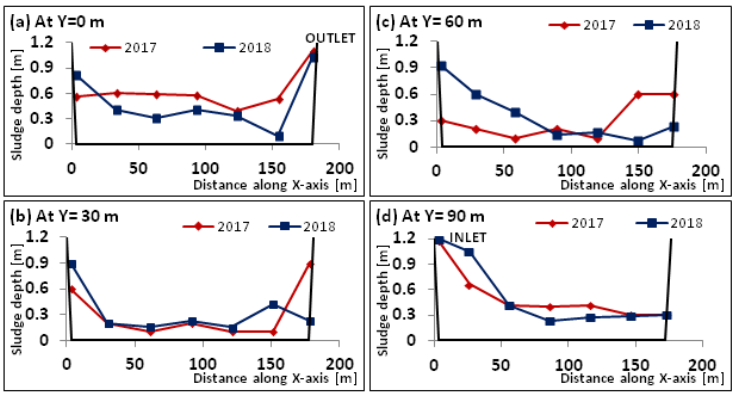

Figure 5.3: Sludge depth variations in sections across the pond length at 30 m intervals.

progressively from the inlet, with the RHS (the inlet side bank) progressing faster and receiving more sludge than the LHS bank.

The popular foot-path discussed in Chapter 2 and shown in Figure 2.6(a,c) runs along the LHS bank. This foot-path results in a lot of debris materials being thrown into and deposited inside the pond on that side which could explain the observed high sludge depth along the outlet bank. Also, during the rainy season, there is a potential of run-off coming into the pond through this path as it is badly worn-out in some areas such as the corner photographed in Figure 2.6 (a). Therefore the LHS bank may have secondary sedimentation resulting from materials that are not related to incoming domestic wastewater. As a result, areas where sedimentation of wastewater particles occur should be regarded as concentrated around the inlet.

The pond has not been dredged recently and assuming the observed sludge depth in the January 2017 has been accumulating since the pond was last de-sludged, possibly in the 2000s, then the pond received incredibly higher amounts of sludge between January 2017 and January 2018. But there were no changes such as a lot of new connections which may result into increased sludge inflow. Given the

nature of the system (sewered to households only), the increased flow must have originated outside the system, most likely from rainfall run-off, entering through the defective sewerage system and roof leakage and seepage into the connected toilets. This is supported by the pattern of sludge in the year 2017 where there seemed to be an extension of sludge deposits along the inlet-outlet line (Figure 5.1a); indicating sludge is pushed towards the outlet by increased discharge. Also, attempt to do particle size analysis immediately after a rainy day, in one of the sampling campaigns of this study failed as the pond water was too diluted for analysis using the Malvern Masterizer 2000, as it depends on light scattering and can only work when the sample has certain obscurity. The dilution of the pond water could only come from rain and it seems to be high enough to reach the pond bottom. The re-suspension of settled sludge during the rain period in the Buguruni WSP has been reported in our previous research, as supported by particle size distribution data (Izdori *et al.*, 2018).

5.3.2 Hydraulic and morphodynamic model results

Simulated flow velocity magnitudes and directions without wind and with different wind scenarios are discussed in Chapter 3. Sedimentation patterns were simulated using cohesive sediment formulation with parameters in Table 5.1, starting with an empty pond (bed level = 0m). In the cohesive sediment formulation, sediment exchange between the bed and flow is calculated by the Partheniades-Krone formulations (equations 5.2, 5.3 and 5.4), which uses the maximum bed shear stress derived from the hydraulic model (Deltares, 2016). Maximum bed shear stress in the pond is $10^{-5}Nm^{-2}$ at the inlet and between $10^{-7}Nm^{-2}$ and $10^{-8}Nm^{-2}$ inside the pond to as low as $10^{-10}Nm^{-2}$ at the corners, resulting into calculation of only the deposition flux while the erosion flux becomes zero. Since materials are transported and eventually deposited along the main flow

Table 5.1: Parameters used in the sedimentation model

Parameter	Value	Remark
Specific density	1020 kgm^{-3}	Density of sludge flocs
Dry bed density	850 kgm^{-3}	Recommended as 20 % less than the specific density
Fresh water settling rate	0.0474 mms^{-1}	Sengupta *et al.* (2011)
Saline water settling rate	0.0474 mms^{-1}	No flocculation
Critical sedimentation shear stress	0.001 Nm^{-2}	Estimated using median particle characteristics
Critical erosion shear stress	0.001 Nm^{-2}	Minimum allowed value in the model

path-line, it is expected that the different wind scenarios will result into modified sedimentation patterns, most likely different to the case without wind.

Simulation of sludge accumulation without wind resulted into accumulations mostly around the inlet (Figure 5.4a). Introduction of wind modified sludge accumulation patterns since the main flow path is changed (Figure 5.4b-d). The North-East and South-West winds result into sludge deposits being pushed towards the inlet side (RHS) bank (Figure 5.4b, c) while the South-East wind results into accumulation along the inlet edge (Figure 5.4d). This confirms that sludge accumulation in WSP tend to follow the areas of high flow velocities hence main flow path-line similar to previously reported ones (Alvarado *et al.*, 2012a).

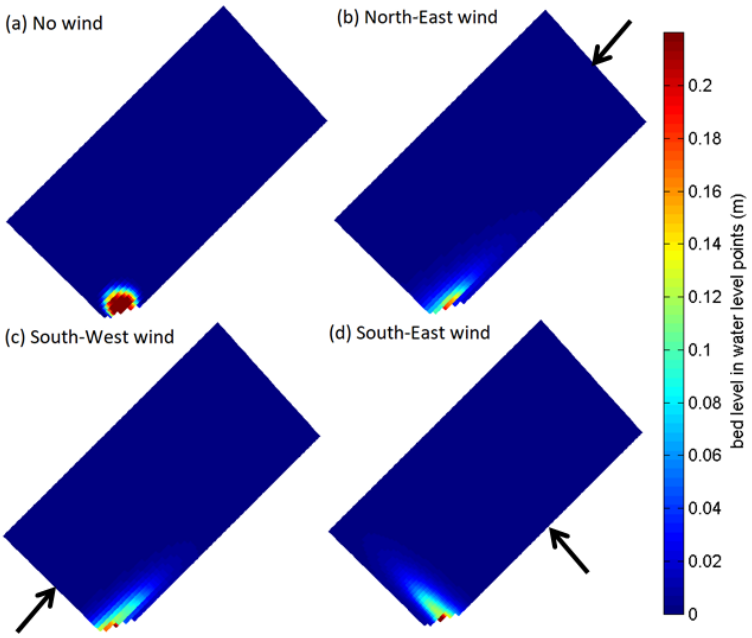

Figure 5.4: Sedimentation patterns from Delft3D simulations for a period of six (6) months, using the design discharge of 0.0077 $m^3 s^{-1}$, average measured suspended solids concentation of 350 mgL^{-1}. Arrows show wind directions.

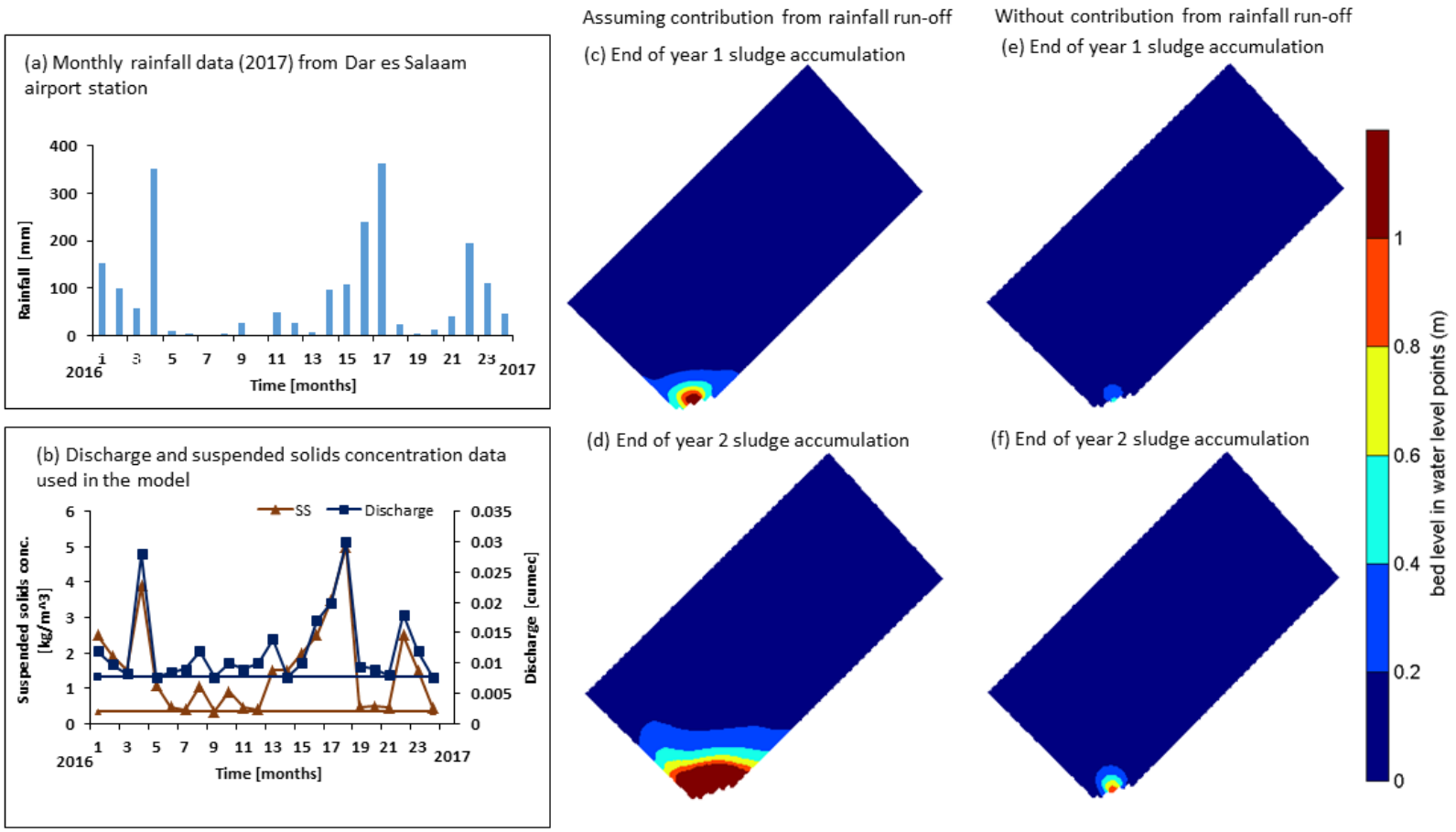

Figure 5.5: (a) Rainfall data for Dar es Salaam airport (2016-2017) (b) Stochastic discharge and suspended solids data, solid horizontal lines represent design data which is taken to be dry season data. Sedimentation patterns from Delft3D using stochastic discharge and suspended solids data (c,d) and with only the design discharge and suspended solids data (e,f)

Wind scenarios from (Figure 5.4), as well as discharge and suspended solids concentration were run in Delft3D simulation to find the set that gives similar sludge accumulation patterns to on-site sludge measurements (Figure 5.1). The best results (Figures 5.5c,d) are obtained by imposing a combination of the observed average wind characteristics, and monthly variable discharge of up to 0.03 m^3s^{-1} and suspended solids concentration as high as 5 kgm^{-3}, whose magnitudes were set to follow the rainfall pattern. A combination of different wind scenarios were tested to check for their contribution. Since the South-East and South-West winds occur in one season, the combinations tested were (i) North-East and South-East and (ii) North-East and South-West. Although the combination of North-East and South-East produce sludge distribution pattern similar to those observed in Figure (5.1), it is more concentrated around the inlet. Introduction of the South-West wind spread the sludge further into the pond, making it more comparable to the observed patterns. The high discharge and suspended solids concentration used in these simulations indicate the important contribution of the storm run-off, resulting from defective system as confirmed by the local technician in-charge of pond maintenance. The use of constant discharge and suspended solids concentration (the design discharge of 0.0077 m^3s^{-1} and suspended solids concentration of 0.35 kgm^{-3}) resulted in sludge accumulation at the inlet only, not spreading further into the pond and neither reaching the measured sludge depths (Figures 5.5e,f).

Generally, the morphodynamic model seemed to fit well, simulating patterns very similar to the observed ones (Figure 5.6a) as well as those reported in literature for facultative ponds (Abis and Mara, 2005; Coggins *et al.*, 2017; Nelson *et al.*, 2004; Alvarado *et al.*, 2012a; Passos *et al.*, 2014a). However, it can be seen that the lower sludge depths are underestimated, severely in some locations (Figure 5.6a), values circled in red). Most of the underestimated depths are measured at nodes located on the LHS bank of the pond, which is thought to have secondary

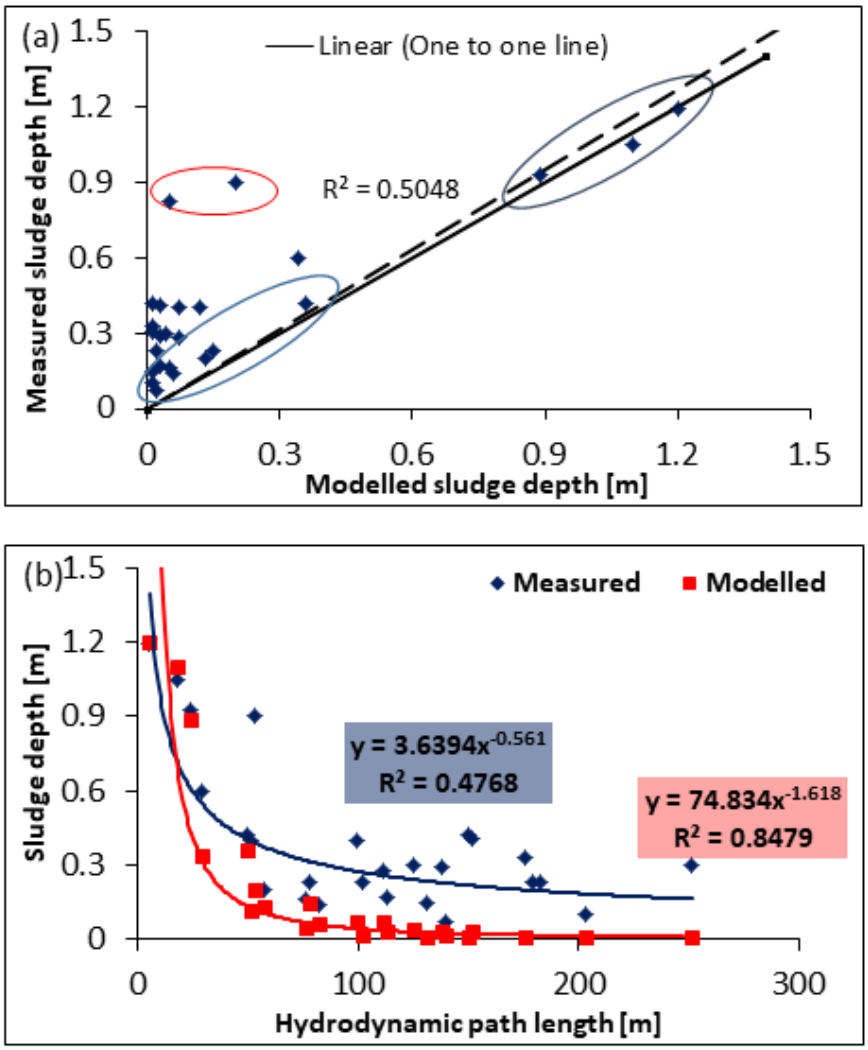

Figure 5.6: Comparison between measured and modelled sludge level (a) their correlation and (b) w.r.t hydrodynamic path length.

sedimentation that is not simulated by the model as it is more likely due to contribution from the footpath. The values circled in red in Figure 5.6a are for nodes 1 and 2 which are at the corner where the path is well worn. Also, both simulated and measured sludge depths follow a negative power function (Figure 5.6b), in which sludge depths decrease with the length of the hydrodynamic path-line from the inlet (the determination of the hydrodynamic path-line is discussed in Section 3.2). The power function for modelled sludge depth reduces to low

numbers close to 0m at around 50m from the inlet, but that for measured sludge depth plateaus to values around 0.3m, hence the observed difference in matching. Although we do not have a clear explanation for this, one reason could be that the measured sludge depths are overestimated by the white towel method, in which visual observation is used to detect the sludge layer thickness on the white cloth. Since water at the bottom of the pond is muddy, the observed sludge depth may actually represent the depth of the 'muddy water' and not settled sludge.

Eventually, sludge accumulation patterns seems to be affected mostly by wind flow and incoming discharge characteristics, which are influenced by rainfall in the Buguruni WSP. Wind seems to push and spread the sludge deposits sideways away from the inlet-outlet path. On the other hand, increased discharge enabled sludge to spread further into the pond along the inlet-outlet path, not concentrating around the inlet only. Although temperature is important in the biodegration of sludge and hence the change in sludge volume in the pond (Papadopoulos *et al.*, 2003), it was not included in this research and could be considered among the avenues to improve the model. Also, the wind scenarios used are long term average of Dar es Salaam city (Mahongo *et al.*, 2012), and the discharge variations were simulated to follow the rainfall trend of Dar es Salaam as it had been observed that there was an increased flow during rainy season which is thought to result from damaged sewer pipes and manholes. Therefore proper representation of the wind and discharge conditions should improve the simulated profiles to fit the observed. We believe that on-site recording of wind and discharge will greatly improve the model.

Re-suspension of settled materials

The increased discharge during the rainy season results into sludge re-suspension and re-distribution, hence pond self-cleaning through discharge of previously

settled sludge particles at the outlet. This poses a health risk as it may result in environmental contamination especially with helminth eggs, as well as other pollutants. In fact, the discharge of re-suspended sludge could be one of the factors for the outbreak of water-borne diseases such as cholera, common during the rainy season. A research by Ndyomugyenyi and Minjas (2001) observed high prevalence of urinary schistosomiasis among school children living in Kigogo area, where the river Msimbazi passes. The prevalence of this disease was linked to water related recreational activities. Buguruni WSP effluent is discharged into this river, upstream of Kigogo area and therefore there is a high likelihood of the river water to be contaminated with this effluent especially during the rain season. Therefore, the possibility of the pond self-cleaning is important and requires further investigation.

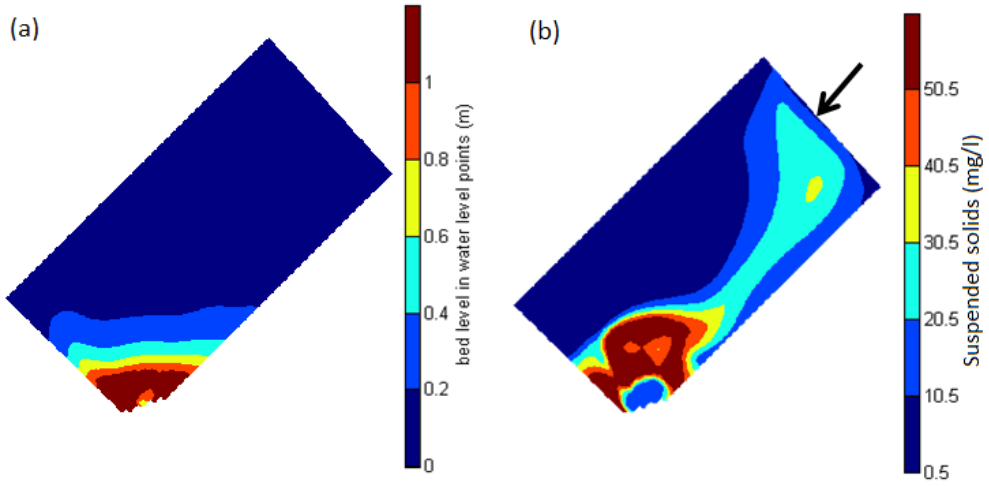

Figure 5.7: Simulation of the re-suspension process in the pond by Delft3D whereby: (a) shows loss of materials hence reduced sludge depth around the inlet and (b) shows the transportation of re-suspended materials towards the outlet. The arrows show wind direction used in the simulation.

The pond has not been dredged since rehabilitation in the year 2000 (personal communication with the DAWASCO techician). According to the research, after 10 years of operation the pond is expected to have accumulated enough sludge

to compromise its efficiency. However, observations as well as data collected show that this is not the case for this pond. The pond seem to self-clean, and simulations (Figures 5.7a, b) show that this could be due to flush-out of the settled sludge from increased flow specifically towards the end of rainy season where the incoming discharge has lesser suspended solids. The re-suspension was simulated by imposing high flows for the last month with suspended solids concentration set to zero. Although this resulted into re-suspension of materials and reduced sludge depth around the inlet, it did not produce patterns similar to January 2017 (Figure 5.5c). Therefore the morphodynamic model is not simulating the re-suspension process very well at present and needs improvement.

Wind effect on particle spreading

Suspended solids concentration as modelled in the pond seem to correspond to the wind direction. During the first wind season that lasts between November and March, particles are transported along the RHS bank of the pond as shown in Figure 5.8(a). This is a result of the differential movement of the different layers whereby, the top layer moves in the wind direction (outlet edge to inlet edge) while the bottom layer moves in the opposite direction (i.e. inlet edge to outlet edge direction). In the second season, from April to October where wind blows in different directions during the day and night, the overall effect seems to be a spreading of the suspended solids across the whole pond width.

5.4 Conclusion

This chapter focused on sludge accumulation in a primary facultative pond of a WSP, and linkage to climate characteristics. It was observed that wind plays a significant role in the pattern of sludge deposition, while increased discharge

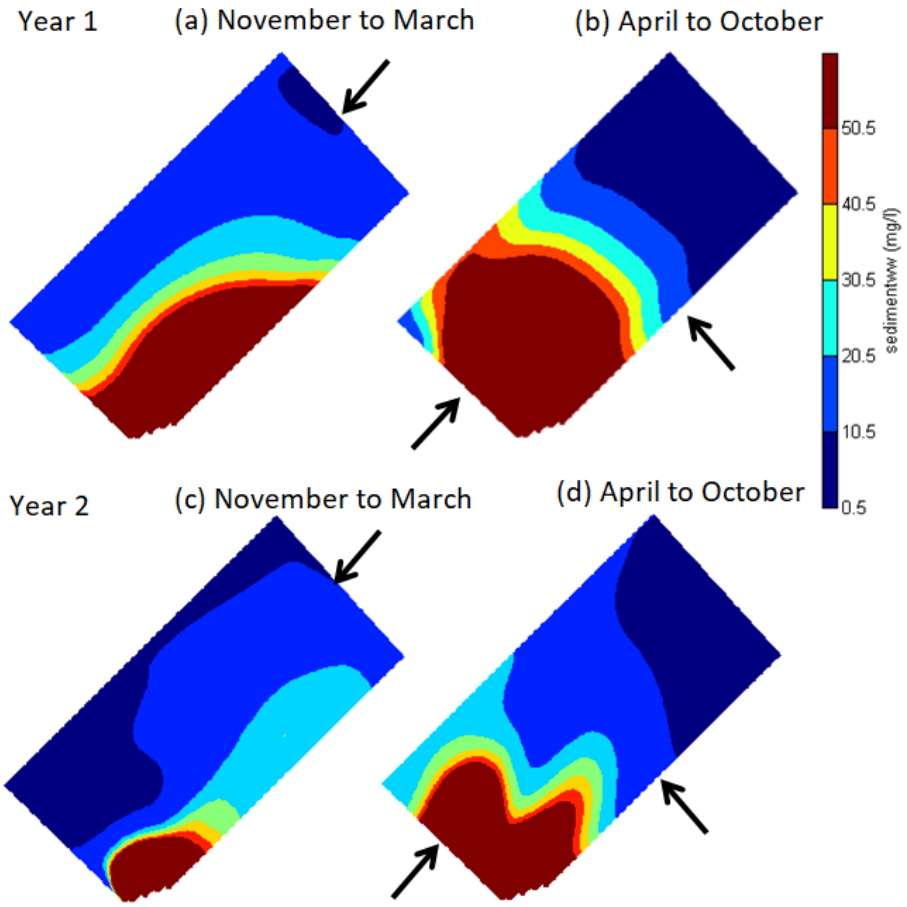

Figure 5.8: Suspended solids concentrations at the bottom layer of the pond for different wind scenarios

.

from rainfall contributed to more sludge materials as well as spreading of sludge further into the pond. The observed role of wind in sludge accumulation patterns may be useful during design for sludge management, for-example positioning of the inlet in a way that wind effect enhance sludge accumulations in only certain sides/areas of the pond. In a properly maintained WSP, the discharge from rainfall should be minimal (mainly origination from precipitation falling over the pond surface). Our research has shown that neglecting maintenance of the pond, as well as the sewer system has potential severe health and environmental effects,

impacting communities downstream of the WSP. Since the introduction of CFD in modelling WSP in the 1990s, numerical models have successful been applied both as a substitute to and in complimenting the laboratory scaled models famously used to study WSP processes (Shilton, 2001; Shilton *et al.*, 2008; Alvarado *et al.*, 2012a,b; Passos *et al.*, 2014b; Ouedraogo *et al.*, 2016; Passos *et al.*, 2019). The use of modelling in WSP, such as the one in this research, is beneficial during design, as well as operation, to simulate different scenarios for the pond inputs. Their use shows that numerical models may be applied both during design and operation to simulate different scenarios for the pond inputs. This is important for sustainable management of the WSP system and maintenance plans.

Chapter 6

Mechanistic model for particle sedimentation in WSP: Application to helminth eggs

6.1 Introduction

Parasites in wastewater pose a public health challenge (Mara and Faechem, 1999; Lloyd and Frederick, 2000), and they are responsible for causing diseases such as helminthiasi; a serious health condition affecting nearly a quarter of the world's population (Hotez *et al.*, 2008a). The parasites cause poor health, retard cognitive development and arrest growth of school children. The infections can also lead to epileptic seizures, maternal death and lower efficacy of tuberculosis (TB) vaccination, causing placental transfer of TB by pregnant women in affected geographies (Mwanjali *et al.*, 2013; Hotez *et al.*, 2008a). The major infection into humans of these parasites is via their eggs which are found abundantly in wastewater in low and middle income countries, as well as food crops irrigated

with contaminated water (Jimenez-Cisneros, 2007). There are several types of helminths (Shuval *et al.*, 1986; Sengupta *et al.*, 2011; Verbyla *et al.*, 2016; Ben Ayed *et al.*, 2009; Konaté *et al.*, 2013; von Sperling *et al.*, 2003), the most common being *ascaris, trichiura* and *taenia* (Mara, 2004). Prevalence of the different species vary between regions (Moodley *et al.*, 2008) and is influenced by climate (Brooker *et al.*, 2006). Helminths eggs' sizes range between 20 to 80 μm and their specific gravity ranges from 1.056 to 1.3 (Jimenez-Cisneros, 2007; Shuval *et al.*, 1986; Sengupta *et al.*, 2011).

In the majority of the tropical countries, helminth eggs are removed by sedimentation in WSP (Sengupta *et al.*, 2011; von Sperling *et al.*, 2003; Ayres *et al.*, 1991; Stott *et al.*, 2003). These water treatment systems are ranked as the best in-terms of helminth eggs removal, especially when sufficient hydraulic retention time (HRT)of atleast twenty (20) days is provided. However, as pointed out earlier, there is a gap in knowledge and a more fundamental understanding of the sedimentation of helminth eggs in WSP is needed; as these eggs have been found in WSP effluents with a HRT higher than 20 days; causing environmental contamination and raising the risk of disease outbreaks and health insecurity. Surveyed literature suggests a high correlation between particles in water and removal of helminth eggs (Sengupta *et al.*, 2011; Chavez *et al.*, 2004; Sengupta *et al.*, 2012a,b). Analysis of densities of wastewater particles in Chapter 4 indicated that, helminth eggs form flocs with other particles in water, resulting in modified physical characteristics which may explain the observed change in settling rates reported in (Sengupta *et al.*, 2012a, 2011).

Furthermore, the role played by the sedimentation process in helminth eggs and other pollutants removal, current design and performance approaches for WSP rarely consider the dynamics of the sedimentation process. We believe that, more nuanced studies on sedimentation in WSP may shed light on strategies to systematically improve helminth eggs removal from wastewater. In Chapter 5,

we successfully simulated the sedimentation process in WSP through application of Delft3D software. However, given the likely existence of limited resources and data, in line with literature we argue that, the use of mechanistic models could provide a simple and cost-effective method for characterizing risk zones (Argyropoulos *et al.*, 2010; Viman *et al.*, 2005), and identify governing processes (Viman *et al.*, 2005; Møller *et al.*, 2016) and sensitive parameters (Møller *et al.*, 2016). Therefore in this section, a mechanistic model for incoming particles dispersion and sedimentation in WSP is developed and applied to the Buguruni WSP to locate areas with sludge most likely to contain helminth eggs.

A number of parameters have been shown to correlate with helminth eggs. First, it has been observed that, areas that have higher sludge depth tend to contain a higher number of helminth eggs (von Sperling *et al.*, 2003). Secondly, the number of helminth eggs has a correlation to volume (in mLm^{-3}) of wastewater particles with sizes between 20 and 80 μm for both influent and effluent, as well as wastewater treated with chemical flocculants (Chavez *et al.*, 2004). Thirdly, the presence of laminar conditions and hydraulic sorting observed in waste stabilization ponds (Chapter 3) facilitates the characterization of particles at different locations inside the pond depending on their physical characteristics (size and density). The above mentioned observations indicate the possibility of using other parameters as a surrogate for presence of helminth eggs in sludge. This could be a useful heuristic tool as current methods for analysis and detection of helminth eggs are tedious,time-consuming and high cost due of chemicals used; that may at times damage the egg structure thereby rendering them undetectable. On the other hand, sludge depth may easily be obtained by the simple white towel method discussed in section 5.2.1, and particle sizes may quickly be obtained if laser equipments such as the Malvern Mastersizer discussed in Section 2.2 are available.

Therefore, in addition to development of a mechanistic sedimentation model

for helminth eggs, this section also explores the reliability of using these other parameters, that is particle size and density as well as sludge depth in the identification of areas with helminth eggs, by comparing results to those observed from the operational facultative pond of Buguruni WSP.

6.2 Model development

The aim is to develop a model that accounts for spatial stochasticity of the distribution and deposition of helminth eggs in WSP based on some measurable parameters. As shown in Figure 6.1, the model simulates the probability distribution of depositional distances inside the pond as a function of flow velocity profile down the pond depth and inlet particle size distribution. Flow profile down the pond depth is determined assuming laminar conditions inside the pond while the particle size distribution is obtained by sampling the incoming wastewater. The model gives the average particle size and their probability of being found at different locations along the pond depth from input data of discharge, particles characteristics (size distribution, density), and pond dimensions assuming no resuspension.

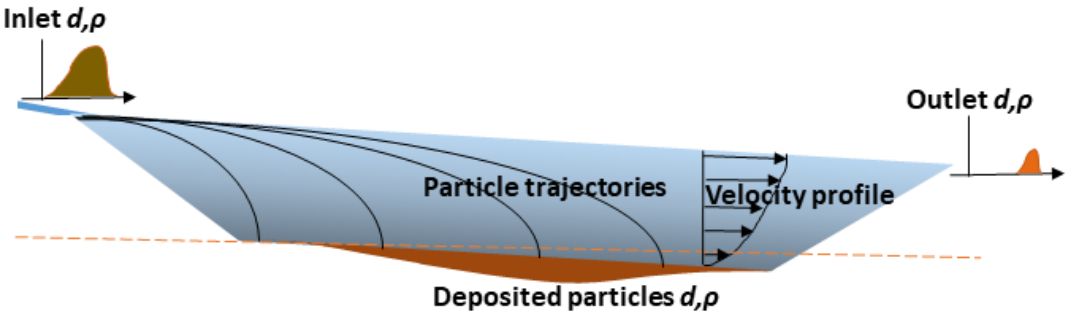

Figure 6.1: Model setup

.

Our model is based on the ballistic formulation by Pasquill and Smith 1983 as

extracted from Greene and Johnson (1989). In the model, the distance L_s that a particle travels before being deposited is obtained as;

$$L_s = \frac{\overline{V}}{w_s} h \tag{6.1}$$

where $\overline{V}$ is the average advection velocity in the pond, w_s is the settling rates of particles and h is the height at which the particles are released (i.e. elevation of the inlet for the case of Buguruni WSP).

Variation in deposition distances are expected to occur due to variations in the flow velocities (V_x, V_y and V_z), release height h and terminal velocities u_s. Since we are interested only in the down-ward movement of the particles to get the distribution of deposition distances, the other variations in flow velocities (V_x, V_y) can be removed by using the average flow velocity along the trajectory and assuming that every single trajectory occurs in a 1-D channel hence particles movements are limited to only forward advection along the pond length. The distribution of deposition distances is defined as the dispersal curve, given as the volume percent of particles at different depositional distances. The small depth of incoming flow at the inlet enables it to be treated as a point source.

The above ballistic equation (6.1) used to estimate the particle deposition distance in this research has been successfully applied for an analogous process of seed dispersal by wind (Nathan *et al.*, 2001; Stephenson *et al.*, 2007; Greene and Johnson, 1989; Murren and Ellison, 1998). In this equation, the distance traveled by a particle is determined from the medium mean flow velocity, particle terminal velocity and release height. This model has been successfully used to model seed dispersal incorporating distributions and variance in horizontal and vertical wind speeds (Nathan *et al.*, 2001; Anderson, 1991; Greene and Johnson, 1989), and terminal velocities (Greene and Johnson, 1989). The model performs well for simple case of point source (Greene and Johnson, 1989), and at low flow velocity

and release height (Murren and Ellison, 1998), conditions which are satisfied in WSP. The model is able to give the characteristics of the dispersal curve (Greene and Johnson, 1989) and performs well in estimating the modal dispersal distance (Greene and Johnson, 1989; Murren and Ellison, 1998) under the said conditions.

Flow in the 1-D channel in which the particle trajectories occur is governed by the slope gradient of the water surface, and may be obtained (Batchelor, 2000)

$$Q = \frac{\rho g sin\alpha h^3}{3\mu} \tag{6.2}$$

where Q is the discharge in $m^3 s^{-1}$, ρ is the fluid density, in this case 1000 kgm^{-3} for water, g is the acceleration due to gravity, α is the inclination of the water surface to the downward vertical, h is the depth and μ is the fluid dynamic viscosity in this case $1.0 \times 10^{-3} Nsm^{-2}$.

The velocity profile due to laminar conditions inside the pond will influence the particle trajectory; significantly reducing particle advancement near the bottom where the flow velocity drops to zero. The laminar velocity profile down the pond depth in the 1-D channel is given by the equation below (Batchelor, 2000).

$$V = \frac{\rho g sin\alpha}{\mu}(yh - \frac{y^2}{2}) \tag{6.3}$$

Substituting equation (6.2) in the velocity profile equation (6.3), the velocity profile down the pond depth can be obtained as:

$$V = \frac{3Q}{h}(yh - \frac{y^2}{2}) \tag{6.4}$$

Incorporating equation (6.4) and the Stokes equation for terminal velocity in

equation (6.1), the particle trajectory is given as

$$L_s = \frac{54Q\mu}{gb(\rho_s - \rho)d^2}(yh - \frac{y^2}{2}) \tag{6.5}$$

The maximum distance that a particle travels before being deposited is obtained when $y = h$ in equation (6.5). The probability of particles being deposited at these locations are obtained by applying the derived distribution function outlined in Chapter 4, using the sampled PSD.

6.2.1 Determination of likelihood of finding helminth eggs

The research aim is to locate areas in the pond with a high probability of recovering helminth eggs by using their physical characteristics i.e. size and density as well as sludge depth. The characteristics used are particle size ranging between 20 and 80 μm, density between 1056 and 1300 kgm^{-3} and sludge depth. Also, helminth eggs content of sludge is needed for comparison, to check the performance of the different criteria in predicting where helminth eggs may be found. In this research the water samples at the bottom of the nodes in Figure (6.2) were analysed for helminth eggs instead of sludge.

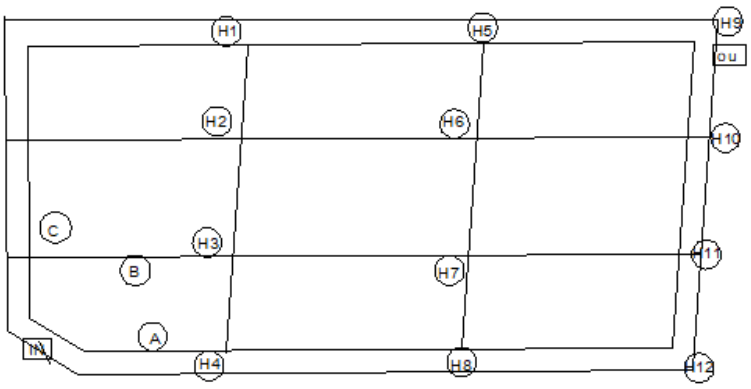

Figure 6.2: Location of data collection points for analysis of helminth eggs

For particle size, the percentage volume of particles between 20 and 80 μm is obtained through summation of all the classes in between. Likelihood is calculated by setting 10 as highest probability of recovering the eggs, corresponding to 100% of particles meeting the criteria and 0 the least representing 0%. For sludge depth, the observed sludge depth was ranked as 10 if it was the same as pond depth, that is 1.2 m (meaning sludge deposits exist to the top of the pond) and 0 for no sludge deposits. The likelihoods calculated through different criteria for all the nodes are then interpolated using the Kriging method in SURFER9 to obtain the spatial distribution of likelihood.

6.3 Results

Several data sets for particle sizes at the inlet were described in Chapter 2. Since particles coming into the pond during the rainy season also contain those from rainfall run-off, they are less likely to contain helminth eggs and are not a good representative for domestic wastewater. Therefore the inlet PSD sampled on the 27^{th} December, 2016, shown in Figure 6.3 was selected to be used in this analysis as this period was a peak of the dry period for that year, hence there is no chance for any contribution from rainfall run-off. This sample showed that the incoming PSD is a unimodal distribution skewed towards larger particles of 100 μm or more. The values for dissolved, colloidal, supracolloidal, and settleable fractions are 0%, 1.5%, 52.9%, and 45.6% respectively, with about 26 % of particles coming into the Buguruni WSP fall within the size fraction of helminth eggs (20-80 μm). When one considers the possibility of the eggs to be contained in the sludge flocs with sizes greater than 80 μm, then almost 80 % of particles have a probability of containing helminth eggs.

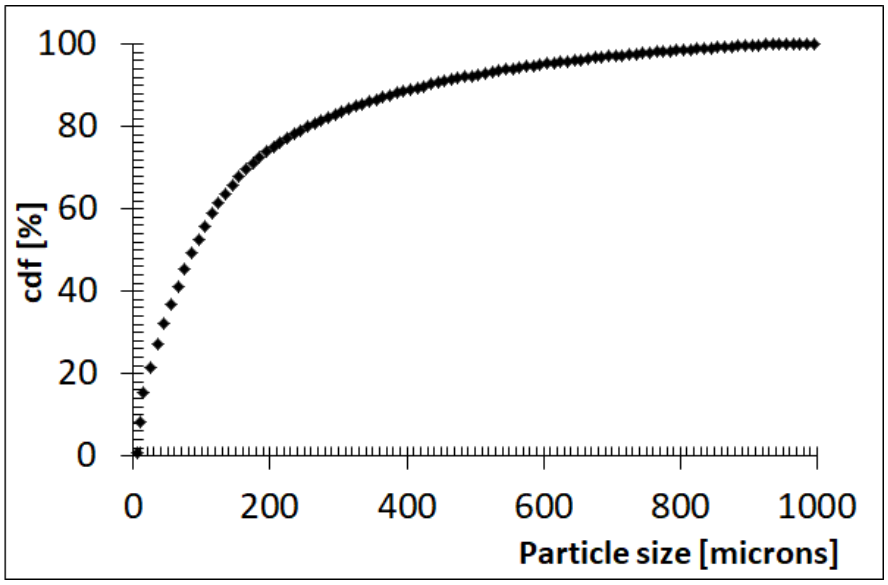

Figure 6.3: Inflow particle sizes from data gathered during fieldwork between 2016 and 2018

.

6.3.1 Deposition distances

The distances travelled by particles of different sizes before being deposited were calculated from equation 6.5, with the design discharge of 0.0077 m^3s^{-1} and the density values of 1000.45 kgm^{-1} (representing lighter flocs) and 1020 kgm^{-1} (representing denser flocs). A discussion for these densities is given in Chapter 4. From the hydraulic modelling in Chapter 3, the maximum path length from the inlet to the outlet is 237.1 m, therefore the plots for deposition distances were limited to this value.

Results show that, using the density value of lighter particles (1000.45 kgm^{-1}), the resulting deposition distance and average particle size matches well the sampled (Figure 6.4, red markers). This confirms the validity of our simple mechanistic model, which utilizes inlet PSD, discharge and pond dimensions to predict where particles will be deposited. The developed model shows that the settling process

acts as a filter, redistributing particles according to their sizes at different locations in the pond. The resulting minimum diameter for a particle to be deposited in the pond is 65 μm and 10 μm for lighter and denser particles respectively. For denser particles, particles as small as 80 μm are deposited within 10 m of the inlet while for lighter particles the size is much greater, coming to around 400 μm (Figure 6.4).

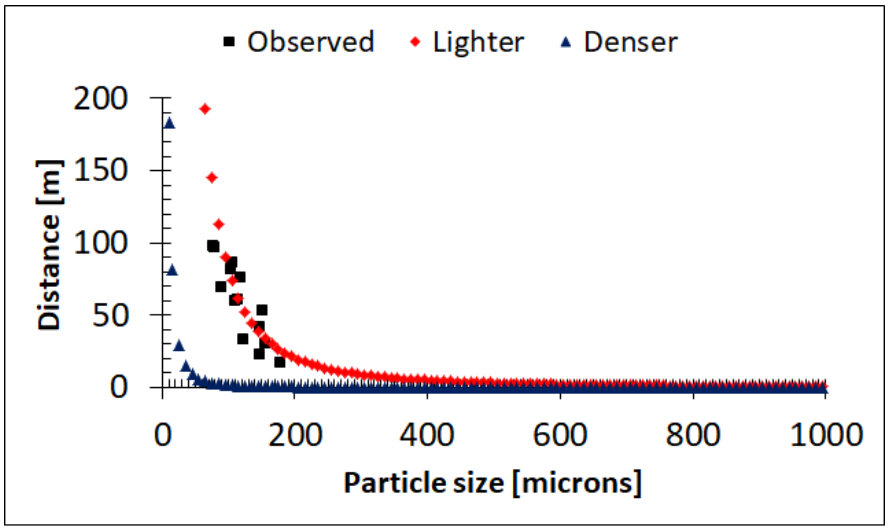

Figure 6.4: Distance travelled by particles of different diameters and densities before deposition, estimated using equation (6.5)

.

The deposition kernels for lighter and denser particles follow the trends shown in Figure 6.5. While most of the denser particles are deposited close to the inlet (blue markers), the lighter particles tend to travel further before they are deposited (red markers). More than 60 % of denser particles are deposited within 10 m of the inlet, making the area with most deposits, known as the modal distance right at the entrance. This is true as observed in the previous chapter (Chapter 5). About 8.3 % and 41.3 % of denser and lighter particles respectively have deposition distances more than the maximum travel distance of 237.1 m in the pond, meaning that these are particles that will be carried out of the facultative

pond. The filtering capacity of the pond should enable location of areas with helminth eggs by tracing their deposition distances from Figure 6.4.

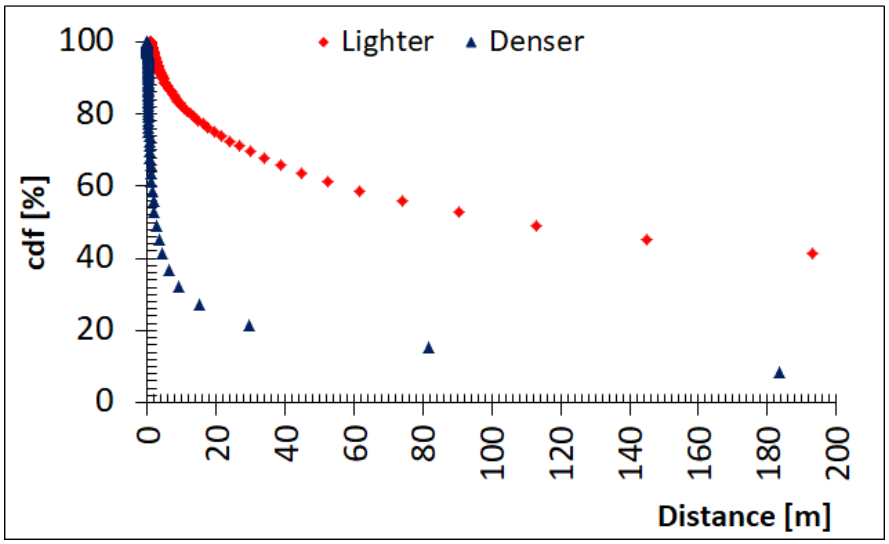

Figure 6.5: Probability of finding particles of different densities at different deposition distances in the pond

.

Although there is clear indication of hydraulic sorting in the pond w.r.t average floc size and percentage of larger particles as observed in the previous chapter (Chapter 4), this information could not be used to identify areas containing helminth eggs using their sizes. From Section 3.4, the average particle sizes which displayed a high correlation with hydraulic characteristics ranges from 160 μm at the inlet to 100 μm mid-pond. On the other hand, helminth eggs sizes range between 20 and 80 μm with an average value of 50 μm both of which are below the sizes that displayed hydraulic sorting. But the application of the mechanistic model developed in this section enabled extension of the deposited particle sizes to the smaller ones, hence identification of areas likely to contain helminth eggs.

From the results of the mechanistic model developed (Figure 6.4), it can be deduced that, if helminth eggs are incorporated in the lighter flocs then the chances for them to sediment in the pond are very slim. This could be the

reason why some helminth eggs have been recovered further from the inlet as well as at the outlet. However, if they are contained in the denser flocs, then they will be deposited from approximately 2.9 m to 45.9 m, giving an average deposition distance of 24.4 m. The probability of finding helminth eggs in denser flocs increases from 19 % at 45.9 m from the inlet to 44.5 % at 2.9 m from the inlet. This implies that, the highest chance of recovering helminth eggs (modal distance) is at around 2.9 m from the inlet.

6.3.2 Observed helminth eggs distribution

Analysis for helminth eggs could not be carried out at the modal distance of 2.9 m for denser particles due to sludge accumulation that was up to the top of the pond as our method involved sampling for wastewater. Therefore sampling and analysis was done for wastewater samples collected at the inlet and outlet, as well as at the bottom of nodes shown in Figure 6.2. The data was then extrapolated in SURFER9 to obtain spatial distribution of recovered helminth eggs. About 552 $eggsL^{-1}$ helminth eggs were recovered in the inlet sample. Inside the pond, the numbers of recovered helminth eggs were 297, 270 and 324 $eggsL^{-1}$ for node A, B and C respectively, and 297 $eggsL^{-1}$ for node H4. No eggs were recovered for the remaining parts of the pond apart from nodes H6, H8 and H10 where 48, 56 and 14 $eggsL^{-1}$ respectively were recovered. No eggs were recovered for the outlet sample.

This data was then ranked to obtain estimation of spatial distribution/ probability of obtaining helminth eggs at different locations. Due to high variability of the recovered number of eggs inside the pond ranging between 324 $eggL^{-1}$ to 0, the numbers were normalized by dividing with the inlet number of eggs. The results, (Figure 6.6), show highest rank of 6 occurs close to the inlet, immediately decreasing to 4.5 at about 21.5 m inside the pond, along the inlet-outlet line/path.

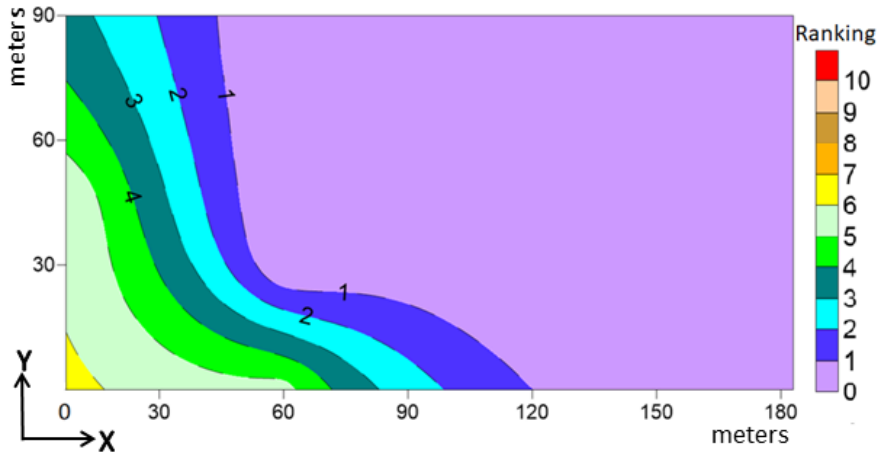

Figure 6.6: Spatial ranking for likelihood of recovering helminth eggs from field sampling. 10 and 0 represent highest and lowest likelihood respectively.

This implies a possibility of recovering up to 60 % of the eggs immediately at the inlet to about 45 % at 21.5 m inside the pond. This comes close to the predicted average distance for recovering helminth eggs using the density of 1020 kgm^{-3} which is 24.4 m, implying that helminth eggs are more likely to be contained in these flocs.

Various species were recovered in the pond as shown in Figure 6.7. The most common species seem to be *S. haematobium* (also known as urinary blood fluke). The eggs of this specie have a narrow oval shape with a terminal spine and have sizes between 100- 170 $\times$ 50- 80 μm. The high recovery of *S. haematobium* could be a result of their larger sizes that makes they detection easier compared to some other smaller eggs. Other recovered species were strongyloides (55 $\times$ 30 μm), *ascaris* 45- 75 $\times$ 35- 50 μm and hookworm (56- 70 $\times$ 35- 50 μm) and *trichuris* (50- 65 $\times$ 22- 30 μm).

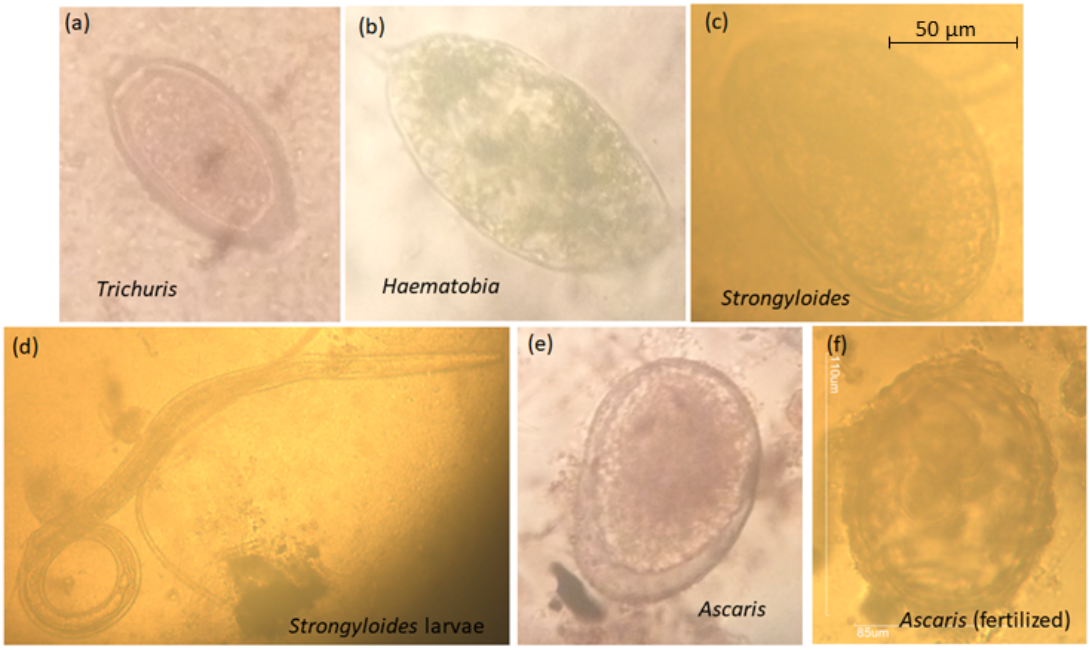

Figure 6.7: Recovered helminth eggs species (plates a, b,c,e,and f) and strongyloides larvae (plate d).

6.3.3 Different criteria for distribution of helminth eggs in the pond

The ranking at the nodes (only for areas with sedimentation) for different criteria were determined as described in the methodology. The node data were then extrapolated using SURFER9 to obtain spatial distribution of ranking. The results are as described below;

Ranking for particle with sizes between 20 to 80 μm increases from the inlet edge (Figure 6.8a). The highest rank is 6 at about mid-pond, and lowest is 4 close to the inlet. However, this is an opposite trend to the expected, as shown in Figure 6.6; whereby the probability of encountering helminth eggs increases from the inlet instead of decreasing. The highest probability of recovering helminth eggs is at around 75 m from the inlet, while for observed data the highest probability is closer to the inlet, decreasing inside the pond.

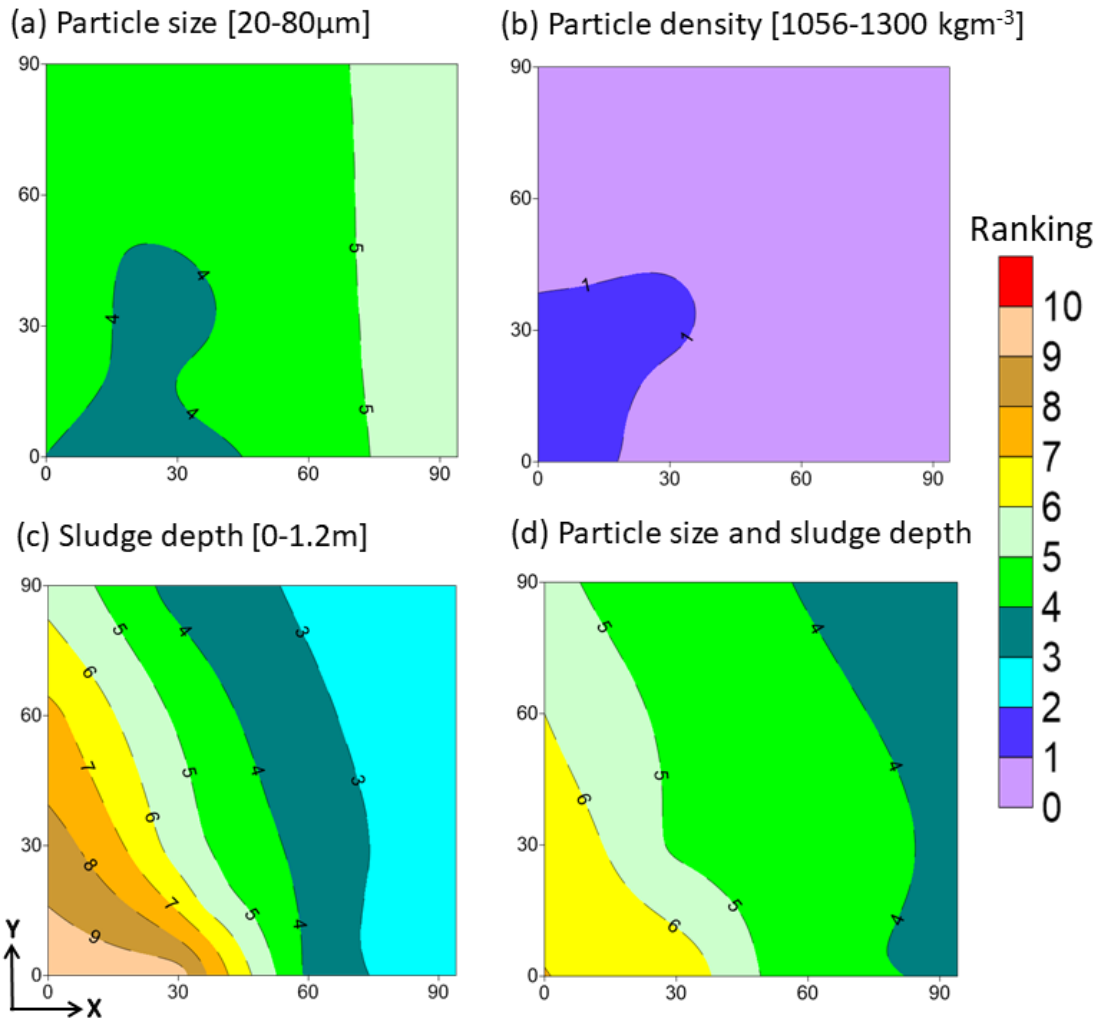

Figure 6.8: Spatial ranking of likelihood to contain helminth eggs through different criteria. 10 and 0 represent highest and lowest likelihood respectively.

Sludge density, although displayed the correct trend, i.e maximum probability at the inlet decreasing inside the pond (Figure 6.8b), the ranking is very poor, with a ranking of 1 close to the inlet and 0 everywhere else. These low probabilities are mainly due to the fact that the floc as well as primary particle densities estimated have lower density values compared to those of helminth eggs which is between 1056 and 1300 kgm^{-3}. These results indicate that, if helminth eggs exist as primary particles inside the pond, not as part of flocs, then they will most likely get deposited very close to the inlet.

Lastly, the ranking for sludge depth shows the expected trend, highest around the inlet decreasing inside the pond, (Figure 6.8c), with very high rankings compared to other criteria. This is because the pond has accumulated so much sludge, coming to the top in areas close to the inlet. This result into the highest ranking of 9 around the inlet, with the rankings decreasing gradually to 2 around mid-pond.

Also, a combination of ranking for particle sizes and sludge depth was calculated by averaging the rankings for the two criteria (Figure 6.8d). Results show the probability of recovering eggs decreases from the inlet to mid-pond, with highest ranking of 6 close to the inlet to minimum of 3 mid-pond.

However, particles in wastewater have been identified as flocs. This implies that, only the lower values for particle sizes can be used as a limit since there is a probability of more than one egg/ particle to be contained in a floc, resulting in a larger size than the upper limit for the eggs. By imposing this condition, the whole pond has about 90% (or ranking 9) possibility of containing helminth eggs as the percent of particles with diameters >20 μm is high in the pond, most likely due to presence of high densities of the algae *A. fusiformis* observed. For the case of particle densities, it is more complicated as there is a probability of eggs being incorporated in either denser or lighter particles, and therefore

their individual densities are irrelevant when considering their sedimentation in wastewater. Therefore, the possibility of using helminth eggs characteristics as a means of locating their depositional areas depends largerly on the characteristics of flocs formed in the pond.

6.4 Conclusion

This chapter aim was to develop a mechanistic model to predict areas of deposition of helminth eggs in WSP. Our results show that, in a properly working WSP system, helminth eggs should settle out within few meters of the inlet. This is supported by results from field data sampling at the facultative pond of the Buguruni WSP, which show that helminth eggs are deposited up to about 44 m inside the pond. The type of floc to which the eggs are incorporated (whether denser or lighter) plays a very significant role in where or if the eggs will be deposited. Since the eggs are incorporated into flocs that have modified physical characteristics (size and density), it is almost impossible to use their characteristics to locate them in sludge. Sludge depth seems to be the only parameter that can be used with confidence to predict areas with more helminth eggs compared to others.

Chapter 7

Conclusions

7.1 Findings

This research was set out to explore the sedimentation processes in the Buguruni WSP- Tanzania, concentrating in particle modifications inside the pond, settlement patterns at the bottom and properties of sedimented particles at different locations inside the pond. By systematically answering the research questions raised in Chapter 1, this research generated new knowledge with regard to sedimentation in the primary facultative pond as summarised below.

Sampled wastewater in this research contained a large number of larger particles ($> 100\mu m$), as discussed in Chapter 2, which is different to the values reported in literature whereby dissolved particles ($< 0.01\mu m$) seem to dominate. For the incoming wastewater, this could be explained by (i) Large soil particles that finds their way into the system because most of the roads and open spaces are unpaved, and therefore there is a high potential of individuals bringing soil particles with them into the wash-rooms that ends up in the pond. Also, sand particles may enter through defective man-holes and broken pipes, weathering of the soil on

the sides of manholes as well as rainfall run-off inflow into the defective system during rainy season. (ii) Fecal characteristics: the characteristic of fecal matter in the low and middle income countries is mostly roughages which are larger in size. Since the system is connected directly to the toilet chambers, the wastewater particles are mostly undigested fecal matter which may account for the large sizes observed. Inside the pond, the high density population of *A. fusiformis*, as observed and discussed in Chapter 4, may be responsible for large volume percent of supra-colloidal particles with sizes between 1 and $100\mu m$ as their helix dimensions vary between 2 and $100\mu m$. This may also account for the large percent of particles that fall within the size class of helminth eggs (20 to $80\mu m$) especially during the dry season, whereby it's above 50% in most of the samples collected at the top of the nodes. Pond hydraulics are a crucial parameter in both design and operation of the pond. With the successful use of CFD models in establishing pond hydraulics, there is a gradual shift from the traditional tracer experiments which are time consuming and sometimes unreliable due to interference of other conditions such as wind and temperature stratification. In Chapter 3, hydraulic conditions in the Buguruni WSP are established by using Delft3D software. The model is calibrated by comparing the average flow velocities and hydraulic retention time in the pond. Perhaps more important is the capability of these models to simulate different hypothetical scenarios which may be very useful especially during design to check for the pond performance under different operational conditions. The model is again employed in Chapter 5 to simulate the sedimentation process, and demonstrate the important role played by wind in sludge accumulation patterns.

Flocs formed inside the pond fall under two categories; lighter and denser flocs (Chapter 4). Estimation of densities inside the pond showed density to be dependent on the discharge as a determinant for minimum possible settling rates at different nodes. Using the design discharge of 0.0077 $m^3 s^{-1}$, the density classes

had modes around 1000.45 and 1020 kgm^{-3} for lighter and denser particles respectively, but these may change depending on the discharge. Again, the proliferation of *A. fusiformis* results into higher volume of the lighter particles that do not settle easily.

Local conditions are important when studying sludge accumulation rates and patterns in WSP. In Buguruni WSP, wind as well as presence of a footpath along one side of a pond are important in determining areas with more sludge accumulations (Chapter 5). Although the pond is fenced, the fence is broken in several places, and there are paths created for people to pass through. Significant sludge deposits observed all along the outlet edge in Chapter 2 and 5 is a result of debris from the foot-path, and possible illegal dumping of waste into the pond. Together with interference of the pond processes, these deposits lead to increased frequency of dredging and hence maintenance cost. On the other hand, damaged pipes and man-holes that are a result of ignoring pond maintenance, allow rainfall run-off discharge into the pond, resulting into modified sludge deposition patterns than expected. Our research has shown that neglecting maintenance of the pond, as well as the sewer system has potential severe health and environmental effects, impacting communities downstream of the WSP.

A simple mechanistic model utilizing the laminar conditions in the pond and the incoming PSD successfully reproduced the hydraulic sorting ability of the pond (Chapter 6). This was then used to locate helminth eggs based on their characteristic sizes and densities. However, since particles in the pond settle as flocs we can only do this as a probability. It appears that, if helminth eggs are embedded in the lighter flocs which are the majority forming on average 80% of the volume of particles in the pond, then they are more likely to be carried out of the system. On the other hand, if the eggs are contained in the denser flocs then they will settle within few meters of the inlet.

The use of modelling in WSP such as the one in this research may be applied during design as well as operation to simulate different scenarios for the pond inputs. This is important for sustainable management of the WSP system and maintenance plans.

Our findings are able to explain the variable settling rates of helminth eggs observed in other researches such as that of Sengupta *et al.* (2011). The eggs attains higher settling rates when embedded in denser flocs and have lower settling rates otherwise. The presence of algal populations in the facultative ponds although beneficial to biological treatment of wastewater, they result into lighter flocs and hence poor sedimentation in the pond. This shows that you can only optimize one process, either biological action or sedimentation in WSP. However, research has shown that a large percent of BOD is normally contained in the sludge where it can be (anaerobically) digested. Therefore, a significant area can be saved by constructing a system that favours sedimentation, followed by a sludge digester.

7.2 Recommendations and way forward

The observed role of wind in sludge accumulation patterns may be employed during design for sludge management, such as positioning of the inlet in a way that wind effect enhance sludge accumulations in only certain sides/areas of the pond. Maintenance of the pond and its system is important as our study has shown that, neglecting pond maintenance turns the WSP into potential disease transmitting vessel. Communities living downstream of discharge zones should be aware that there may be environmental contamination and take care if/ when in contact with natural water bodies. Irrigation using surface waters, play grounds in the discharge zone, stream crossings etc should be carried out with this awareness

in mind and preventive measures for helminth infections, such as wearing gum boots and gloves during irrigation, whenever possible should be taken.

Particle size analysis showed that the incoming wastewater at Buguruni has a higher content of supra-colloidal ($1-100\mu m$) and settleables particles ($> 100\mu m$), despite other researches reporting that dissolved particles ($< 0.01\mu m$) form the majority of particles in municipal wastewaters. It is thought that this is due to limitation of the mastersizer 2000, which measures particles within the range of $0.01 - 1000\mu m$. Therefore, further measurement of particle sizes using methods that measure smaller particle sizes than $0.01\mu m$ is recommended. In addition, studies on the association between the different particle size classes and pollutants will be useful in estimating the efficiency of different methods in pollutants removal.

Since it appears that wastewater particles settle as flocs, there is a higher potential for improving the sedimentation process in WSP through application of flocculants. Therefore future research should focus on addition of flocculants to WSP, especially locally available and natural ones. Also it will be useful to know the effect of flocculants addition on other wastewater parameters if any.

Although the simple mechanistic model developed in this research was calibrated using the average particle size data, it is recommended that laboratory experiments that are able to study the particles trajectories, forexample through image velocimetry (imaging) are undertaken. Particle tracking in the laboratory experiment should aim to observe the interaction of particles of different characteristic sizes and densities, and the impact on their trajectories.

The possibility of the pond self-cleaning under increased discharge (for this case during rainy season) also requires further research and confirmation. This process is important as it explains the prevalence of helminth eggs in the discharge zone,

as well as water-borne disease outbreak common during the rainy season. This also emphasizes on the importance of system maintenance by municipals.

Bibliography

Abbas, H., Nasr, R. and Seif, H. (2006). Study of waste stabilization pond geometry for the wastewater treatment efficiency. *Ecological Engineering*, **28**, 25–34.

Abis, K.L. and Mara, D. (2005). Research on Waste Stabilization Ponds in the United Kingdom: Sludge Accumulation in Pilot-scale Primary Facultative Ponds. *Environmental Technology*, **26**, 449–458.

Al-Sammarraee, M., Chan, A., Salim, S.M. and Mahabaleswar, U.S. (2009). Large-eddy simulations of particle sedimentation in a longitudinal sedimentation basin of a water treatment plant. Part I: Particle settling performance. *Chemical Engineering Journal*, **152**, 307–314.

Alvarado, A., Sanchez, E., Durazno, G., Vesvikar, M. and Nopens, I. (2012a). CFD analysis of sludge accumulation and hydraulic performance of a waste stabilization pond. *Water Science and Technology*, **66**, 2370–2377.

Alvarado, A., Vedantam, S., Goethals, P. and Nopens, I. (2012b). A compartmental model to describe hydraulics in a full-scale waste stabilization pond. *Water Research*, **46**, 521–530.

Amoah, I.D., Reddy, P. and Stenström, T.A. (2017). Effect of reagents used during detection and quantification of Ascaris suum in environmental samples on egg viability. *Water Science and Technology*, **76**, 2389–2400.

Anderson, M. (1991). Mechanistic Models for the Seed Shadows of Wind-Dispersed Plants. *The American Naturalist*, **137**, 476–497.

Argyropoulos, C.D., Sideris, G.M., Christolis, M.N., Nivolianitou, Z. and Markatos, N.C. (2010). Modelling pollutants dispersion and plume rise from large hydrocarbon tank fires in neutrally stratified atmosphere. *Atmospheric Environment*, **44**, 803–813.

Ayres, R.M., Stott, R., Lee, D.L., Mara, D.D. and Silva, S.A. (1991). Comparison of techniques for the enumeration of human parasitic helminth eggs in treated wastewater. *Environmental Technology*, **12**, 617–623.

Ayres, R.M., Alabaster, G.P., Mara, D.D. and Lee, D.L. (1992). A design equation for human intestinal nematode egg removal in waste stabilization ponds. *Water Research*, **26**, 863–865.

Ayres, R.M., Mara, D.D. and Rachel, M. (1996). Analysis of Wastewater for Use in Agriculture - A Laboratory Manual of Parasitological and Bacteriological Techniques. Tech. rep., World Health Organization.

Azema, N., Pouet, M.F. and Berho, C. (2002). Wastewater suspended solids study by optical methods. *Colloids and Surfaces A: Physicochem. Eng. Aspects*, **204**, 131–140.

Badrot-Nico, F., Guinot, V. and Brissaud, F. (2009). Fluid flow pattern and water residence time in waste stabilisation ponds. *Water Science and Technology*, **59**, 1061–1068.

Batchelor, G.K. (2000). *An Introduction to Fluid Dynamics*. Cambridge University Press, Cambridge, United Kingdom.

Ben Ayed, L., Schijven, J., Alouini, Z., Jemli, M. and Sabbahi, S. (2009). Presence of parasitic protozoa and helminth in sewage and efficiency of sewage treatment in Tunisia. *Parasitol Res*, **105**, 393–406.

Bethony, J., Brooker, S., Albonico, M., Geiger, S.M., Loukas, A., Diemert, D. and Hotez, P.J. (2006). Soil-transmitted helminth infections : ascariasis , trichuriasis , and hookworm. *The lancet*, **367**, 1521–1532.

Brissaud, F., Tournoud, M.G., Drakides, C. and Lazarova, V. (2003). Mixing and its impact on faecal coliform removal in a stabilisation pond. *Water Science and Technology*, **48**, 75–80.

Brooker, S., Clements, A.C.A. and Bundy, D.A.P. (2006). Global Epidemiology, Ecology and Control of Soil-Transmitted Helminth Infections. *Advanced parasitology*, **62**, 221–261.

Brooker, S., Akhwale, W., Pullan, R., Estambale, B., Clarke, S.E., Snow, R.W. and Hotez, P.J. (2007). Epidemiology of Plasmodium-Helminth Co-Infection in Africa: Populations at Risk, potential impact of anemia and prospects for combining control. *American Journal of Tropical Medicine and Hygiene*, **77**, 88–98.

Camnasio, E., Erpicum, S., Orsi, E., Pirotton, M., Anton, J.S. and Dewals, B. (2013). Coupling between flow and sediment deposition in rectangular shallow reservoirs. *Journal of Hydraulic Research*, **51**, 535–547.

Chavez, A., Jimenez, B. and Maya, C. (2004). Particle size distribution for microbial detection. *Water Science and Technology*.

Coggins, L.X., Ghisalberti, M. and Ghadouani, A. (2017). Sludge accumulation and distribution impact the hydraulic performance in waste stabilisation ponds. *Water Research*, **110**, 354–365.

David, E.D. and Lindquist, W.D. (1982). Determination of the Specific Gravity of Certain Helminth Eggs Using Sucrose Density Gradient Centrifugation. *The Journal of Parasitology*, **68**, 916–919.

Deltares (2016). Simulation of multi-dimensional hydrodynamic flow and transport phenomena, including sediments. In *User manual*, chap. Delft3D-FL, 679, Deltares.

DFID (2008). Water and Sanitation Policy- Water: An increasing precious resource. Sanitation: A matter of dignity.

Dominic, J.A. and Aris, A.Z. (2016). Discriminant analysis for the prediction of sand mass distribution in an urban stormwater holding pond using simulated depth average flow velocity data. *Environment Monitoring Assessment*.

Dufresne, M., Dewals, B.J., Erpicum, S., Archambeau, P. and Pirotton, M. (2010). Experimental investigation of flow pattern and sediment deposition in rectangular shallow reservoirs. *International Journal of Sediment Research*, **25**, 258–270.

Greene, D.F. and Johnson, E.A. (1989). A Model of Wind Dispersal of Winged or Plumed Seeds. *Ecology*, **70**, 339–347.

Gu, R. and Stefan, H.G. (1995). Stratification dynamics in wastewater stabilization pond. *Water Science and Technology*, **29**, 1909–1923.

Haranas, I., Gkigkitzis, I. and Zouganelis, G.D. (2012). g Dependent particle concentration due to sedimentation. *Astrophysics and Space Science*, **342**, 31–43.

Hotez, P.J., Brindley, P.J., Bethony, J.M., King, C.H., Pearce, E.J. and Jacobson, J. (2008a). Helminth infections: the great neglected tropical diseases. *J Clin Invest*, **118**, 1311–1321.

Hotez, P.J., Brindley, P.J., Bethony, J.M., King, C.H., Pearce, E.J. and Jacobson, J. (2008b). Review series Helminth infections : the great neglected tropical diseases. *The Journal of Clinical Investigation*, **118**, 1311–1321.

Izdori, F., Semiao, A.J.C. and Perona, P. (2018). Empirical Characterization of Particle Size Distribution Spatial Dynamics for Helminth Eggs Detection in Waste Stabilization Ponds (WSP). *Water*, **2**, 138.

Jimenez, B. and Alma, C. (2002). Low cost technology for reliable use of Mexico City's wastewater for agricultural irrigation. *Journal of Technology*, **9**, 95–108.

Jimenez-Cisneros, B.E. (2007). *Helminth Ova Control in Wastewater and Sludge for Agricultural Reuse*, book section Water and, 23. Encyclopedia of Life Support Systems, Eolss Publishers, Oxford ,UK.

Johnson, C.P., Li, X. and Logan, B.E. (1996). Settling velocities of fractal aggregates. *Environmental Science and Technology*, **30**, 1911–1918.

Kantoush, S.A., Bollaert, E. and Schleiss, A.J. (2008). Experimental and numerical modelling of sedimentation in a rectangular shallow basin. *International Journal of Sediment Research*, **23**, 212–232.

Keffala, C., Harerimana, C. and Vasel, J.L. (2013). A review of the sustainable value and disposal techniques, wastewater stabilisation ponds sludge characteristics and accumulation. *Environ Monit Assess*, **185**, 45–58.

Keller, R. (2004). Pathogen removal efficiency from UASB + BF effluent using conventional and UV post-treatment systems. *Water Science and Technology*, **50**, 1–6.

Keraita, B., Drechsel, P. and Konradsen, F. (2008a). Using on-farm sedimentation ponds to improve microbial quality of irrigation water in urban vegetable farming in Ghana. *Water Sci Technol*, **57**, 519–525.

Keraita, B., Drechsel, P., Konradsen, F. and Vreugdenhil, R.C. (2008b). Potential of simple filters to improve microbial quality of irrigation water used in urban vegetable farming in Ghana. *J Environ Sci Health A Tox Hazard Subst Environ Eng*, **43**, 749–755.

Khelifa, A. and Hill, P.S. (2006). Models for effective density and settling velocity of flocs. *Journal of Hydraulic Research*, **44**, 390–401.

Kihampa, C. (2013). Heavy metal contamination in water and sediment downstream of municipal wastewater treatment plants. *Int. J. Environ. Sci*, **3**, 1407–1415.

Konaté, Y., Maiga, A.H., Basset, D., Casellas, C. and Picot, B. (2013). Parasite removal by waste stabilisation pond in Burkina Faso, accumulation and inactivation in sludge. *Ecological Engineering*, **50**, 101–106.

Kottegoda, N.T., Rosso, R. and Kottegoda, N.T. (2008). *Applied statistics for civil and environmental engineers*. Blackwell Pub., Oxford, UK; [Malden, MA].

Krishnappan, B., Marsalek, J., Watt, W. and Anderson, B. (1999). Seasonal size distributions of suspended solids in a stormwater management pond. *Water Science and Technology*, **39**, 127–134.

Kunert, J. (1992). On the mechanism of penetration of ovicidal fungi through egg-shells of parasitic nematodes. Decomposition of chitinous and ascaroside layers. *Folia Parasitologica*, **39**, 61–66.

Lawler, D.F., O'Melia, C.E. and Tobiason, J.E. (1980). Integral water treatment plant design: from particle size to plant performance. In M.C. Kavanaugh and J.O. Leckie, eds., *In "Particulates in water: characterization, fate, effects, and removal"*, Am. Chem. Soc., Washington D.C.

Levine, A.D., Tchobanoglous, G. and Asano, T. (1991). Size Distributions of Particulate Contaminants in Wastewater and their Impact on Treatability. *Wat. Res.*, **25**, 911–922.

Levine, A.D., Tchobanoglous, G., Asano, T., Levine, A.D., Tchobanoglous, G. and Asano, T. (2017). Characterization of the size distribution of contaminants in wastewater : treatment and reuse implications. *Water Pollution Control Federation*, **57**, 805–816.

Lloyd, B.J. and Frederick, G.L. (2000). Parasite removal by waste stabilisation pond systems and the relationship between concentrations In sewage and prevalence in the community. *Water Science and Technology*, **42**, 375–386.

Logan, B.E. and Wilkinson, D.B. (1990). Fractal Geometry of Marine Snow and Other Biological Aggregates. *Limnology and Oceanography*, **35**, 130–136.

Lorang, M.S., Hauer, F.R., Journal, S., American, N., Society, B., December, N. and Auer, F.R.I.H. (2003). Flow competence and streambed stability : an evaluation of technique. *Journal of the North American Benthological Society*, **22**.

Madera, C.A., Mara, D. and Pena, M.R. (2002). Microbial quality of wsp effluent used for restricted irrigation in valle del Cauca, Colombia. *Water Science and Technology*, **45**, 139–143.

Mahongo, S.B., Francis, J. and Osima, S.E. (2012). Wind Patterns of Coastal Tanzania : Their Variability and Trends. *Western Indian Ocean*, **10**, 107–120.

Makoye, K. (2018). Tanzania's New Health Policy To Recognise Neglected Tropical Diseases.

Mara, D. and Sleigh, A. (2010). Estimation of Ascaris infection risks in children under 15 from the consumption of wastewater-irrigated carrots. *J Water Health*, **8**, 35–38.

Mara, D.D. (2004). *Domestic Wastewater Treatment in Developing Countries*. Earthscan Publications, London.

Mara, D.D. and Faechem, G.A. (1999). Water- and Excreta-Related Diseases:Unitary Environmental Classification. *Environmental Engineering*, **125**, 334–339.

Mara, D.D. and Pearson, H.W. (1999). Technical note a hybrid waste stabilization pond and wastewater storage and treatment reservoir system for wastewater reuse for both restricted and unrestricted crop irrigation. *Water Research*, **33**, 591–594.

Maya, C., Jimenez, B. and Schwartzbrod, J. (2006). Comparison of Techniques for the Detection of Helminth Ova in Drinking Water and Wastewater. *Water Environment Research*, **78**, 118–124.

Mayo, A.W. and Abbas, M. (2014). Removal mechanisms of nitrogen in waste stabilization ponds. *Physics and Chemistry of the Earth*, **72–75**, 77–82.

Møller, C.C., Weisser, J.J., Msigala, S., Mdegela, R., Jørgensen, S.E. and Styrishave, B. (2016). Modelling antibiotics transport in a waste stabilization pond system in Tanzania. *Ecological Modelling*, **319**, 137–146.

Moodley, P., Archer, C., Hawksworth, D. and Leibach, L. (2008). Standard Methods for the Recovery and Enumeration of Helminth Ova in Wastewater, Sludge, Compost and Urine–Diversion Waste in South Africa. Report, Water Research Commission.

Murphy, C. (2012). *Quantifying the Impact of Sludge Accumulation on the Hydraulic Performance of Waste Stabilisation Ponds*. Bachelor thesis, The University of Western Australia.

Murren, C.J. and Ellison, A.M. (1998). Seed Dispersal Characteristics of Brassavola Nodosa (Orchidaceae). *American Journal of Botany*, **85**, 675–680.

Mwanjali, G., Kihamia, C., Kakoko, D.V., Lekule, F., Ngowi, H., Johansen, M.V., Thamsborg, S.M. and Willingham A. L., r. (2013). Prevalence and risk factors associated with human Taenia solium infections in Mbozi District, Mbeya Region, Tanzania. *PLoS Negl Trop Dis*, **7**, e2102.

Nathan, R., Safriel, U.N. and Noy-Meir, I. (2001). Field Validation and Sensitivity Analysis of a Mechanistic Model for Tree Seed Dispersal by Wind. *Ecology*, **82**, 374.

Ndetto, E.L. and Matzarakis, A. (2013). Basic analysis of climate and urban bioclimate of Dar es Salaam , Tanzania. *Theor Appl Climatol*, **114**, 213–226.

Ndyomugyenyi, R. and Minjas, J.N. (2001). Urinary schistosomiasis in schoolchildren in Dar-es-Salaam , Tanzania , and the factors in uencing its transmission. *Annals of tropical medicine and parasitology*, **95**, 697–607.

Nelson, K.L., Cisneros, B.J., Tchobanoglous, G. and Darby, J.L. (2004). Sludge accumulation, characteristics, and pathogen inactivation in four primary waste stabilization ponds in central Mexico. *Water Res*, **38**, 111–127.

Ockenden, M.C. (1993). A Model for the Settling of Non-Uniform Cohesive Sediment in a Laboratory Flume and an Estuarine Field Setting. *Coastal Research*, **9**, 1094–1105.

Olukanni, D.O. and Ducoste, J.J. (2011). Optimization of waste stabilization pond design for developing nations using computational fluid dynamics. *Ecological Engineering*, **37**, 1878–1888.

Onyango, V. (1992). *Hydraulic sorting of bed-surface sediments in a shallow lake*. Masters thesis, University of Montreal, Canada.

Ouedraogo, F.R., Zhang, J., Cornejo, P.K., Zhang, Q., Mihelcic, J.R. and Tejada-Martinez, A.E. (2016). Impact of sludge layer geometry on the hydraulic performance of a waste stabilization pond. *Water Research*, **99**, 253–262.

Papadopoulos, A., Parisopoulos, G., Papadopoulos, F. and Karteris, A. (2003). Sludge accumulation pattern in an anaerobic pond under Mediterranean climatic conditions. *Water Research*, **37**, 634–644.

Passos, R.G., von Sperling, M. and Bressani Ribeiro, T. (2014a). Performance evaluation and spatial sludge distribution at facultative and maturation ponds treating wastewater from an international airport. *Water Science and Technology*, **70**, 226–233.

Passos, R.G., Von Sperling, M. and Ribeiro, T.B. (2014b). Hydrodynamic evaluation of a full-scale facultative pond by computational fluid dynamics (CFD) and field measurements. *Water Science and Technology*, **70**, 569–575.

Passos, R.G., Ferreira, V.V.M. and Sperling, M.V. (2019). A dynamic and unified model of hydrodynamics in waste stabilization ponds. *Chemical Engineering Research and Design*, **144**, 434–443.

Pearson, H.W., Silva Athayde, S.T., Athayde, G.B. and Silva, S.A. (2005). Implications for physical design: The effect of depth on the performance of waste stabilization ponds. *Water Science and Technology*, **51**, 69–74.

Poister, D. and DeGuelle, C. (2005). The influence of particle size distribution and composition on seasonal sedimentation rates in a temperate lake. *Hydrobiologia*, **537**, 37–46.

Ramirez, J.A. (2018). Derived Distribution Approach.

Reinoso, R., Torres, L.A. and Becares, E. (2008). Efficiency of natural systems for removal of bacteria and pathogenic parasites from wastewater. *Sci Total Environ*, **395**, 80–86.

Rodrigues, V., Possmoser-Nascimento, T., Dias, D., Passos, R.G., Von Sperling, M. and Vasel, J. (2015). Performance comparison between two equal stabilization ponds operating with and without sludge layer. *Water Science And Technology*, **71**, 929–937.

Sears, K., Alleman, J.E., Barnard, J.L. and Oleszkiewicz, J.A. (2006). Density and Activity Characterization of Activated. *Journal of Environmental Engineering*, **132**, 1235–1242.

Semadeni-Davies, A. (2009). Fall Velocities of Stormwater Sediment Particles. Literature Review. Report, Auckland Regional Council.

Sengupta, M.E., Thamsborg, S.M., Andersen, T.J., Olsen, A. and Dalsgaard, A. (2011). Sedimentation of helminth eggs in water. *Water Research*, **45**, 4651–4660.

Sengupta, M.E., Andersen, T.J., Dalsgaard, A., Olsen, A. and Thamsborg, S.M. (2012a). Resuspension and settling of helminth eggs in water interaction with cohesive sediments. *water research*, **46**, 3903–3912.

Sengupta, M.E., Keraita, B., Olsen, A., Boateng, O.K., Thamsborg, S.M., Pálsdóttir, G.R. and Dalsgaard, A. (2012b). Use of Moringa oleifera seed extracts to reduce helminth egg numbers and turbidity in irrigation water. *Water Research*, **46**, 3646–3656.

Shanthala, M., BB, H. and R, S. (2007). Removal helminth Parasitic eggs from Waste Stabilization Ponds at Shimoga. *The Bioscan*, **2**, 9–14.

Shilton, A. (2001). *Studies into the Hydraulics of Waste Stabilization Ponds*. Phd thesis, Massey University, Turitea Campus, Palmerston North, New Zealand.

Shilton, A., Kreegher, S. and Grigg, N. (2008). Comparison of Computation Fluid Dynamics Simulation against Tracer Data from a Scale Model and Full-Sized Waste Stabilization Pond. *Journal of Environmental Engineering*, **134**, 845–850.

Shuval, H.I., Adin, A., Fattal, B., Rawitz, E. and Yekutiel, P. (1986). Wastewater Irrigation in Developing Countries: Health Effects and Technical Solutions. Report, World Bank.

Sochan, A., Polakowski, C. and Łagód, G. (2014). Impact of optical indices on particle size distribution of activated sludge measured by laser diffraction method. *ECOL CHEM ENG S.*, **21**, 137–145.

Somes, N.L.G., Bishop, W.A. and Wong, T.H.F. (1999). Numerical Simulation Hydrodynamics. *Environment International*, **25**, 773–779.

Stephenson, C., Kohn, D., Park, K., Atkinson, R., Edwards, C. and Travis, J. (2007). Testing mechanistic models of seed dispersal for the invasive Rhododendron ponticum (L.). *Perspectives in Plant Ecology, Evolution and Systematics*, **9**, 15–28.

Stott, R., May, E. and Mara, D.D. (2003). Parasite Removal by Natural Wastewater Treatment Systems, Performance of Wastewater Stabilization Ponds and Constructed Wetlands. *Water Science and Technology*, **48**, 97–104.

Sweeney, D.D., Nixon, J.B., Cromar, N.J. and Fallowfield, H.J. (2005). Profiling and modelling of thermal changes in a large waste stabilisation pond. *Water Science and Technology*, **51**, 163–172.

Tyagi, V.K., Kazmi, A.A. and Chopra, A.K. (2008). Removal of Fecal Indicators and Pathogens in a Waste Stabilization Pond System Treating Municipal Wastewater in India. *Water Environment Research*, **80**, 2111–2117.

Tyagi, V.K., Sahoo, B.K., Khursheed, A., Kazmi, A.A., Ahmad, Z. and Chopra, A.K. (2010). Fate of coliforms and pathogenic parasite in four full-scale sewage treatment systems in India. *Environ Monit Assess*, **181**, 123–135.

Vega, G.P., Peńa, M.R., Ramírez, C. and Mara, D.D. (2003). Application of CFD modelling to study the hydrodynamics of various anaerobic pond configurations. *Water Science and Technology*, **48**, 163–171.

Verbyla, M.E., Oakley, S.M., Lizima, L.A., Zhang, J., Iriarte, M., Tejada-martinez, A.E. and Mihelcic, J.R. (2013). Taenia eggs in a stabilization pond system with poor hydraulics : concern for human cysticercosis ? *Water Science and Technology*, **68**, 2698–2703.

Verbyla, M.E., Iriarte, M.M., Guzmán, A.M., Coronado, O., Almanza, M. and Mihelcic, J.R. (2016). Pathogens and fecal indicators in waste stabilization pond systems with direct reuse for irrigation : Fate and transport in water , soil and crops. *Science of the Total Environment*, **551-552**, 429–437.

Viman, V., Mihaly Cozmuta, L., Mihaly Cozmuta, A., Vatca, G., Varga, C. and Oprea, G. (2005). Mathematical Modelling of Pollutants' Dispersion in Soil I. Case Study of Copper Dispersion. *American Journal of Envioronmental Sciences*, **1**, 126–129.

von Sperling, M., Chernicharo, C.A.L., Soares, A.M.E. and Zerbini, A.M. (2003). Evaluation and modelling of helminth eggs removal in baffled and unbaffled ponds treating anaerobic effluent. *Water Science and Technology*, **48**, 113–120.

WHO (2002). Prevention and Control of Schistosomiasis and Soil-Transmitted Helminthiasis: Report of a WHO Expert committee. Report, World Health Organisaztion.

Wu, J. and He, C. (2010). Experimental and modeling investigation of sewage solids sedimentation based on particle size distribution and fractal dimension. *International Journal of Environmental Science and Technology*, **7**, 37–46.